Report No. BMI-1437

UC-25 Metallurgy and Ceramics
(TID-4500, 15th Ed.)

Contract No. W-7405-eng-92

DEVELOPMENT OF CORROSION-RESISTANT NIOBIUM-BASE ALLOYS

by

Daniel J. Maykuth
William D. Klopp
Robert I. Jaffee
Warren E. Berry
Frederick W. Fink

May 12, 1960

BATTELLE MEMORIAL INSTITUTE
505 King Avenue
Columbus 1, Ohio

DISCLAIMER

TABLE OF CONTENTS

DEVELOPMENT OF CORROSION-RESISTANT NIOBIUM-BASE ALLOYS

Daniel J. Maykuth, William D. Klopp, Robert I. Jaffee,
Warren E. Berry, and Frederick W. Fink

The hot-water corrosion resistance and mechanical properties of niobium and a number of its alloys were evaluated with a view toward determining their usefulness in pressurized-water thermal reactors.

Unalloyed niobium is rapidly attacked by 600 and 680 F water and 750 F steam. However, a number of alloying additions were found which markedly improve the corrosion resistance of niobium. Of these, binary and ternary combinations of chromium, molybdenum, titanium, vanadium, and zirconium were among the most effective. Many of these alloys show as low or lower weight gains than those obtained for Zircaloy-2 under similar test conditions. Most of the niobium-base alloys tested for strength also show excellent resistance to creep at temperatures up to 1200 F under stresses through 20,000 psi.

INTRODUCTION

The objective of this research program was the development of a high-strength, low-neutron-absorption, corrosion-resistant niobium-base alloy suitable for use in pressurized-water thermal reactors. Concurrent niobium corrosion programs are also underway at Bettis and Knolls Atomic Power Laboratories.

Prior to the initiation of this work, relatively little information concerning the hot-water corrosion resistance of niobium or its alloys was available. Some work by Griess, et al. (1) indicated that unalloyed niobium showed moderately good resistance to 480 F water. Other reported data on the corrosion behavior in water of alloys containing niobium were those given by Ivanoff and Grigorovich(2). This work, however, was primarily concerned with zirconium-base alloys.

Work at Battelle(3) and elsewhere had shown that the hot-air oxidation resistance of niobium could be improved significantly by alloying. Moreover, principles were developed in the Battelle work by which the effectiveness of alloying elements on the air oxidation resistance of niobium could be explained or predicted. This was believed to be of great practical significance since both the air and water oxidation reactions were believed to be basically the same.

Chromium, molybdenum, titanium, tungsten, vanadium, and zirconium are foremost among the binary addition elements which are known to improve the hot-air oxidation resistance of niobium. Thus, it was of interest to determine the hot-water corrosion resistance of these binary-alloy systems to establish the suspected correlation between the hot-air and hot-water oxidation resistance of these alloys.

(1) References are at end of report.

In addition a number of ternary niobium-base alloys were also evaluated. Initially, zirconium was most strongly favored as the major addition in the ternary alloys because of its low cross section and the high thermodynamic stability of its oxide. Later, as experimental results became available, several series of ternary alloys using vanadium as the major alloying addition were prepared for evaluation.

The experimental work on this program was actually begun with the corrosion testing of a group of wrought, commercial-purity niobium-base alloys which were available from the previous Battelle work[3]. Additional alloys, using high-purity niobium as a base material, were made to screen and evaluate other compositions of interest as described above.

In the alloy-development work, emphasis was directed toward alloys which were fabricable and which would have a total calculated thermal-neutron-absorption cross section as low as possible, the cross section not to exceed the value of 2.8 barns per atom for an 18 w/o chromium-8 w/o nickel stainless steel. Although not a primary objective of the program, useful information was obtained concerning the melting and fabrication properties of the alloys.

EXPERIMENTAL PROCEDURES

Materials

All of the niobium and niobium-base alloys prepared for this study were made from 3 to 4-in.-diameter niobium ingots which had been purified to the analyses shown in Table 1 by double electron-beam zone melting. As indicated, the results of a check analysis at Battelle on one of these ingots were in good agreement with the supplied analysis. The alloying additions were of comparably high purity as indicated by the data of Table 2.

Some evaluations were also conducted on a series of alloys made with commercially pure niobium of the following representative analysis:

Impurity	Amount, ppm	Impurity	Amount, ppm
Aluminum	40	Molybdenum	100
Carbon	50	Nitrogen	100
Calcium	20	Nickel	60
Copper	30	Oxygen	500
Iron	200	Silicon	100
Hydrogen	1	Titanium	50
Magnesium	<10	Zirconium	100 to 6000
Manganese	10		

These alloys were made using alloy additions of the same or similar quality indicated in Table 2 for the higher purity niobium-base alloys.

TABLE 1. ANALYSES AND HARDNESS OF DOUBLE ELECTRON-BEAM-MELTED NIOBIUM USED AS BASE MATERIAL FOR ALLOY INGOTS[a]

	Analyses, ppm			
	Lot 405-599 P37 [Bhn (500-Kg Load) = 55.7]		Lot 405-599-162A3 [Bhn (500-Kg Load) = 59.3]	Lot 405-645-168A3 [Bhn (500-Kg Load) = 51]
Element	Battelle	Supplier	Supplier	Supplier
Aluminum	20	<20	<20	<20
Boron	--	<1	<1	<1
Carbon	70	100	<30	<30
Cadmium	--	<1	--	<1
Chromium	<50	<20	<20	<20
Copper	<10	70	--	<40
Iron	<30	<100	<100	<100
Magnesium	<5	<20	<20	<20
Manganese	<20	<20	<20	<20
Molybdenum	300	40	20	<20
Nitrogen	70	103	50	40
Nickel	<20	<20	<20	<20
Oxygen	130	131	52	50
Lead	30	40	50	<20
Silicon	30	<100	<100	<100
Tin	--	<20	--	<20
Tantalum	<1500	960	780	620
Titanium	<30	<150	<150	<150
Vanadium	--	<20	<20	<20
Tungsten	--	<300	287	<300
Zinc	--	<20	--	<20
Zirconium	<10	<500	--	<500

(a) Niobium purity was >99.8 per cent, material and data received from the Wah Chang Corporation.

TABLE 2. ANALYSES OF ALLOYING ADDITIONS USED TO MAKE HIGH-PURITY NIOBIUM-BASE ALLOYS

Base Metal	Method of Preparation or Source	Supplier's Analyses, ppm													
		Al	C	Cr	Cu	Fe	H	Mg	Mn	N	O	Si	Ti	V	Cl
Cr	Iodide process	1	10	--	--	1.5	1	1	--	3	10	--	--	--	--
Fe	Electrolytic flake	<30	40	<30	<10	--	--	<5	10	--	500	10	<10	<50	--
Mo	Commercial, sintered rod	--	40	--	--	--	--	--	--	40	70	--	--	--	--
Mo	Vacuum-fusion purified	--	<30	<5	5	<50	<1	<20	<5	<10	<10	<20	<10	--	--
Ni	Commercial, Nivac P sheet	<50	26	<10	40	130	--	--	<30	1.2	58	20	--	--	--
Ti	Fused-salt electrolysis	<300	120	<50	<60	<50	70	<10	100	20	180	100	--	<50	600
V	Calcium reduction	--	--	--	--	--	--	--	--	--	25[a]	--	--	--	--
Zr	Iodide process	<35	33	--	<25	27	--	<10	--	8	300	--	<25	--	--

(a) Estimated on the basis of lattice-parameter measurements.

Alloy Preparation

All alloys were prepared by arc melting in either of two sizes, i.e., as 50-g "button" ingots or as 2-in.-diameter, consumable-electrode-melted ingots.

The button ingots were used to obtain a broad composition coverage for screening the alloys according to their 680 F water corrosion resistance and hot hardness. These ingots were inversion melted with a tungsten electrode, under an absolute helium pressure of 20 to 30 cm of mercury, on a rocking, water-cooled copper crucible. Each alloy received a minimum of three, separate inversion-arc-melting operations.

The 2-1/2-lb ingots were prepared by double consumable-electrode arc melting under an absolute helium pressure of 25 cm of mercury. After the first melt, the ingots were sectioned longitudinally and joined end to end, by inert-atmosphere arc welding, to form a new electrode for the second melting operation.

Most of both types of alloy ingots were made using elemental charges of the desired addition metals. The only exceptions were for the ternary, 50-g alloy ingots containing combinations of niobium and vanadium with chromium or aluminum. In these instances, master alloys containing 51.4 w/o vanadium-48.6 w/o chromium and 40.6 w/o vanadium-59.4 w/o aluminum were first prepared by inert-electrode arc melting. These were then used in the alloy charges.

After melting, the hardnesses of all ingots were determined. Generally, for the 50-g-size screening alloy ingots, direct cold rolling to sheet was attempted where the as-cast hardnesses did not exceed a value of 150 VHN. Ingots of higher hardness were ground to a rectangular shape and fitted into a Type 304 stainless steel pack of welded construction for hot rolling to sheet at 1800 F. Prior to rolling, the packs were evacuated and sealed. A parting compound, made up of a slurry of chromic oxide in water glass was used to prevent bonding of the alloys with the steel cover plates during rolling.

For the 2-1/2-lb scaleup alloy ingots, several fabrication techniques were investigated. These included direct hot forging of the unprotected, 2-in.-diameter ingots in air and forging and rolling of the as-cast stainless steel-clad ingots. Generally, the most satisfactory procedure involved longitudinal sectioning of the ingots into roughly rectangular slabs, of about 3/4-in. thickness, and cladding of these slabs in stainless steel packs of the same type used for the 50-g alloy ingots. The clad slabs were then rolled directly to sheet in air at 1800 F.

After pack rolling, all of the alloys were cleaned by pickling, then grinding prior to vacuum annealing.

Corrosion-Test Procedures

Specimen Preparation

Corrosion specimens were cut from the annealed sheet. Specimens were shaper finished to a rectangular cross section. A minimum of 0.005 in. of metal was removed

from each surface to insure that no surface contamination remained. Specimens were then measured, degreased, dried, and weighed prior to corrosion testing.

The specimens were inserted in individual Chromel A* wire baskets. Numbered stainless steel tags were attached to each basket to maintain specimen identity. The baskets were hung from stainless steel supports, and no effort was made to insulate them from the autoclave.

Test Conditions

The corrosion tests were conducted in static, 1-liter-capacity autoclaves. The autoclaves and all auxiliary fittings and fixtures in contact with the water were AISI Type 316 stainless steel. An exception was the seal gasket which was made of "A" nickel.

Corrosion behavior was evaluated in 600 and 680 F degassed water and 750 F, 1500-psi degassed steam. The test water was once distilled and then passed through a mixed-bed ion-exchange column. The specific resistivity of the starting water was in excess of 1 megohm-cm. The water was degassed for the 600 and 680 F tests by (1) boiling for 1 hr, (2) transferring quickly to the autoclave which was sealed, and (3) boiling off the excess water at 300 F to further purge the autoclave of entrapped air. In the 750 F steam tests, 100 ml of water was added to the cold autoclave which was then sealed. The autoclave was opened to a vacuum pump three successive times with 5-min intervals between pumpings. The autoclave temperature was then raised to 600 F and the excess steam was bled off periodically to keep the pressure at 1500 psi. Fresh water was added after each exposure period.

The schedule of corrosion-specimen examination was as follows:

(1) 600 F water: 7, 14, 28, 42, 56 days and every 28 days thereafter

(2) 680 F water: 3, 7, 14, 28, 42, 56 days and every 28 days thereafter

(3) 750 F, 1500-psi steam: 1, 3, 7, 14, 21, 28, 42 days and every 14 days thereafter.

Evaluation

Corrosion behavior during the course of the experiment was evaluated on the basis of appearance and weight change of specimens. Specimens were brushed prior to weighing to remove any loose corrosion product. The microstructures of most specimens were examined when the corrosion tests were terminated. On selected samples, hardness traverses were made to determine the depth of contamination in the metal beneath the oxide film, and corrosion films were identified and hydrogen analyses were obtained.

*80 w/o nickel-20 w/o chromium alloy.

Hot-Hardness Testing

Hot-hardness measurements were conducted on annealed sheet specimens of each alloy in a vacuum atmosphere at 600, 900, 1200, 1400, and 1650 F. Allowed heating times for the 600 and 900 F measurements were 60 and 45 min, respectively, with 10-min periods being used for each of the higher temperatures. A sapphire indenter with a 730-g load was used in all of the tests.

Leak rates for the vacuum system were checked before and after each run and were found not to exceed a value of 0.6 μ per min for any run. As a check against possible contamination on heating, the room-temperature hardness of each sample was measured after as well as before heating to 1650 F.

Tensile and Creep Testing

All tensile and creep tests were conducted on annealed sheet samples, approximately 45 mils thick, with a reduced section approximately 1/4 in. wide and a gage length of 1 in.

All tensile tests were carried out at a crosshead speed of 0.02 in. per min, with testing at room temperature and 600 F being performed in air and tests at 1200 F being performed in helium.

The creep tests were all conducted in vacuum. Prior to testing, the reduced section of each sample was wrapped with niobium foil to minimize contamination.

EXPERIMENTAL RESULTS

Alloy Preparation

Screening Alloys

The compositions, cross sections, hardness, and fabrication data for all of the 50-g screening alloy ingots evaluated to date are listed in Table 3. This table includes data for the 22 binary and 9 ternary alloys prepared using commercial-purity niobium in the previous Battelle program.[3]

Generally, weight losses during melting of the alloys containing molybdenum, nickel, titanium, vanadium, and zirconium were quite low. However, the weight-loss data and subsequent analyses showed that almost all of the chromium and most of the aluminum and iron added to the alloy charges were lost during arc melting.

TABLE 3. COMPOSITIONS, HARDNESSES, AND FABRICATION DATA FOR 50-G, INERT-ELECTRODE ARC-MELTED NIOBIUM-BASE ALLOYS

Alloy	Alloy Content (Balance Niobium)[a], a/o	Weight Loss in Melting, per cent	Thermal-Neutron-Absorption Cross Section, barns per atom	Fabrication Procedure[b]	Sheet Quality[c]	Annealing Temperature, F	Vickers Hardness (10-Kg Load)	
							As Cast	As Annealed
			Commercial-Purity[d]					
--	100 Nb	--	1.15	CR	E	2730	120	120
138	10.5 Zr	--	1.05	HR	G	2730	187	199
139	26.1 Zr	--	0.90	HR	G	2730	212	266
140	35.7 Zr	--	0.81	HR	G	2730	283	306
141	45.7 Zr	--	0.71	HR	G	2730	289	302
163	1.1 W	--	1.3	CR	G	2730	147	--
164	4.7 W	--	2.0	CR	G	2730	175	--
165	9.6 W	--	2.8	HR	G	2730	230	266
152	2.45 Mo	--	1.18	CR	G	2730	128	126
153	5.2 Mo	--	1.21	CR	G	2730	154	146
154	7.4 Mo	--	1.26	CR	F	2730	175	205
150	4.4 V	--	1.30	CR	G	2730	152	143
147	6.6 V	--	1.38	CR	G	2730	168	169
148	8.9 V	--	1.48	CR	G	2730	196	191
149	10.7 V	--	1.54	CR	F	2730	209	210
158	13.7 V	--	1.65	HR	G	2730	264	281
151	24.2 V	--	2.06	HR	G	2730	285	314
169	4.9 Fe	--	1.22	CR	G	2730	167	127
142	9.4 Ti	--	1.58	CR	E	2730	123	127
143	18.8 Ti	--	2.02	CR	E	2730	145	154
144	24.3 Ti	--	2.26	CR	E	2730	145	162
145	30.5 Ti	--	2.58	CR	E	2730	151	160
146	33.8 Ti	--	2.72	CR	E	2730	155	169
175	12.0 Ti-0.5 Cr	--	1.72	HR	E	2730	136	240
176	20.2 Ti-2.1 Cr	--	2.12	HR	E	2730	192	235
177	28.2 Ti-6.1 Cr	--	2.56	HR	G	2730	230	348

TABLE 3. (Continued)

Alloy	Alloy Content (Balance Niobium)[a], a/o	Weight Loss in Melting, per cent	Thermal-Neutron-Absorption Cross Section, barns per atom	Fabrication Procedure[b]	Sheet Quality[c]	Annealing Temperature, F	Vickers Hardness (10-Kg Load) As Cast	Vickers Hardness (10-Kg Load) As Annealed
				Commercial-Purity[d] (Continued)				
172	12 Ti-4.2 Mo	--	1.78	HR	G	2730	171	177
173	17.4 Ti-6.2 Mo	--	2.06	HR	G	2730	192	227
174	23.1 Ti-7.8 Mo	--	2.35	HR	G	2730	206	260
178	10.4 Ti-5.0 V	--	1.57	HR	E	2730	175	268
179	16.1 Ti-8.4 V	--	1.80	HR	G	2730	199	262
180	22.6 Ti-11.0 V	--	2.05	HR	G	2730	243	287
				High-Purity				
N1	100 Nb	--	1.15	CR	E	2190	95	105
N40	100 Nb	--	1.15	CR	E	2190	101	109
N44	100 Nb	--	1.15	CR	E	2190	93	110
N56	100 Nb	--	1.15	CR	E	2190	93	94
N2	1.1 Zr	0	1.14	CR	G	2190	129	96
N3	2.2 Zr	0.3	1.13	HR	G	2190	151	--
N4	5 Zr[e]	0	1.10	HR	G	2730	173	165
N5	10.2 Zr	0	1.05	HR	G	2730	207	192
N41	25 Zr[e]	0.1	0.91	HR	G	2730	264	--
N42	35 Zr[e]	0.2	0.81	HR	G	2730	279	--
N6	40 Zr[e]	0	0.76	HR	G	2730	276	293
N43	45 Zr[e]	0.1	0.72	HR	G	2730	266	--
N8	65 Zr[e]	0	0.52	HR	G	2730	212	234
N9	75 Zr[e]	0	0.42	HR	G	2730	193	195
N10	90 Zr[e]	0	0.27	HR	G	2730	304	435
N11	3.2 Ti	0.4	1.30	CR	E	2190	98	83
N12	10.5 Ti	2.0	1.60	CR	E	2190	122	106
N13	25 Ti[e]	2.4	2.30	CR	E	2190	146	123
N14	<0.02 Cr	0.8	1.15	CR	E	2190	84	74
N15	0.5 Cr	5.6	1.16	CR	G	2190	90	78
N48	0.5 Cr	5.2	1.16	CR	G	2190	84	113

TABLE 3. (Continued)

Alloy	Alloy Content (Balance Niobium)[a], a/o	Weight Loss in Melting, per cent	Thermal-Neutron-Absorption Cross Section, barns per atom	Fabrication Procedure[b]	Sheet Quality[c]	Annealing Temperature, F	Vickers Hardness (10-Kg Load) As Cast	Vickers Hardness (10-Kg Load) As Annealed
				High-Purity (Continued)				
N45	<0.08 Fe	0.6	1.15	CR	G	2190	89	96
N46	0.3 Fe	2.8	1.16	HR	G	2190	116	107
N47	10 Fe[e]	3.2	1.28	HR	G	2190	238	232
N57	1 Ce[e]	1.7	1.13	CR	G	2190	73	71
N59	1 Y[e]	1.2	1.15	CR	G	2190	86	94
N60	5 Y[e]	5.0	1.16	CR	G	2190	67	109
N61	1 Ni[e]	0.2	1.18	HR	G	2190	140	144
N62	2.5 Ni[e]	1.2	1.23	HR	F	2190	192	171
N63	5 Ni[e]	0.6	1.32	HR	P	2190	223	186
N64	1 Pd[e]	0.4	1.21	CR	G	2190	107	134
N16	1.6 V	0.8	1.18	CR	G	2190	106	91
N81	5 V[e]	0	1.34	CR	G	2190	159	151
N49	2 V-2.5 Ti	2.4	1.34	CR	G	2190	115	118
N50	2 V-2.3 Mo	0.6	1.29	CR	G	2190	127	134
N51	2.2 V-0.54 Fe	1.6	1.24	CR	G	2190	136	134
N52	2.2 V-0.87 Ni	1.4	1.24	HR	G	2190	177	174
N53	1.8 V-<0.02 Cr	2.2	1.19	CR	G	2190	106	105
N54	1.8 V-0.14 Al	1.0	1.19	CR	G	2190	105	109
N55	2.5 V-2.5 Zr[e]	0.6	1.22	HR	G	2190	149	146
N65	5 V-2.5 Ti[e]	0.5	1.49	CR	G	2190	150	150
N66	5 V-2.5 Mo[e]	0.3	1.38	HR	G	2190	144	158
N67	5 V-2.5 Fe[e]	0.1	1.38	HR	G	2190	177	169
N68	5 V-2.5 Cr[e]	0.4	1.39	CR	G	2190	149	149
N69	5 V-2.5 Ni[e]	0.7	1.48	HR	G	2190	232	211
N70	5 V-2.5 Al[e]	1.3	1.32	CR	G	2190	150	144
N71	2.5 V-0.5 C[e]	0.4	1.24	HR	G	2190	153	130
N72	5 V-0.5 C[e]	0	1.34	HR	G	2190	198	163

TABLE 3. (Continued)

Alloy	Alloy Content (Balance Niobium)[a], a/o	Weight Loss in Melting, per cent	Thermal-Neutron-Absorption Cross Section, barns per atom	Fabrication Procedure[b]	Sheet Quality[c]	Annealing Temperature, F	Vickers Hardness (10-Kg Load) As Cast	Vickers Hardness (10-Kg Load) As Annealed
				High-Purity (Continued)				
N73	2.5 V-0.25 Ti-0.5 O[e]	0.3	1.29	HR	G	2190	162	161
N74	5 V-0.25 Ti-0.5 O[e]	0	1.41	HR	G	2190	179	186
N75	2.5 V-0.25 Zr-0.5 O[e]	0	1.24	HR	G	2190	165	158
N76	5 V-0.25 Zr-0.5 O[e]	0.1	1.34	HR	G	2190	188	163
N77	2.5 V-0.5 Ti-0.5 C[e]	0.3	1.30	HR	G	2190	150	127
N78	5 V-0.5 Ti-0.5 C[e]	0.3	1.42	HR	G	2190	199	163
N79	2.5 V-0.5 Zr-0.5 C[e]	0	1.24	HR	G	2190	160	163
N80	5 V-0.5 Zr-0.5 C[e]	0	1.34	HR	G	2190	203	198
N17	2.3 Zr-4.0 V	1.7	1.26	HR	G	2190	101	168
N18	25 Zr-5 V[e]	0.2	1.10	HR	G	2730	283	286
N19	35 Zr-5 V[e]	0.1	1.00	HR	G	2730	297	313
N20	45 Zr-5 V[e]	0.1	0.90	HR	G	2730	304	321
N21	10.9 Zr-5.1 Ti	1.8	1.24	HR	G	2730	202	210
N22	25 Zr-5 Ti[e]	1.1	1.10	HR	G	2730	258	271
N23	25 Zr-15 Ti[e]	0.6	1.56	HR	G	2730	253	277
N24	25 Zr-25 Ti[e]	0.4	2.04	HR	G	2730	253	265
N25	35 Zr-5 Ti[e]	1.0	1.00	HR	G	2730	262	274
N26	35 Zr-15 Ti[e]	0.8	1.50	HR	G	2730	264	306
N28	45 Zr-5 Ti[e]	0.6	0.92	HR	G	2730	253	280
N29	10 Zr-5 Mo[e]	0.3	1.13	HR	G	2730	236	244
N30	35 Zr-5 Mo[e]	0.6	0.88	HR	G	2730	323	325
N31	45 Zr-5 Mo[e]	0.2	0.78	HR	G	2730	321	313
N32	35 Zr-5 Al[e]	0.4	0.76	HR	G	2730	325	329
N33	35 Zr-15 Al[e]	0.2	0.68	HR	NG	--	429	--
N34	45 Zr-5 Al[e]	0	0.67	HR	G	2730	311	329
N35	10 Zr-5 Cr[e]	2.7	1.14	HR	G	2730	194	219
N36	35 Zr-5 Cr[e]	1.0	0.99	HR	NG	--	312	--
N37	45 Zr-5 Cr[e]	0.5	0.93	HR	G	2730	330	332
N38	10 Zr-5 Fe[e]	1.2	1.12	HR	G	2730	266	341
N39	45 Zr-5 Fe[e]	0	0.78	HR	NG	--	348	--

Footnotes appear on following page.

Footnotes for Table 3.

(a) By chemical analysis unless otherwise indicated.
(b) CR designates cold rolling to 45-mil-thick strip, with interstage annealing at 75 per cent reduction, HR designates hot rolling in evacuated stainless steel pack at 1800 F to 45-mil-thick strip.
(c) E designates excellent, G designates good, F designates fair, NG designates no good.
(d) Alloys made in earlier Battelle program, see BMI-1317, "Oxidation and Contamination Reactions of Niobium and Niobium Alloys", February 3, 1959.
(e) Nominal composition.

The earlier Battelle work indicated that binary additions to niobium of titanium, molybdenum, zirconium, vanadium, iron, and tungsten (in the approximate order listed) resulted in alloys of increasingly higher hardnesses. This same work indicated the approximate limiting alloy contents for good cold workability in 50-g binary-alloy ingots were as follows:

Titanium	>33.8 a/o	Iron	~5 a/o
Vanadium	10.7 a/o	Tungsten	~5 a/o
Molybdenum	~7.5 a/o	Chromium	<3 a/o
Zirconium	<10.5 a/o		

In the present work, the alloy limits for good cold workability were more closely defined for binary niobium-zirconium and niobium-iron alloys at levels of about 1 per cent each for both alloying elements.

The only alloys which could not be fabricated to useful sheet by cold- or hot-pack rolling were those ternaries containing 35 a/o zirconium-15 a/o aluminum, 35 a/o zirconium-5 a/o chromium, and 45 a/o zirconium-5 a/o iron.

After fabrication and cleanup, each alloy was vacuum annealed. Initially, 1 hr at 2730 F (1500 C) was used as the annealing treatment as in the previous work. Later, however, the annealing temperature was dropped to 2190 F (1200 C) for alloys containing a total of 10 per cent additions or less in order to keep the recrystallized grain sizes as small as possible.

As indicated in Table 3, four unalloyed 50-g ingots of niobium were prepared to act as control samples for the alloys. The niobium for each of the unalloyed ingots was taken from the same lot of electron-beam-melted material (Lot 405-599-P37) which had an as-received hardness of 81 VHN. Alloys N1, N40, and N44 were each melted three times, and Alloy N56 was melted twice. In addition, separate niobium getter buttons were melted prior to each melting operation for Alloys N44 and N56. In spite of these precautions, the hardnesses of all four arc-melted samples were 20 to 30 VHN higher than that of the base material, indicating that some contamination had occurred during melting.

Scaleup Alloys

Table 4 lists the compositions, cross sections, hardnesses, and fabrication data for the fourteen 2-1/2-lb alloy ingots which were prepared to obtain mechanical-property data on selected compositions of interest.

In order to obtain comparative data for unalloyed niobium, a portion of one as-received, electron-beam-melted ingot (Lot 405-599-P37) was cold rolled directly from the 4-in. ingot to 70-mil-thick sheet. After degreasing and pickling, this material was vacuum annealed for 1 hr at 2730 F. Analyses of this material for interstitial content are given in Table 5. Comparison of these data with those for the as-received material (Table 1) shows that about 70 ppm oxygen pickup occurred as a result of contamination during the cold rolling and/or vacuum annealing of this material.

TABLE 4. COMPOSITIONS, HARDNESSES, AND FABRICATION DATA FOR 2-1/2-LB, CONSUMABLE-ELECTRODE ARC-MELTED ALLOY INGOTS

Alloy	Alloy Content (Balance Niobium), a/o		Thermal-Neutron-Absorption Cross Section, barns per atom	As-Cast Hardness (1500-Kg Load), Bhn	Fabrication Conditions[a]	Results
	Charged	Analyzed				
NL-1	45.9 Zr	--	0.70	255	Forged in SS at 1950 F and rolled in SS at 1800 F	Partial liquation, sheet no good
NL-2	13.1 V	12.6 V	1.61	201	Ditto	Some edge cracking, fair quality sheet
NL-3	7.5 Mo	7.2 Mo	1.25	160	Ditto	Ditto
NL-4	45.1 Zr-5.0 Ti	46.8 Zr-5.1 Ti	0.92	238	(1) Forged in air at 2200 F	(1) Ingot cracked in initial upsetting
					(2) Ingot slabs rolled in SS at 1800 F	(2) Rolled to very good quality sheet
NL-5	44.8 Zr-3.0 V	--	0.83	272	(1) Forged in air at 2200 F	(1) Ingot cracked in initial upsetting
					(2) Ingot slabs rolled in SS at 1800 F	(2) No good, slices fragmented severely
NL-5R	45.0 Zr-3.1 V	--	0.83	258	Ingot slabs rolled in SS at 1800 F	No good, slices fragmented severely
NL-6	16.4 Ti-8.3 Mo	18.8 Ti-8.7 Mo	2 15	198	(1) Forged in air at 2200 F	(1) Ingot cracked in initial upsetting
					(2) Ingot slabs rolled in SS at 1800 F	(2) Rolled to very good quality sheet
NL-7	11 2 Ti-3.6 Mo	11.2 Ti-3.2 Mo	1.72	151	Ingot slabs rolled in SS at 1800 F	Rolled to very good quality sheet
NL-8	9.9 V-9.9 Zr	9.4 V-9.9 Zr	1.39	228	Ditto	Rolled to good quality sheet
NL-9	12.8 V-6.3 Zr	11.4 V-5.7 Zr	1.50	237	Ditto	Ditto
NL-10	9.9 Ti-6.7 Cr	9.6 Ti-3.3 Cr[b]	1.75	196	Ditto	Ditto
NL-11	7.6 V	7.6 V	1.44	168	Ditto	Rolled to very good quality sheet
NL-12	8.8 V-0.22 N	8.7 V-0.26 N[c]	1.47	182	Ditto	Ditto
NL-13	7.4 V-2.5 Ti	7.3 V-2.4 Ti	1.55	172	Ditto	Ditto
NL-14	7.5 V-2.5 Mo	7.6 V-2.3 Mo	1.48	185	Ditto	Ditto

(a) SS designates evacuated stainless steel pack.
(b) Chromium content variable, see text.
(c) Equivalent to 0.040 w/o nitrogen.

TABLE 5. ANALYSES OF SELECTED NIOBIUM-BASE ALLOYS FOR INTERSTITIAL CONTAMINANTS[a]

Alloy	Alloy Content (Balance Niobium), a/o	Interstitial Content, ppm			
		Oxygen	Nitrogen	Carbon	Hydrogen
TP-37	100 Nb[b]	200	90	70	3
NL-2	12.6 V	360	140	180	7
NL-3	7.2 Mo	440	90	60	19
NL-4	46.8 Zr-5.1 Ti	--	70	60	--
NL-6	18.8 Ti-8.7 Mo	200	100	70	11
NL-7	11.2 Ti-3.2 Mo	290	90	100	17
NL-8	9.4 V-9.9 Zr	270	560	420	9
NL-9	11.4 V-5.7 Zr	1780	220	250	19
NL-10	9.6 Ti-3.3 Cr	226	60	160	2
NL-11	7.6 V	240	160	160	7
NL-12	8.7 V-0.26 N	280	400	200	21
NL-13	7.3 V-2.4 Ti	300	170	110	18
NL-14	7.6 V-2.3 Mo	244	150	130	10

(a) All materials analyzed after fabrication and vacuum annealing.
(b) Fabricated from electron-beam-melted stock (without remelting) by cold rolling.

Radiographs made for each of the double consumable-electrode-melted alloy ingots indicated that each was sound and free of porosity. After surface cleanup by light machining, the first three alloy ingots (NL-1, NL-2, and NL-3 in Table 4) were simply inserted in 1-5/8-in.-ID by 3-in.-OD stainless steel cans which were closed by welding in end plugs under a partial pressure of helium. For these as for all pack-rolled materials, the chromic oxide-water glass slurry was used to prevent bonding of the alloys to the stainless steel.

The canned ingots were then forged in air at 1950 F to 1-in.-thick billets. X-ray inspection of the canned billets showed the niobium-45.9 a/o zirconium alloy was badly cracked while the niobium-12.6 a/o vanadium and niobium-7.2 a/o molybdenum alloy billets showed only minor edge cracking. All three billets were then rolled to 1/8-in.-thick sheet at 1800 F.

On attempted stripping of the alloys from the stainless steel, it was found that the niobium-45.9 a/o zirconium alloy was too badly fragmented to be salvageable. Visible evidences of wetting of the stainless steel indicated that liquation had occurred in the contact areas between this alloy and the steel. This was apparently caused by the formation of a low-melting eutectic due to interdiffusion of the zirconium (from the alloy), chromium, iron, and nickel (from the stainless steel) at 1950 F. The other two alloy sheets were readily removed from the stainless and had moderately rough surfaces with edge cracking that was no more severe than that observed on these same alloy ingots after forging.

In an attempt to expedite fabrication, forging of the next three alloy ingots (NL-4, -5, and -6, in Table 4) was attempted in air at 2200 F. However, when each of the three ingots developed radial cracks during the initial upsetting operations, forging was stopped and abandoned in the fabrication process for the large, arc-melted alloy ingots. Instead, the practice of direct hot rolling stainless steel-clad slabs cut from the ingots was adopted, as described earlier in this report.

As shown in Table 4, sheet of good to very good quality was obtained from all of the ingots rolled using this technique excepting only the niobium-45 a/o zirconium-3.1 a/o vanadium alloy which fragmented severely.

As a check on the homogeneity of the alloys, samples from the ends and centers of two 30-in.-long alloy strips were analyzed for major metallic additions with the following results:

	Alloy Content (Balance Niobium), a/o				
		Analyzed			
Alloy	Charged	End A	Center	End B	Average
NL-2	13.1 V	12.65 V	12.81 V	12.28 V	12.58 V
NL-3	7.5 Mo	7.22 Mo	7.02 Mo	7.30 Mo	7.18 Mo

These results indicated good alloy homogeneity was obtained in melting and, on this basis, single analyses only were obtained on the balance of the fabricated alloy sheets. An exception was made in the case of the nominal 9.9 a/o titanium-6.7 a/o chromium alloy sheet (Alloy NL-10) for which two separate samples were analyzed for chromium content. Here, due to variable losses in melting, the chromium content ranged from 0.44 a/o at one end of the sheet to 6.3 a/o at the other.

Analyses for interstitial contaminants were obtained on each of the annealed alloy sheets with the results shown in Table 5. Marked increases in interstitial content were observed for several alloys, especially those containing vanadium. It appears possible that the higher oxygen contents of Alloys NL-2 and NL-3 resulted from heating these ingots to a higher temperature (1950 F) during fabrication than the other ingots (1800 F max). On the other hand, the higher-than-average levels of carbon, nitrogen, and oxygen in the vanadium-containing alloys suggest that appreciable amounts of these contaminants were contained in the vanadium. The very high oxygen content (1780 ppm) of the niobium-11.4 a/o vanadium-5.7 a/o zirconium alloy shows that significant oxygen contamination, from an unknown source, also occurred in this alloy.

Metallography

The structures of most of the binary alloys and some of the ternary alloys were examined in the vacuum-annealed condition. As indicated in Table 6, most of these alloys consisted of a single-phase solid-solution structure based on the niobium. Figures 1a and 1b show representative equiaxed structures observed for the base material and the alloys.

As noted in Table 6, binary alloys containing 10 a/o iron or 10.5 through 45.7 a/o zirconium contained two phases. Similarly, each of the ternary alloys containing zirconium also contained varying amounts of apparently the same zirconium-rich second phase observed in the binary zirconium alloys. In the 2.5 a/o vanadium-2.5 a/o zirconium, this phase occurred in the form of widely spaced, randomly distributed particles as shown in Figure 1c. The alloys with 10.5 to 45.7 a/o zirconium contained appreciably more of this phase which was distributed both inter- and intragranularly as a very fine dispersion. Similar structures were found in the 11.4 a/o vanadium-5.7 a/o zirconium (Figure 1d) and 9.4 a/o vanadium-9.9 a/o zirconium ternary alloys. Lesser amounts of apparently the same phase were observed in the annealed 46.8 a/o zirconium-5.1 a/o titanium alloy as shown in Figure 1e.

One metallographic sample of the segregated 9.6 a/o titanium-3.3 a/o chromium alloy (illustrated in Figure 1f) showed traces of a second phase at the grain boundaries. Three other titanium-chromium alloys of higher titanium:chromium ratios, prepared as smaller ingots, were all single phase. Accordingly, the extraneous phase in the 9.6 a/o titanium-3.3 a/o chromium alloy was tentatively identified as a chromium-rich phase resulting from chromium segregation and is probably based on the $NbCr_2$ compound.

Corrosion Testing

Corrosion tests were conducted under degassed conditions in static high-purity 600 and 680 F water and in 750 F, 1500-psi steam. Corrosion behavior was established by noting changes in weight and surface appearance for successive exposure periods. Metallographic examinations and hydrogen assays also were conducted on selected specimens.

TABLE 6. SUMMARIZED DESCRIPTION OF METALLOGRAPHIC STRUCTURES OBSERVED IN ANNEALED NIOBIUM-BASE ALLOYS

Composition Range (Balance Niobium)[a], a/o	
Single-Phase Alloy Structures	Two-Phase Alloy Structures
Binary Alloys	
0-33.8 Ti	--
0-24.2 V	--
0-7.4 Mo	--
0-4.9 Fe	10 Fe[b]
0-4.7 W	--
--	10.5-45.7 Zr
Ternary Alloys	
12 Ti-0.5 Cr	--
20.2 Ti-2.1 Cr	--
28.2 Ti-6.1 Cr	--
11.2 Ti-3.2 Mo	--
12 Ti-4.2 Mo	--
17.4 Ti-6.2 Mo	--
18.8 Ti-8.7 Mo	--
10.4 Ti-5 V	--
16.1 Ti-8.4 V	--
22.6 Ti-11 V	--
--	2.5 V-2.5 Zr[b]
--	9.4 V-9.9 Zr
--	11.4 V-5.7 Zr
--	46.8 Zr-5.1 Ti

(a) All vacuum annealed 1 hr at 2730 F and furnace cooled unless otherwise indicated.

(b) Vacuum annealed 1 hr at 2190 F and furnace cooled.

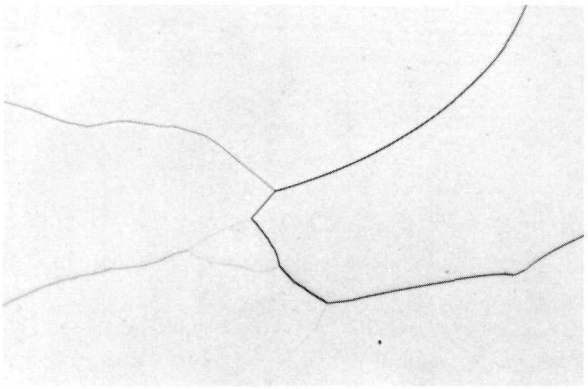

100X N57528

a. 100 a/o Niobium

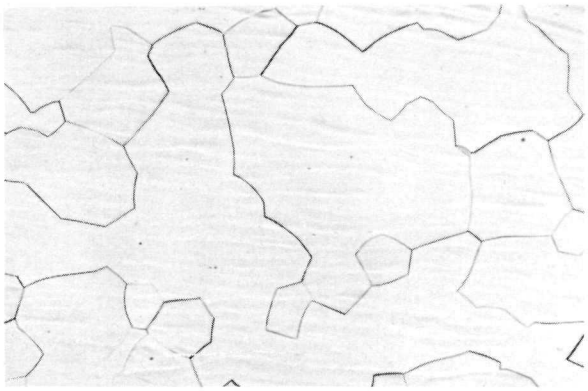

100X N57994

b. Niobium-18.8 a/o Titanium-8.7 a/o Molybdenum

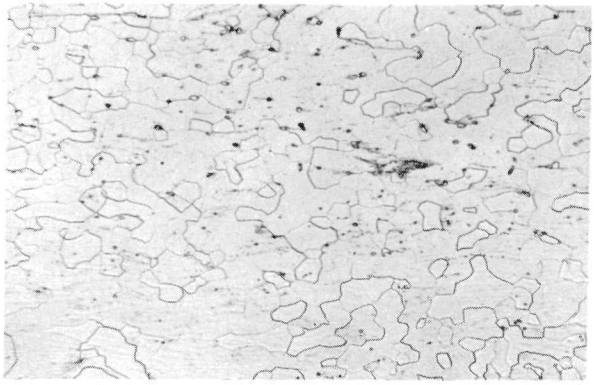

100X N61330

c. Niobium 2.5 a/o Vanadium-2.5 a/o Zirconium

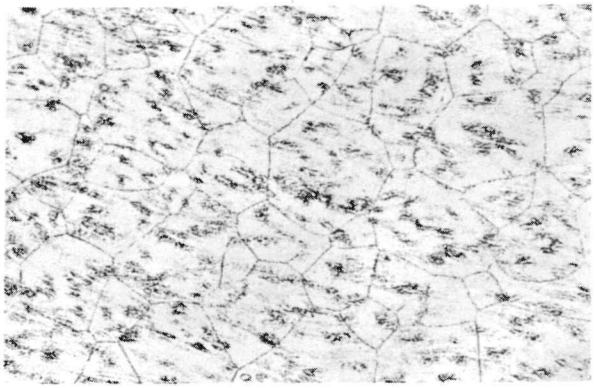

100X N61366

d. Niobium-11.4 a/o Vanadium-5.7 a/o Zirconium

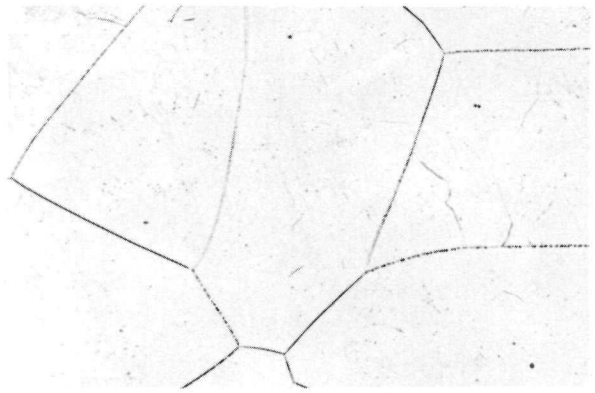

100X N57997

e. Niobium-46.8 a/o Zirconium-5.1 a/o Titanium

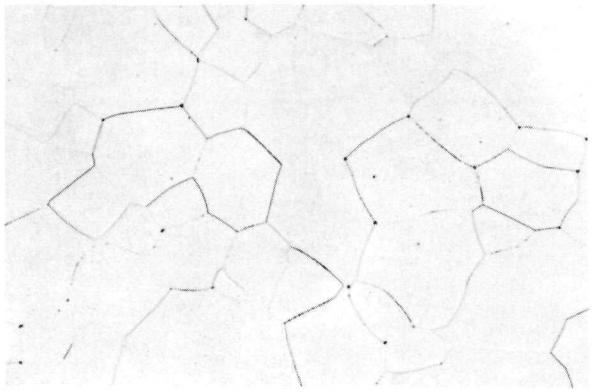

100X N61367

f. Niobium-9.6 a/o Titanium-3.3 a/o Chromium

FIGURE 1. REPRESENTATIVE MICROSTRUCTURES OF VACUUM-ANNEALED NIOBIUM-BASE ALLOYS

Appearance of Corroded Samples

The corrosion film on unalloyed niobium was dark gray to black in all test conditions. It was adherent during initial exposures, but eventually began to spall. Of the alloys studied, those containing more than 40 to 45 a/o zirconium, a ternary with 28.2 a/o titanium-6.1 a/o chromium and a ternary with 10.9 a/o zirconium-5.1 a/o iron exhibited adherent tarnish films throughout the course of the tests (196 days in 680 F water). The alloys which contained zirconium were covered with an adherent shiny black film while the titanium-chromium alloy possessed an iridescent tarnish during the entire exposure. A number of alloys exhibited tarnish films which were replaced by a dark-gray or brown film upon continued exposure. Included among these were binary alloys containing 25 to 35 a/o zirconium, 7.5 a/o molybdenum, 10 to 25 a/o vanadium, 20 to 35 a/o titanium, and ternaries containing at least one of the above elements in the composition range listed. All other alloy specimens were covered with dark-gray or brown films after the initial exposure.

Identification of Surface Oxides

Attempts were made using X-ray diffraction techniques to identify the species of oxides which occurred on the surfaces of several corroded alloy samples. The results are summarized in Table 7. The low-temperature T-type modification[4] of Nb_2O_5 was observed as the major constituent in the oxide scales of unalloyed niobium and the 4.7 a/o tungsten alloy. On the other hand, new oxides of $6ZrO_2 \cdot Nb_2O_5$ and TiO_2 rutile were found in the 45.7 a/o zirconium and 28.2 a/o titanium-6.1 a/o chromium alloy scales, respectively.

TABLE 7. IDENTIFICATION OF SURFACE OXIDES BY X-RAY DIFFRACTION

Alloy	Alloy Content (Balance Niobium), a/o	Corrosion Time in 680 F Water, days	Phases in Scale
--	100 Nb	28	T-Nb_2O_5[a]
149	10.7 V	196	Unidentifiable phase plus trace of NbO
151	24.2 V	196	Unidentifiable
164	4.7 W	196	T-Nb_2O_5
141	45.7 Zr	42	$6ZrO_2 \cdot Nb_2O_5$
144	24.3 Ti	196	Two unidentifiable phases, one of which is similar to niobium-24.2 vanadium phase
177	28.2 Ti-6.1 Cr	42	Unidentifiable
		196	TiO_2[b]

(a) A phase believed to be hydrogen-distorted niobium was also noted in scrapings from sample surface.
(b) Identification is tentative.

Corrosion Rates

Commercial-Purity Niobium-Base Alloys. Corrosion tests of a screening nature were conducted in 680 F water on the commercial-purity niobium-base alloys listed in Table 8. Where sufficient material was available, specimens from the same alloys were also exposed to 750 F, 1500-psi steam.

Weight-change data obtained at the intermediate exposure periods were somewhat erratic. Plotted curves exhibited a "wavy" appearance which suggested occasional loss of corrosion product. Contributing factors were believed to be: (1) slight powdering of the gray or brown corrosion films, (2) small specimen size, and (3) exposure of occasional defects which had been smeared over and not removed during specimen preparation. As a result of this erratic behavior, weight change-versus-time plots were not obtained, although the data seemed to follow a parabolic rate law for several of the alloys. The cumulative weight-change data after 196 days' exposure for the alloys investigated are included in Table 8. The unalloyed niobium was completely oxidized after 42 days' exposure, while the 9.6 a/o tungsten alloy cracked within 7 days. Alloys containing 1.1 and 4.7 a/o tungsten or 2.45 and 5.2 a/o molybdenum were losing weight. All other alloy specimens gained weight. The most resistant alloy appeared to be the 45.7 a/o zirconium binary and the 28.2 a/o titanium-6.1 a/o chromium ternary which exhibited adherent shiny black and iridescent tarnish films, respectively.

Corrosion results for the commercial-purity niobium-base alloys exposed to 750 F steam also are presented in Table 8. The accelerated nature of attack was quite pronounced on the less-corrosion-resistant alloys. The unalloyed niobium was completely oxidized within 28 days' exposure, while the 2.45 a/o molybdenum and 4.9 a/o iron alloys were completely oxidized at 98 days' exposure. The remaining alloys have survived 210 days' exposure, although weight losses are very high on the 10.5 a/o zirconium, 1.1 a/o tungsten, and 5.2 a/o molybdenum alloys running 3,970, 6,420, and 18,450 mg per dm^2, respectively. The 4.4 a/o vanadium alloy also is losing weight at 2400 mg per dm^2, while the 6.6 and 8.9 vanadium and the 9.4 a/o titanium alloys possess weight gains in the range of 120 to 125 mg per dm^2. The latter were about double those observed for replicate specimens after 196 days' exposure to 680 F water.

High-Purity Niobium-Base Alloys. Corrosion tests were conducted on high-purity niobium-base alloys taken from two sizes of arc melts: (1) consumable-electrode melts weighing several pounds and (2) rocking-hearth arc melts weighing 50 g. The former were used for extensive mechanical-property evaluation, while the latter were used as screening alloys in the search for improved properties.

Consumable-Electrode Arc Melts. The quantity of material available from the consumable-electrode melts was sufficient to conduct corrosion studies at all three test temperatures. The results after exposures of up to 280 days are summarized in Table 9. It is apparent from comparing the data in Tables 8 and 9 that the high-purity unalloyed niobium exhibits a much longer corrosion life than does the commercial-purity stock. However, in the initial stages of corrosion there is little difference between the two as illustrated in Figure 2.

TABLE 8. SUMMARY OF CORROSION RESULTS FOR COMMERCIAL-PURITY NIOBIUM-BASE ALLOYS EXPOSED TO WATER AND STEAM

Alloy	Alloy Content (Balance Niobium), a/o	Thermal-Neutron-Absorption Cross Section, barns per atom	600 F Water		680 F Water		750 F Steam	
			Exposure Time, days	Total Weight Change, mg per dm^2	Exposure Time, days[a]	Total Weight Change, mg per dm^2	Exposure Time, days	Total Weight Change, mg per dm^2
--	100 Nb	1.15	196	-1860	42	Disintegrated	28[a]	Disintegrated
138	10.5 Zr	1.05	--	--	196	67	210	-3,970
139	26.1 Zr	0.90	--	--	196	7	--	--
140	35.7 Zr	0.81	--	--	196	66	--	--
141	45.7 Zr	0.71	--	--	196	55	--	--
163	1.1 W	1.3	--	--	196	-260	210	-6,420
164	4.7 W	2.0	--	--	196	-2,930	--	--
165	9.6 W	2.8	--	--	7	Cracked	--	--
152	2.45 Mo	1.18	--	--	196	-710	98[a]	Disintegrated
153	5.2 Mo	1.21	--	--	196	-130	210	-18,450
154	7.4 Mo	1.26	--	--	196	62	--	--
150	4.4 V	1.30	--	--	196	42	210	-2,400
147	6.6 V	1.38	--	--	196	73	210	127
148	8.9 V	1.48	--	--	196	59	210	118
149	10.7 V	1.54	--	--	196	78	--	--
158	13.7 V	1.65	--	--	196	50	--	--
151	24.2 V	2.06	--	--	196	0	--	--
169	4.9 Fe	1.22	--	--	196	10	98[a]	Disintegrated
142	9.4 Ti	1.58	--	--	196	65	210	119
143	18.8 Ti	2.02	--	--	196	48	--	--
144	24.3 Ti	2.26	--	--	196	52	--	--
145	30.5 Ti	2.58	--	--	196	40	--	--
146	33.8 Ti	2.72	--	--	196	33	--	--
175	12.0 Ti-0.5 Cr	1.72	--	--	196	66	--	--
176	20.2 Ti-2.1 Cr	2.12	--	--	196	39	--	--
177	28.2 Ti-6.1 Cr	2.56	--	--	196	20	--	--
172	12 Ti-4.2 Mo	1.78	--	--	196	64	--	--
173	17.4 Ti-6.2 Mo	2.06	--	--	196	54	--	--
174	23.1 Ti-7.8 Mo	2.35	--	--	196	45	--	--
178	10.4 Ti-5.0 V	1.57	--	--	196	56	--	--
179	16.1 Ti-8.4 V	1.80	--	--	196	40	--	--
180	22.6 Ti-11.0 V	2.05	--	--	196	48	--	--
--	Zircaloy-2	0.19	200	22[b]	200	66[b]	200	243[b]

(a) Specimens off test.

(b) Reference (5).

TABLE 9. SUMMARY OF CORROSION RESULTS FOR CONSUMABLE-ELECTRODE-MELTED HIGH-PURITY NIOBIUM-BASE ALLOYS EXPOSED TO WATER AND STEAM

Alloy Addition (Balance Niobium) a/o	Thermal-Neutron-Absorption Cross Section, barns per atom	600 F Water		680 F Water		750 F Steam	
		Exposure Time, days	Total Weight Change, mg per dm^2	Exposure Time, days	Total Weight Change, mg per dm^2	Exposure Time, days	Total Weight Change, mg per dm^2
100 Nb[b]	1.15	280	76	280	-722	224[a]	-5400
7.2 Mo	1.25	280	73	224[a]	Cracked	70[a]	Cracked
12.6 V	1.61	280	40	280	72	280	76
46.8 Zr-5.1 Ti	0.92	280	24	280	103	280	254
11.2 Ti-3.2 Mo	1.72	280	36	280	66	280	36[c]
18.8 Ti-8.7 Mo	2.15	280	22	280	66	280	53[c]
11.4 V-5.7 Zr	1.50	196	6	196	43	196	-237
9.4 V-9.9 Zr	1.39	196	14[c]	196	23[c]	196	-682
9.6 Ti-3.3 Cr	1.75	196	-4	196	50	196	-553
Zircaloy-2	0.19	200	22[d]	200	66[d]	200	243[d]

(a) Specimens off test.
(b) Portion of as-received electron-beam-melted ingot.
(c) Specimens are losing weight.
(d) Reference (5).

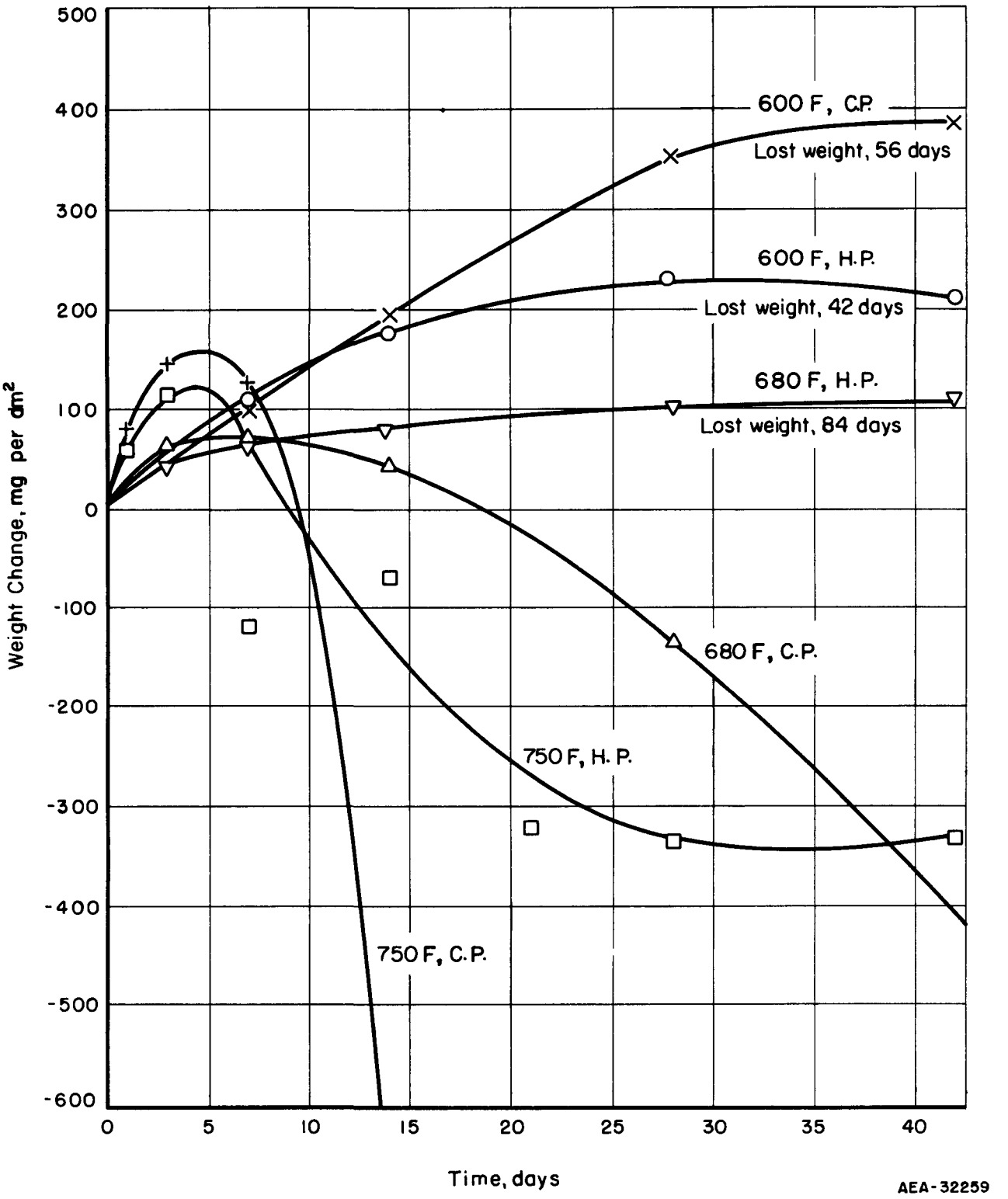

FIGURE 2. WEIGHT CHANGES FOR COMMERCIAL PURITY (C.P.) AND HIGH-PURITY (H.P.) NIOBIUM IN 600 AND 680 F WATER AND IN 750 F STEAM

Weight-change data for the consumable-electrode-melted alloys were quite consistent. Smooth curves could be drawn through the cumulative weight-change data. With one or two exceptions, all alloys gained weight. Typical weight change-time curves for the alloys are presented in Figures 3, 4, and 5. It is obvious from the plots that unalloyed niobium is not so resistant to high-temperature water as several of its alloys. The corrosion curve for Zircaloy-2 also is included in these plots for comparison purposes. Several of the alloys, notably 12.6 a/o vanadium, 11.2 a/o titanium-3.2 a/o molybdenum, and 18.8 a/o titanium-8.7 a/o molybdenum, exhibit weight changes which are comparable with those for Zircaloy-2.

The corrosion reaction kinetics can be expressed by the equation:

$$W = Kt^n \quad , \tag{1}$$

where

W = total weight gain, mg per dm^2

K = 1-day intercept of a log-log plot of weight gain versus time (also in mg per dm^2)

t = exposure time, days

n = slope of the resulting straight line on the log-log plot.

The values obtained for K and n for all of the consumable-electrode-melted alloys are presented in Table 10. The value of n for most of the alloys approached 0.5 indicating that the corrosion rate appeared to follow the parabolic rate law. The 12.6 a/o vanadium alloy appeared to be the most corrosion resistant of the group studied. It has exhibited relatively low values for K and n and still possesses an adherent film after 280 days' exposure at all three test temperatures. The 46.8 a/o zirconium-5.1 a/o titanium alloy and the 18.8 a/o titanium-8.7 a/o molybdenum alloy also appears to possess good corrosion resistance.

Rocking-Hearth Arc Melts. The screening alloys prepared in the rocking-hearth arc furnace were tested in 680 F water only. Included in the study were binary alloys containing cerium, chromium, iron, nickel, palladium, titanium, yttrium, or zirconium and ternary alloys containing vanadium or zirconium plus one of the following: aluminum, chromium, iron, molybdenum, nickel, titanium, vanadium, or zirconium. Total weight changes obtained after exposure times ranging from 56 to 224 days are presented in Table 11. The values of K and n describing the reaction-rate kinetics for these alloys [see Equation (1)] are summarized in Table 12.

At the exposure times indicated in Table 11 all alloy specimens were gaining weight at a uniform rate except the following:

Unalloyed niobium	1 a/o cerium
1 to 10 a/o zirconium	1 to 5 a/o yttrium
3.2 a/o titanium	2.5 a/o vanadium-2.5 a/o nickel or zirconium
<0.02 to 0.5 a/o chromium	10 a/o zirconium-5 a/o molybdenum
<0.08 to 10 a/o iron	

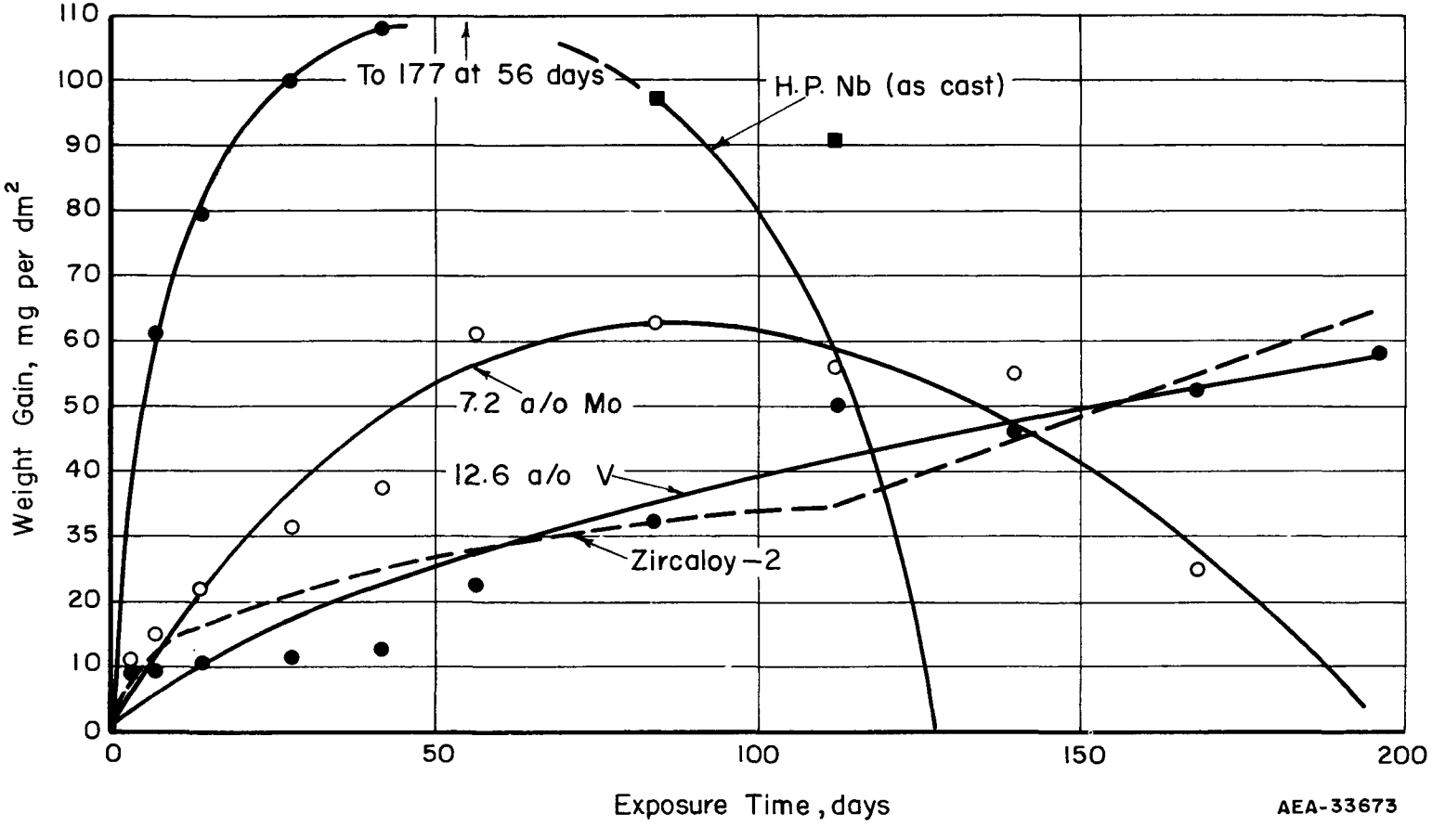

FIGURE 3. CORROSION RESULTS FOR HIGH-PURITY AND COMMERCIAL-PURITY NIOBIUM-BASE ALLOYS EXPOSED TO 680 F WATER

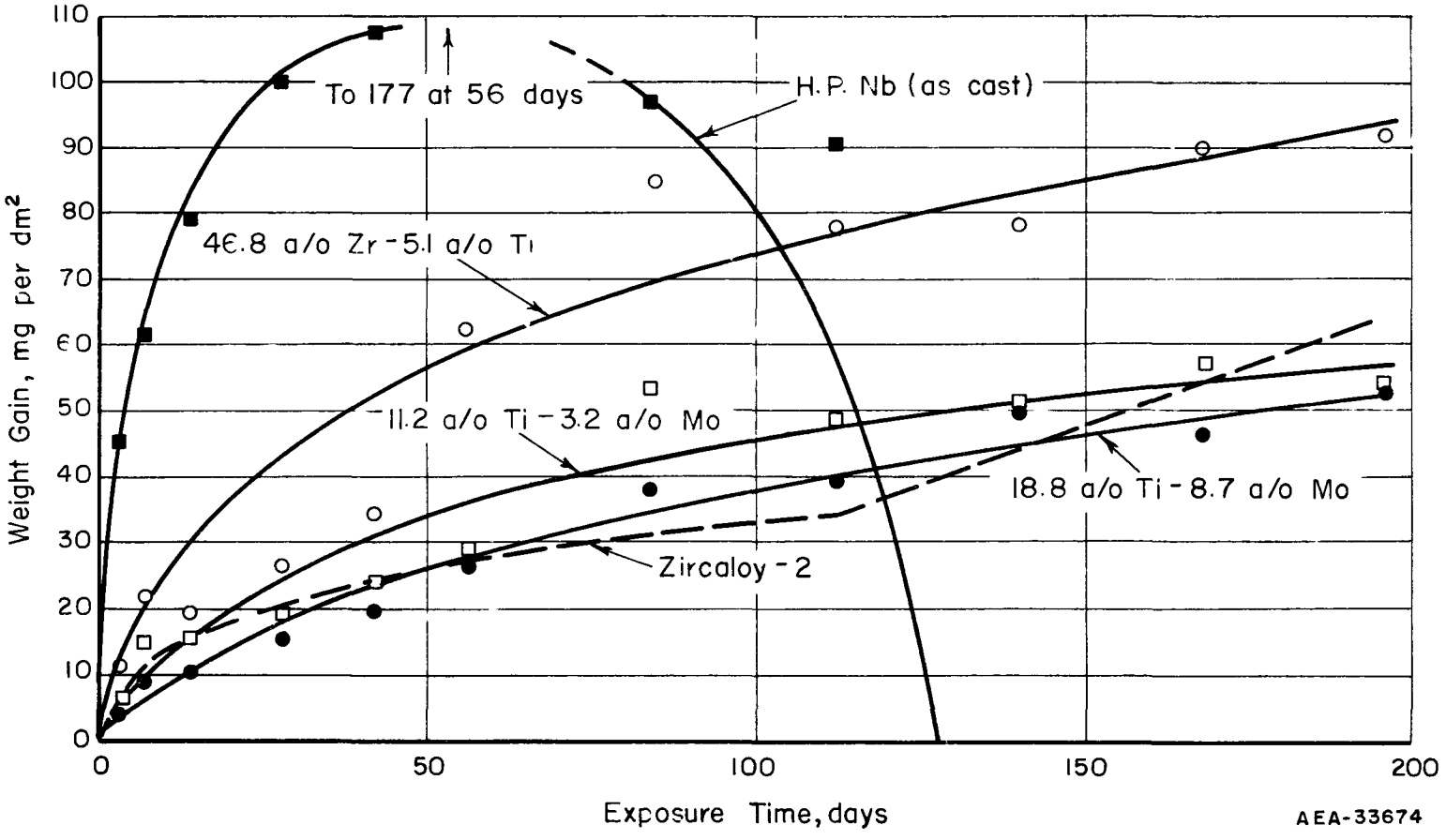

FIGURE 4. CORROSION RESULTS FOR HIGH-PURITY NIOBIUM-BASE ALLOYS EXPOSED TO 680 F WATER

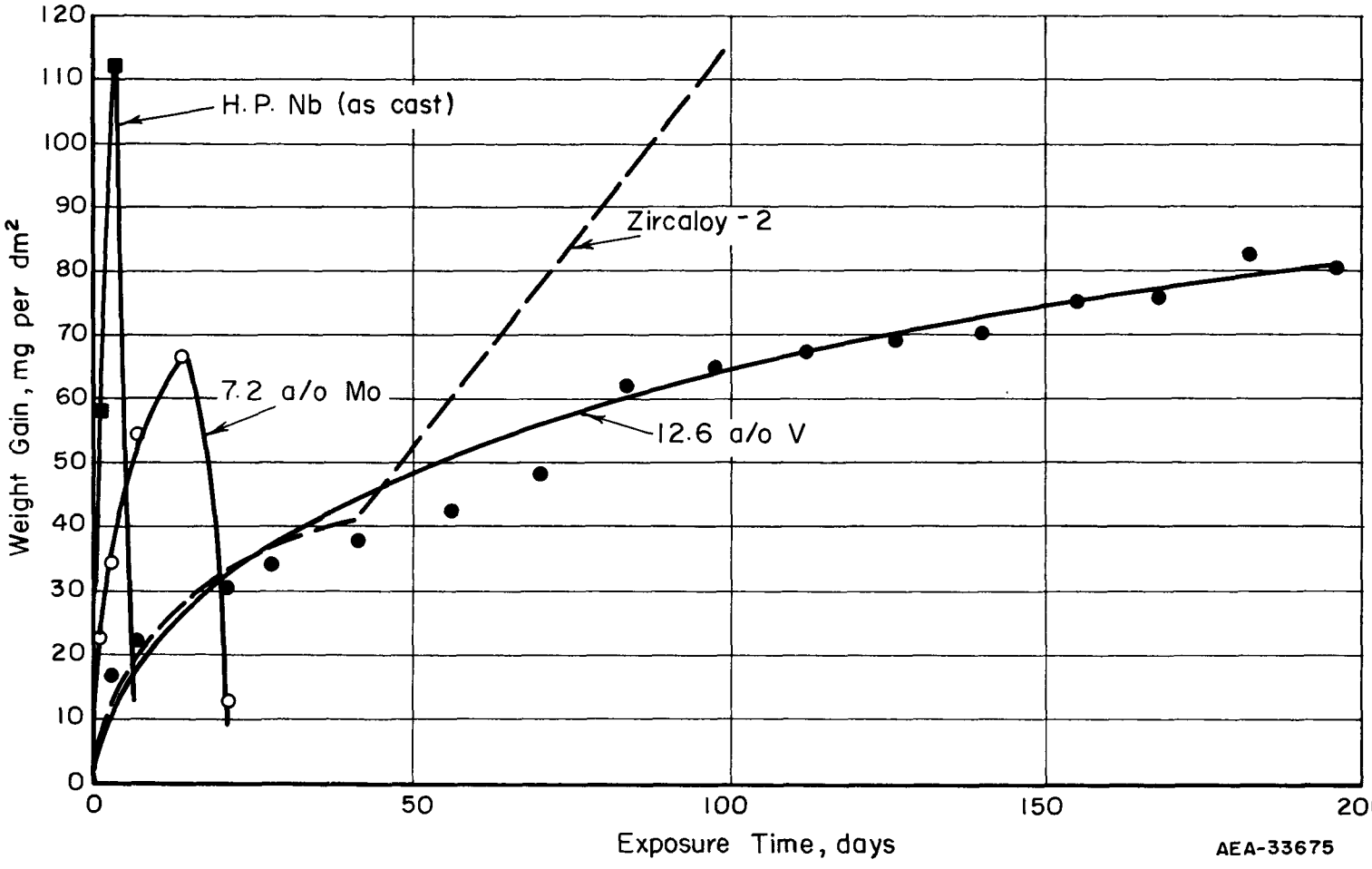

FIGURE 5. CORROSION RESULTS FOR HIGH-PURITY NIOBIUM-BASE ALLOYS EXPOSED TO 750 F, 1500-PSI STEAM

TABLE 10. RATE CONSTANTS FOR THE CORROSION OF CONSUMABLE-ELECTRODE-MELTED HIGH-PURITY NIOBIUM-BASE ALLOYS IN HIGH-TEMPERATURE WATER AND STEAM

Alloy Addition (Balance Niobium), a/o	600 F Water			680 F Water			750 F, 1500-PSI Steam		
	Exposure Time, days	K[a], mg per dm^2, 1 Day	n, Dimensionless	Exposure Time, days	K[a], mg per dm^2, 1 Day	n, Dimensionless	Exposure Time, days	K[a], mg per dm^2, 1 Day	n, Dimensionless
100 Nb	28[b]	3.0	0.62	42[b]	3.1	0.34	3[b]	58	0.60
12.6 V	280	1.6	0.58	280	2.5	0.63	280	12	0.36
7.2 Mo	280	1.0	0.79	112[b]	6.6	0.44	14[b]	22	0.46
46.8 Zr-5.06 Ti	280	1.3	0.57	280	6.5	0.50	266	13	0.56
11.2 Ti-3.2 Mo	280	2.5	0.54	280	3.4	0.55	154[b]	10	0.43
18.8 Ti-8.7 Mo	280	2.0	0.47	280	2.2	0.60	196[b]	7.6	0.40
11.4 V-5.7 Zr	84[b]	2.5	0.40	196	13	0.22	28[b]	20	0.11
9.4 V-9.9 Zr	84[b]	4.1	0.41	140[b]	21	0.06	21[b]	25	0.13
9.6 Ti-3.3 Cr	84[b]	1.7	0.60	196	11	0.26	21[b]	15	0.09

(a) From the equation $W = Kt^n$, where t = time, days.

(b) Specimen began to lose weight after exposure time indicated.

TABLE 11. SUMMARY OF CORROSION RESULTS OF ROCKING-HEARTH-MELTED HIGH-PURITY NIOBIUM-BASE ALLOYS EXPOSED TO 680 F WATER

Alloy	Alloy Content (Balance Niobium), a/o	Thermal-Neutron-Absorption Cross Section, barns per atom	Exposure Time, days	Total Weight Change, mg per dm^2
N1	100 Nb	1.15	224	-531
N40	100 Nb	1.15	224	-615
N44	100 Nb	1.15	84[a]	Disintegrated
N56	100 Nb	1.15	196	-39
N2	1.1 Zr	1.14	140	-20,400 (disintegrated 168 days)
N3	2.2 Zr	1.13	196	-1,780
N4	5 Zr[c]	1.10	196	-1,450
N5	10.2 Zr	1.05	196	-3
N6	40 Zr[c]	0.76	196	78
N8	65 Zr[c]	0.52	196	-112 (edge cracking)
N9	75 Zr[c]	0.42	196	128
N10	90 Zr[c]	0.27	196	142
N11	3.2 Ti	1.30	224	-1,030
N12	10.5 Ti	1.60	224	76
N13	25.0 Ti[c]	2.30	224	48
N14	<0.02 Cr	1.15	224	-387
N15	0.5 Cr	1.16	224	-135
N48	0.5 Cr	1.16	196	-495
N45	<0.08 Fe	1.15	196	-182
N46	0.3 Fe	1.16	112	-1,180
N47	10 Fe[c]	1.28	28[a]	-2,000 (cracked)
N21	10.9 Zr-5.1 Ti	1.24	224	60
N22	25 Zr-5 Ti[c]	1.10	224	-22 (edge cracking)
N23	25 Zr-15 Ti[c]	1.56	224	47
N24	25 Zr-25 Ti[c]	2.04	224	47
N25	35 Zr-5 Ti[c]	1.00	224	71
N26	35 Zr-15 Ti[c]	1.50	224	59
N28	45 Zr-5 Ti[c]	0.92	224	71
N29	10 Zr-5 Mo[c]	1.13	224	17[b]
N30	35 Zr-5 Mo[c]	0.88	224	53
N31	45 Zr-5 Mo[c]	0.78	224	70
N32	35 Zr-5 Al[c]	0.76	196	62
N34	45 Zr-5 Al[c]	0.67	196	60
N35	10 Zr-5 Cr[c]	1.14	196	48
N37	45 Cr-5 Cr[c]	0.93	196	48
N38	10 Zr-5 Fe[c]	1.12	196	44
N16	1.6 V	1.18	224	111

TABLE 11. (Continued)

Alloy	Alloy Content (Balance Niobium), a/o	Thermal-Neutron-Absorption Cross Section, barns per atom	Exposure Time, days	Total Weight Change, mg per dm^2
N49	2 V-2.5 Ti	1.34	196	88
N50	2 V-2.3 Mo	1.29	196	114
N51	2.2 V-0.54 Fe	1.24	196	79
N53	1.8 V-<0.02 Cr	1.19	196	58
N54	1.8 V-0.14 Al	1.19	196	88
N55	2.5 V-2.5 Zr(c)	1.22	112	-243
N52	2.2 V-0.87 Ni	1.24	28(a)	-100
N17	2.3 Zr-4 V	1.26	196	60
N18	25 Zr-5 V(c)	1.10	196	-284 (edge cracking)
N19	35 Zr-5 V(c)	1.00	196	-352 (pitted)
N20	45 Zr-5 V(c)	0.90	196	60
N57	1 Ce(c)	1.13	56	-1,180(a)
N59	1 Y(c)	1.15	56	-1,020
N60	5 Y(c)	1.16	56	-6,420(a)
N61	1 Ni(c)	1.18	28	4(b)
N62	2.5 Ni(c)	1.23	7(a)	Cracked
N63	5 Ni(c)	1.32	7(a)	Disintegrated
N64	1 Pd(c)	1.21	28(a)	-834 (split in two)
N70	5 V-2.5 Al(c)	1.32	56	58
N68	5 V-2.5 Cr(c)	1.39	56	60
N65	5 V-2.5 Ti(c)	1.49	56	51
--	Zircaloy-2	0.19	200	66(d)

(a) Specimens off test.
(b) Specimens losing weight.
(c) Nominal composition.
(d) Reference (5).

TABLE 12. RATE CONSTANTS FOR THE CORROSION OF ROCKING-HEARTH ARC-MELTED HIGH-PURITY NIOBIUM-BASE ALLOYS EXPOSED TO 680 F WATER

Alloy	Alloy Content (Balance Niobium), a/o	Exposure Time, days	K[a], mg per dm^2, 1 Day	n, Dimensionless
N1	100 Nb	112[c]	54	0.21
N40	100 Nb	112[c]	42	0.30
N56	100 Nb	112[c]	39	0.18[b]
N44	100 Nb	3[c]	--	--
N2	1.1 Zr	3[c]	--	--
N3	2.2 Zr	3[c]	--	--
N4	5 Zr[d]	28[c]	19	0.43
N5	10.2 Zr	56[c]	5.5	0.38[b]
N6	40 Zr[d]	196	6.0	0.49
N8	65 Zr[d]	112[c]	7.5	0.53
N9	75 Zr[d]	196	17	0.39
N10	90 Zr[d]	196	6.4	0.59
N11	3.2 Ti	42[c]	37	0.11
N12	10.5 Ti	224	9.0	0.40
N13	25 Ti[d]	224	8.0	0.33
N14	<0.02 Cr	42[c]	37	0.30
N15	0.5 Cr	14[c]	27	0.32
N48	0.5 Cr	14[c]	28	0.23
N45	<0.08 Fe	28[c]	36	0.24
N46	0.3 Fe	3[c]	--	--
N47	10 Fe[d]	3[c]	--	--
N21	10.9 Zr-5.1 Ti	196	9.5	0.36
N22	25 Zr-5 Ti[d]	84[c]	21	0.23[b]
N23	25 Zr-15 Ti[d]	196	12	0.32[b]
N24	25 Zr-25 Ti[d]	196	5.0	0.42
N25	35 Zr-5 Ti[d]	196	7.3	0.42
N26	35 Zr-15 Ti[d]	196	5.5	0.46
N28	45 Zr-5 Ti[d]	196	4.4	0.49
N29	10 Zr-5 Mo[d]	112[c]	3.9	0.44
N30	35 Zr-5 Mo[d]	196	12	0.30
N31	45 Zr-5 Mo[d]	196	5.2	0.50
N32	35 Zr-5 Al[d]	196	15	0.26
N34	45 Zr-5 Al[d]	196	4.5	0.53
N35	10 Zr-5 Cr[d]	196	7.5	0.41
N37	45 Zr-5 Cr	196	5.6	0.42
N38	10 Zr-5 Fe[d]	196	8.0	0.33
N16	1.6 V	224	20	0.30[b]

TABLE 12. (Continued)

Alloy	Alloy Content (Balance Niobium), a/o	Exposure Time, days	K[a], mg per dm^2, 1 Day	n, Dimensionless
N49	2 V-2.5 Ti	196	10.0	0.42
N50	2 V-2.3 Mo	196	7.2	0.52
N51	2.2 V-0.54 Fe	196	19	0.29
N53	1.8 V-<0.02 Cr	196	11	0.34[b]
N54	1.8 V-0.14 Al	196	20	0.28
N55	2.5 V-2.5 Zr[d]	7[c]	--	--
N52	2.2 V-0.87 Ni	3[c]	--	--
N17	2.3 Zr-4 V	196	2.8	0.55
N18	25 Zr-5 V[d]	28[c]	18	0.35
N19	35 Zr-5 V[d]	84[c]	14	0.38
N20	45 Zr-5 V[d]	112	3.0	0.52[b]
N57	1 Ce[d]	14[c]	--	--
N59	1 Y[d]	3[c]	--	--
N60	5 Y[d]	3[c]	--	--
N61	1 Ni[d]	3[c]	--	--
N62	2.5 Ni[d]	3[c]	--	--
N63	5 Ni[d]	3[c]	--	--
N64	1 Pd[d]	28[c]	170	0.85
N70	5 V-2.5 Al[d]	56	6.5	0.53[b]
N68	5 V-2.5 Cr[d]	56	7.0	0.53[b]
N65	5 V-2.5 Ti[d]	56	7.5	0.47

(a) From the equation $W = Kt^n$, where t = time, days.

(b) Slope obtained from erratic data.

(c) Specimen began to lose weight after exposure time indicated.

(d) Nominal composition.

A binary 65 a/o zirconium alloy and ternary alloys containing 25 a/o zirconium plus 5 a/o titanium or 5 a/o vanadium also were losing weight, apparently at edge cracks. The cracks probably were present after fabrication and were not entirely removed during sample preparation. Pitting was observed on a 35 a/o zirconium-5 a/o vanadium alloy.

One set of the arc-melted, unalloyed control samples (N44 in Table 10) processed with these alloys began to flake and lose weight rapidly after 7 days' exposure in much the same fashion as the unalloyed commercial-purity niobium specimen. One of the specimens was completely oxidized after 84 days' exposure. The other three sets of unalloyed control samples (N1, N40, and N56 in Table 11) showed lower weight gains after 84 days' exposure. The variance among these data suggests that the interstitial content of niobium may have a profound effect on its water corrosion resistance. It would appear, for example, from the weight-gain data that the interstitial content of the N44 material had been raised to the level of that for commercial-purity niobium as a result of contamination during melting and fabrication. Hardness measurements (see Table 3) on each of the unalloyed high-purity samples indicated that only minor differences existed in the total interstitial content of all four of these control samples. The wide variance in corrosion rates suggests, therefore, that one or more of the contaminants has a greater detrimental effect on the corrosion resistance of niobium than the others.

While the high-purity unalloyed niobium exhibits longer corrosion life than does commercial-purity material, there appears to be little effect of purity of the base metal on the corrosion behavior of niobium alloys. Comparison of the results obtained in 680 F water for alloys of similar composition prepared from the two melting stocks reveals no significant difference in weight change (see Tables 8, 9, and 11).

Selective Attack

Visual examination revealed that several of the niobium alloys failed prematurely from cracking or other forms of selective attack during corrosion. The microstructure of two of the specimens was examined to gain an insight into the mode of failure. These specimens were commercial-purity unalloyed niobium and a 7.2 a/o molybdenum alloy. Corrosion results for these alloys were presented in Tables 8 and 9, respectively.

The appearance of the microstructures of these specimens is shown in Figure 6. The unalloyed niobium had been exposed 28 days to 680 F water. A companion specimen in the same test was completely oxidized after 42 days' exposure. Laminar-type attack is evident from the oxide pattern in the structure of the unalloyed niobium. Attack apparently occurred either at grain boundaries, which were elongated during rolling, or more probably at cold shuts introduced during cold reduction. The complete oxidation of the companion specimen probably occurred when the selective attack progressed to such an extent that the specimen was reduced to small metal particles. The particles, in turn, were completely oxidized because of their large surface-to-volume ratio.

The 7.2 a/o molybdenum alloy cracked after 70 days' exposure to 750 F steam. A duplicate specimen cracked after 224 days' exposure to 680 F water. The cracking was found to be transgranular in nature. The reasons for the cracking are not yet apparent.

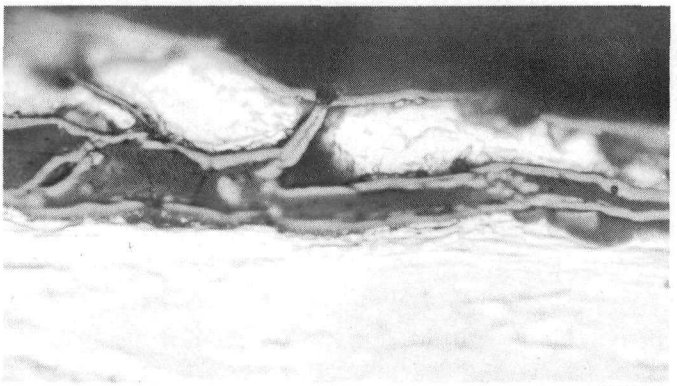

1000X N57992

a. Unalloyed Commercial-Purity Niobium Exposed
28 Days to 680 F Water

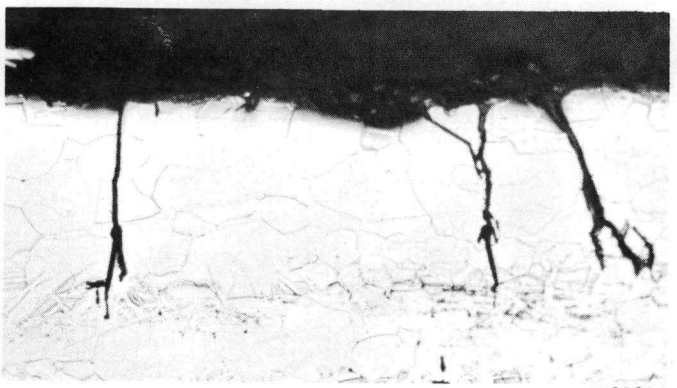

100X N62684

b. Niobium-7.2 a/o Molybdenum Exposed
70 Days to 750 F Steam

FIGURE 6. SELECTIVE ATTACK IN NIOBIUM SAMPLES EXPOSED TO HIGH-TEMPERATURE WATER AND STEAM

Note lamellar separation in unalloyed niobium and transgranular cracking in alloy.

Oxygen Contamination

Samples of each commercial-purity niobium-base alloy were withdrawn for metallographic evaluation after 42- and 196-day exposures to 680 F water and their oxide-scale thicknesses were measured where these could be retained in polishing. For selected alloys, Knoop-hardness traverses were obtained and used to calculate the depth of contamination hardening. On the assumption that this hardening was due entirely to oxygen absorbed from the water-corrosion reaction, the contamination coefficients for oxygen in the alloys were calculated*. In alloys where no reaction occurs with the diffusing oxygen, i. e., in unalloyed niobium and in alloys with molybdenum, tungsten, and vanadium, the contamination rates equal the oxygen-diffusion rates. Table 13 summarizes the results obtained.

The oxide scales on the corroded alloys were generally found to increase in thickness and porosity with increasing corrosion rates. The range of scale thicknesses ranged from less than 0. 1 mil for the most corrosion-resistant alloys (niobium-45. 7 a/o zirconium and niobium-28. 2 a/o titanium-6. 1 a/o chromium) to about 0. 8 mil for the least corrosion-resistant alloy (niobium-4. 7 a/o tungsten) remaining on test after 196 days. It should be noted, however, that this tungsten alloy was losing weight rapidly near the end of the corrosion test period. Hence, its true scale thickness was probably much greater than 0. 8 mil.

The calculated contamination coefficient for oxygen in unalloyed niobium in 680 F water was found to be 2.7×10^{-12} cm^2 per sec. This value is in good agreement with a value of 4.5×10^{-12} cm^2 per sec obtained by extrapolation of the diffusion data of Ang[6] to this temperature. The effect of alloying additions on the contamination rate of oxygen in niobium is more clearly shown by reference to Figure 7. As shown, additions of titanium, vanadium, and zirconium reduce the contamination rate of oxygen in niobium significantly. Both titanium and zirconium reduce the rates by a factor of about 40. This corresponds to about a sixfold reduction in the depth of contamination. Vanadium, molybdenum, and tungsten additions, in that order, have increasingly less effect on reducing the depth of contamination. It is noted, however, that even the least corrosion-resistant alloys were contaminated to a depth of only about 5 mils after 196 days' exposure.

Micrographs of scale-metal interfaces on several corroded niobium alloys are shown in Figure 8. The decrease in thickness and porosity of the scale is apparent as the corrosion resistance changes from poor (niobium-4. 7 a/o tungsten) to excellent (niobium-45. 7 a/o zirconium).

Hydrogen Absorption

It is known that zirconium alloys absorb hydrogen during corrosion in high-temperature water. A similar effect might be expected with niobium since it also is an excellent getter for reactive gases. Accordingly, hydrogen analyses were obtained on unalloyed niobium and several alloys after exposures ranging up to 252 days for the three test conditions. These data are presented in Table 14.

*The techniques used for calculating diffusion coefficients of oxygen in niobium from hardness data were described in Reference (3).

TABLE 13. METALLOGRAPHIC DATA ON COMMERCIAL-PURITY NIOBIUM-BASE ALLOYS EXPOSED TO 680 F WATER

Alloy	Alloy Content (Balance Niobium), a/o	7 to 42 Days of Exposure: Exposure Time, days	Thickness of Adhering Scale, mils	Diffusion Coefficient of Oxygen[a], cm^2 per sec	Depth of Contamination Hardening[b], mils	196 Days of Exposure: Thickness of Adhering Scale, mils	Diffusion Coefficient of Oxygen[a], cm^2 per sec	Depth of Contamination Hardening[b], mils
--	100 Nb	28	0.3	2.7×10^{-12}	2.4	--	--	--
150	4.4 V	42	(c)	--	--	--	5×10^{-13}	2.8
147	6.6 V	42	(c)	--	--	0.2	--	--
149	10.7 V	42	0.1	--	--	--	2×10^{-13}	1.6
158	13.7 V	42	(c)	1.3×10^{-12}	3.2	--	1×10^{-12}	~4
151	24.2 V	42	(c)	--	--	0.2	1.1×10^{-12}	<4
154	7.4 Mo	42	(c)	1.3×10^{-12}	2.4	0.5	1.6×10^{-12}	<4
163	1.1 W	42	0.15	--	--	--	--	--
164	4.7 W	42	0.1-0.2	--	--	0.8	--	--
165	9.6 W	7	0.6	2×10^{-12}	1.6	--	--	--
169	4.9 Fe	42	0.1	--	--	--	--	--
138	10.5 Zr	42	0.02	--	--	0.2	7×10^{-14}	1.6
139	26.1 Zr	42	(c)	--	--	--	3×10^{-14}	0.8
140	35.7 Zr	42	0.1	--	--	--	--	--
141	45.7 Zr	42	0.02-0.03	6.1×10^{-13}	0.8	0.05	7×10^{-14}	1.2
142	9.4 Ti	42	0.1-0.3	--	--	0.2	7×10^{-14}	1.6
144	24.3 Ti	42	(c)	$<5 \times 10^{-13}$	<0.4	--	5×10^{-14}	0.8
146	33.8 Ti	42	0.05	--	--	0.1	--	--
177	28.2 Ti-6.1 Cr	42	(c)	$<5 \times 10^{-13}$	<0.4	0.07	5×10^{-14}	1.2
172	12 Ti-4.2 Mo	42	(c)	$<5 \times 10^{-13}$	<0.4	--	--	--
174	23.1 Ti-7.8 Mo	42	(c)	--	--	0.13	5×10^{-14}	0.8
180	22.6 Ti-11 V	42	(c)	--	--	0.1	--	--

(a) Calculated from hardness-traverse data.

(b) Distance from surface where hardness returns to within 10 KHN of base hardness.

(c) Scale thickness not estimated due to poor preservation of sample edges.

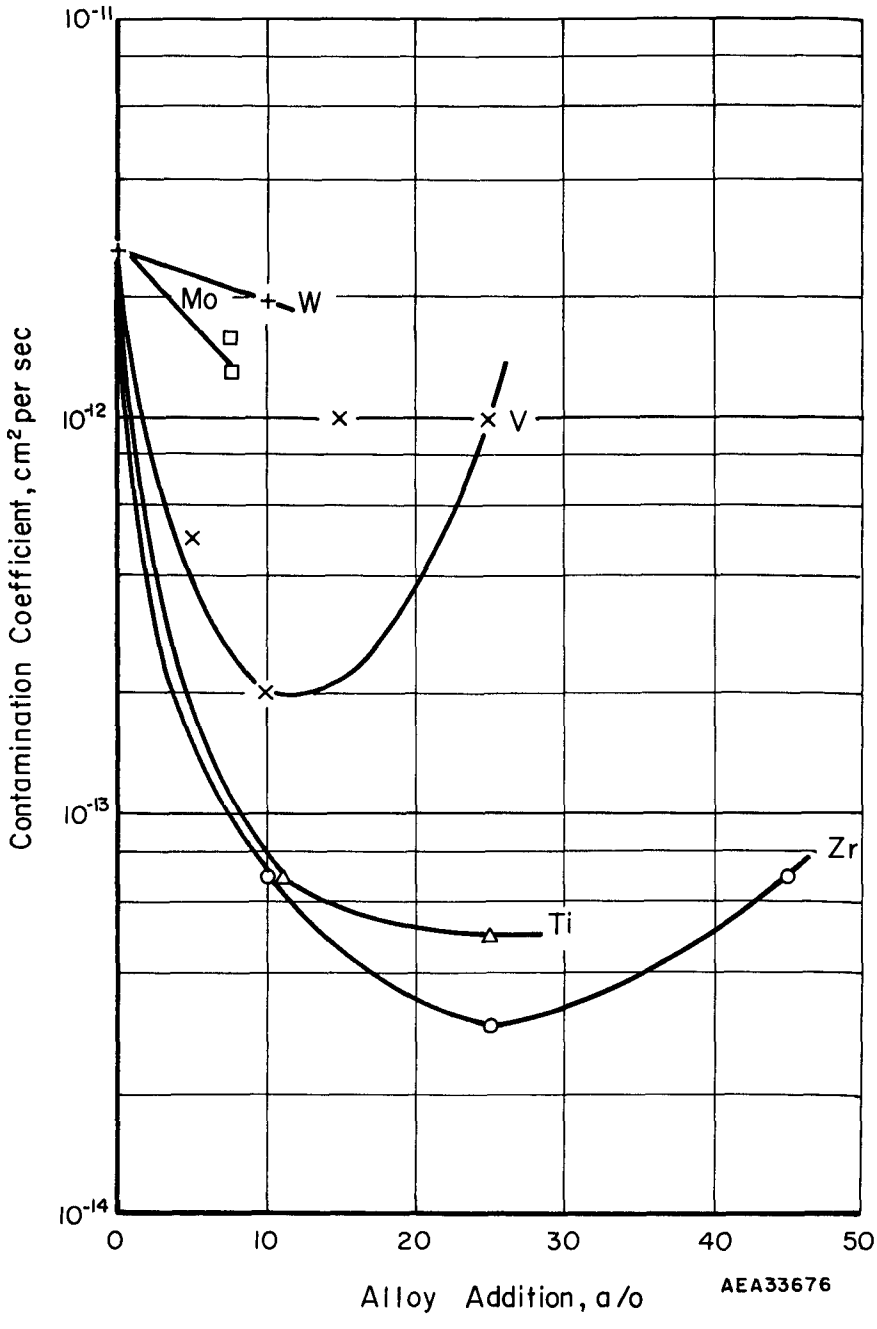

FIGURE 7. EFFECTS OF ALLOYING ON THE CONTAMINATION RATE OF NIOBIUM EXPOSED TO 680 F WATER FOR 196 DAYS

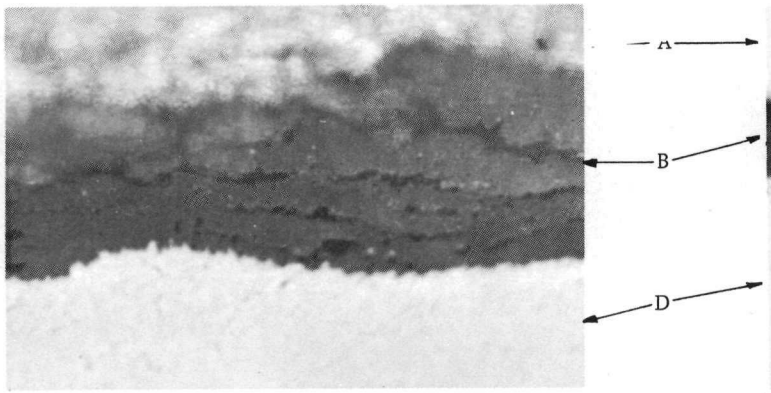

1500X N61536

a. Niobium-4.7 a/o Tungsten

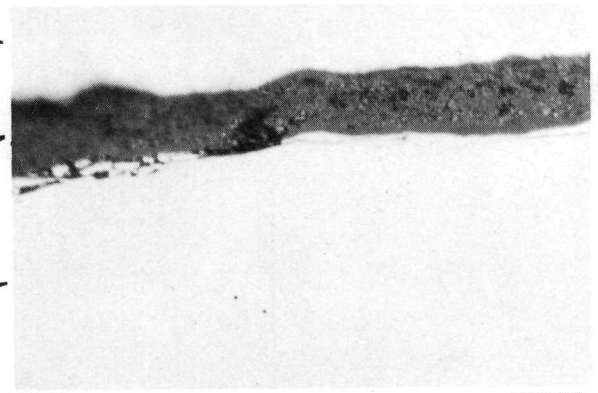

1500X N61539

b. Niobium-10.5 a/o Zirconium

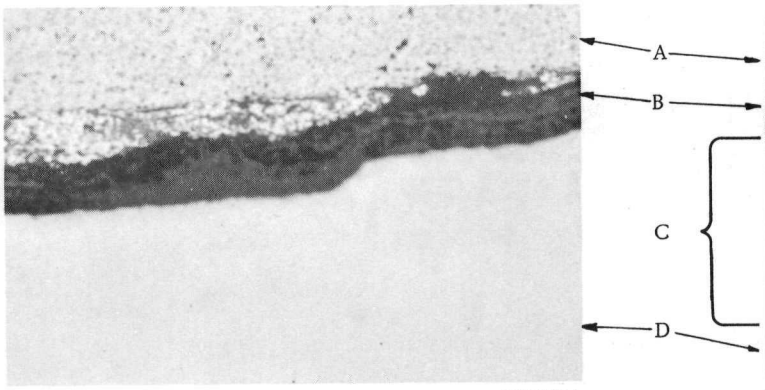

1500X N61534

c. Niobium-6.6 a/o Vanadium

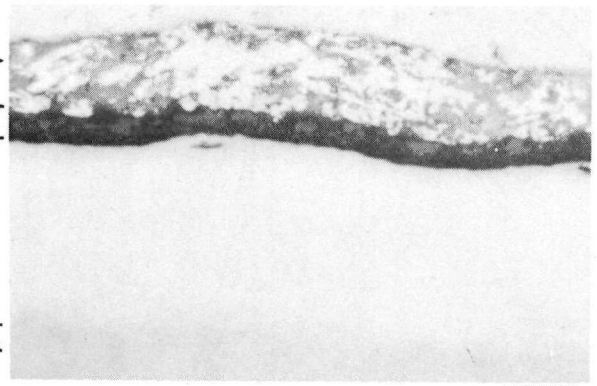

1500X N61538

d. Niobium-33.8 a/o Titanium

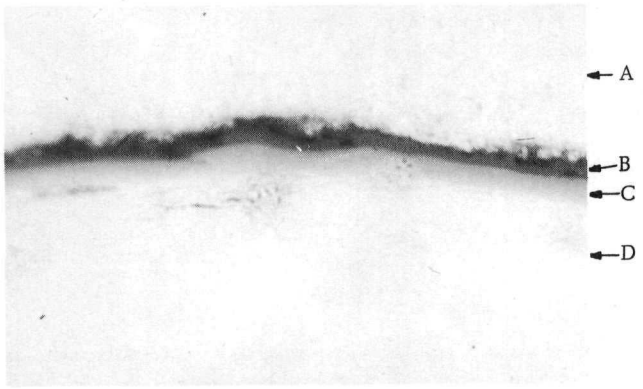

1500X N61540

e. Niobium-45.7 a/o Zirconium

FIGURE 8. MICROSTRUCTURES OF CORRODED NIOBIUM ALLOYS

All alloys were exposed 196 days to 680 F water.
A is backup material; B is scale; C is subscale;
D is unaffected base.

TABLE 14. HYDROGEN ANALYSES OF ALLOYS AFTER VARIOUS EXPOSURES TO HOT WATER AND STEAM

Alloy	Alloy Content (Balance Niobium), a/o	Type of Niobium Base[a]	Corrosion-Test Conditions: Temperature, F	Corrosion-Test Conditions: Time, days	Weight Change During Water Exposure, mg per dm^2	Hydrogen Content: Before Corrosion, ppm	Hydrogen Content: After Corrosion: PPM	Hydrogen Content: After Corrosion: Mg per Dm^2
--	100 Nb	C. P.	600	252	-3740	<2	224	4.4
		C. P.	680	28	-5210	<2	590	5.9
--	100 Nb[b]	H. P.	600	252	64[c]	3	11	1.2
		H. P.	680	224	-982	3	62	6.8
		H. P	750	168	-5280	3	211	21.5
		H. P.	750	224	-5400	3	225	23.2
N44	100 Nb	H. P.	680	84	-2030	--	944	29.7
150	4.4 V	C. P.	680	196	42	--	5	0.18
147	6.6 V	C. P.	680	196	73	--	18	0.67
148	8.9 V	C. P.	680	196	59	--	6	0.24
149	10.7 V	C. P.	680	196	78	--	30	1.1
NL-2	12.6 V	H. P.	600	252	45	7	5	0.22
		H. P.	680	224	61	7	31	1.3
		H. P.	750	224	84	7	44	1.9
158	13.7 V	C. P.	680	196	50	--	8	0.37
151	24.2 V	C. P.	680	196	0	--	5	0.18
138	10.5 Zr	C. P.	680	196	67	--	18	0.48
141	45.7 Zr	C. P.	680	42	16	35	61	2.2
163	1.1 W	C. P.	680	196	-260	--	34	1.4
164	4.7 W	C. P.	680	196	-2930	--	140	5.5
NL-3	7.2 Mo	H. P.	680	224	-96	19	422	8.5
154	7.4 Mo	C. P.	680	196	62	--	38	1.5
169	4.9 Fe	C. P.	750	84	-283	--	388	13.5
N47	10 Fe	H. P.	680	28	-760	--	511	13.5
142	9.4 Ti	C. P.	680	196	65	--	24	0.86
177	28.2 Ti-6.1 Cr	C. P.	680	42	10	--	33	1.4
			680	196	20	--	29	1.2
N52	2.2 V-0.87 Ni	H. P	680	56	-738	--	1660	32.1

(a) C P designates commercial-purity niobium base, H. P. designates high-purity niobium base.

(b) Tested in as-received electron-beam-melted condition.

(c) Losing weight, maximum gain was 24.8 mg per dm^2 at 28 days.

Analyses of the unalloyed niobium revealed hydrogen contents ranging from 11 to 944 ppm. In general, hydrogen content increased with increasing corrosion attack, thus indicating that the source of the hydrogen was the corrosion reaction. On this assumption, the hydrogen contents were recalculated on the basis of amount absorbed per unit of surface area. The resulting values ranged between 1.2 and 29.7 mg per dm^2 and again indicated that hydrogen absorption increased with increasing corrosion.

In some instances, hydrogen analyses were not obtained prior to corrosion testing because sample materials were limited. The maximum content found in any specimen before corrosion was 35 ppm. Since all specimens were vacuum annealed prior to corrosion testing, it appears probable that none of the alloys contained more than 35 ppm hydrogen. Thus it is apparent from Table 14 that hydrogen absorption in the vanadium alloys was quite low. Hydrogen pickup in the zirconium and titanium binaries and the 28 a/o titanium-6 a/o chromium ternary also was low, while that in the iron, molybdenum, and tungsten alloy was moderately high and that in the 2.2 a/o vanadium-0.87 a/o nickel alloy was very high. In all instances, high hydrogen absorption could be correlated with poor corrosion resistance.

Correlation of Corrosion-Test Results

For purposes of discussion, the 680 F water corrosion behavior of all of the alloys tested is summarized in Table 15 and compared with the behavior of the most-corrosion-resistant unalloyed niobium sample and with Zircaloy-2, after comparable exposure periods. Table 16 contains a similar comparison for the alloys tested in 750 F steam.

As is apparent from Table 15, the weight changes for six unalloyed niobium samples in 680 F water varied considerably. Highest corrosion rates were observed for the commercial-purity niobium which disintegrated in 42 days. While lower rates were obtained for the higher purity samples, the variance was still great. These values ranged from disintegration after 84 days, for the "worst" samples, to weight losses of 39 mg per dm^2 after 196 days for the "best" samples.

No significant effects of base-metal purity were observed on the corrosion behavior of the alloys. This is apparent by comparison of the data in Table 15 for binary alloys, made with both bases, containing about 10 a/o zirconium, 10 a/o titanium, 13 a/o vanadium, and 7 a/o molybdenum, as well as for several ternary titanium-molybdenum alloys.

Of the binary-alloy additions studied, titanium, vanadium, and zirconium were outstanding in improving the corrosion resistance of niobium. The most effective concentration range for zirconium appears to extend from about 10.5 through 45.7 a/o. For titanium and vanadium, the corrosion resistance continues to improve with titanium additions over the range of 9.4 through 33.8 a/o and with vanadium additions of 4.4 through 24.2 a/o.

In 680 F water, most of the binary titanium, vanadium, and zirconium alloys, within the above-defined ranges, show weight changes which are comparable with or lower than those for Zircaloy-2. In 750 F steam, the 9.4 a/o titanium and 6.6, 8.9, and 12.6 a/o vanadium alloys were the only binary alloys of those tested which showed improved corrosion behavior over Zircaloy-2. These data, as well as the comparative 680 F weight-change data of Table 15, indicate that titanium and vanadium are more effective in improving the corrosion resistance of niobium than zirconium.

The data of Table 15 further indicate that binary additions of cerium, chromium, iron, molybdenum, nickel, palladium, tungsten, or yttrium, over the range of 1 to 5 a/o, either have no significant beneficial effect on corrosion resistance or actually decrease it. For example, these alloys are characterized either by weight losses of similar or greater magnitude than those obtained with unalloyed niobium or by cracking or disintegration. However, the favorable results obtained with the 7.4 a/o molybdenum alloy (Alloy 154 in Table 15) indicate that some of these elements may have beneficial effects at higher concentration levels than those investigated here.

All of the ternary alloys prepared included either titanium, vanadium, or zirconium additions. As mentioned above, these elements were the most effective binary additions in improving the corrosion resistance of niobium. Consequently, it is not surprising to find that most of the ternary alloys based on these metals also show excellent corrosion resistance.

The lowest weight gains were most consistently found for those ternary alloys containing 10 a/o or more of titanium or zirconium. The effect of the other ternary additions to these alloys is not clear since the presence of either titanium or zirconium alone (in these concentrations) is apparently sufficient to give comparably low weight changes. On the other hand, ternary combinations of vanadium and zirconium appear no more effective than binary additions of either element alone, and are probably less effective than binary additions of vanadium alone. Similarly, the 750 F steam data suggest that the ternary addition of molybdenum to a 10 a/o titanium binary alloy may have a detrimental effect.

On this basis, it would appear that no significant improvements in the corrosion behavior of binary titanium, vanadium, or zirconium alloys are obtained through ternary additions of aluminum, chromium, iron, molybdenum, or nickel. However, weight-change data alone are not the only important criteria in water-corrosion resistance. The character of the corrosion film formed is also of considerable importance. Thus, it is important to recognize that, of all the niobium alloys tested in 680 F water, only the 28.2 a/o titanium-6.1 a/o chromium ternary alloy and the binary and ternary zirconium alloys containing 45 a/o zirconium showed adherent tarnish films. Those on the former were iridescent while those on the latter were of the type obtained on Zircaloy-2.

Binary titanium alloys with titanium contents in the range of this ternary-alloy composition were also fairly corrosion resistant, but did not exhibit the iridescent tarnish film. The same qualification holds for the titanium-chromium alloys of lower titanium and chromium content. It would thus appear that the combination of large amounts of titanium and chromium is necessary to obtain the iridescent film. Thus, ternary modifications of binary zirconium, titanium, or vanadium alloys may have a considerably important effect. As will be discussed shortly, these modifications can most likely be expected to occur at high alloy-concentration levels through modifications in the character of the surface oxide film.

The slight powdery character of the corrosion film which formed on the other alloys which showed low weight changes may be a foreseeable deterrent to their use as cladding materials. It is well known that stainless steels also exhibit tarnish films with a thin powdery layer during corrosion in static high-temperature water. In the presence of flowing water, at velocities up to 30 fps, the corrosion rate is increased severalfold. A more serious consequence of flow is that the stainless steel corrosion product (principally Fe_3O_4) is transported by the coolant water and can become radioactive when

TABLE 15. COMPARATIVE CORROSION RESISTANCE

Alloy	Alloy Content (Balance Niobium), a/o	Thermal-Neutron Absorption Cross Section, barns per atom	Type of Niobium Base[a]	Exposure Time, days	Weight Change, mg per dm^2
--	100 Nb	1.15	C.P.	42	Disintegrated
N44	100 Nb	1.15	H.P.	84	Disintegrated
N40	100 Nb	1.15	H.P.	196	-625
N1	100 Nb	1.15	H.P.	196	-510
TP-37	100 Nb	1.15	H.P.	196	-61
N56	100 Nb	1.15	H.P.	196	-39
N2	1.1 Zr	1.14	H.P.	140	-20,400
N3	2.2 Zr	1.13	H.P.	196	-1,780
N4	5 Zr[c]	1.10	H.P.	196	-1,450
N5	10.2 Zr	1.05	H.P.	196	-3
138	10.5 Zr	1.05	C.P.	196	67
139	26.1 Zr	0.90	C.P.	196	7
140	35.7 Zr	0.81	C.P.	196	66
N6	40 Zr[c]	0.76	H.P.	196	78
141	45.7 Zr	0.71	C.P.	196	55
N8	65 Zr[c]	0.52	H.P.	196	-112
N9	75 Zr[c]	0.42	H.P.	196	128
N10	90 Zr[c]	0.27	H.P.	196	142
N11	3.2 Ti	1.30	H.P.	196	-796
142	9.4 Ti	1.58	C.P.	196	65
N12	10.5 Ti	1.60	H.P.	196	76
143	18.8 Ti	2.02	C.P.	196	48
144	24.3 Ti	2.26	C.P.	196	52
N13	25 Ti[c]	2.30	H.P.	196	45
145	30.5 Ti	2.58	C.P.	196	40
146	33.8 Ti	2.72	C.P.	196	33
N16	1.6 V	1.18	H.P.	196	107
150	4.4 V	1.30	C.P.	196	42
147	6.6 V	1.38	C.P.	196	73
148	8.9 V	1.48	C.P.	196	59
149	10.7 V	1.54	C.P.	196	78
NL-2	12.6 V	1.61	H.P.	196	58
158	13.7 V	1.65	C.P.	196	50
151	24.2 V	2.06	C.P.	196	0
163	1.1 W	1.3	C.P.	196	-260
164	4.7 W	2.0	C.P.	196	-2930
165	9.6 W	2.8	C.P.	7	Cracked
152	2.45 Mo	1.18	C.P.	196	-710
153	5.2 Mo	1.21	C.P.	196	-130
NL-3	7.2 Mo	1.25	H.P.	196	0[d]
154	7.4 Mo	1.26	C.P.	196	62
N14	<0.02 Cr	1.15	H.P.	196	-328
N15	0.5 Cr	1.16	H.P.	196	-80
N48	0.5 Cr	1.16	H.P.	196	-495

OF NIOBIUM ALLOYS IN 680 F WATER

Corrosion Resistance					
	Compared With Zircaloy-2				
Compared With "Best" 100 Nb[b]	Higher Weight Change		Equivalent,	Lower Weight Change	
	>20 Per Cent	10 to 20 Per Cent	±10 per cent	10 to 20 Per Cent	>20 Per Cent
-	X				
-	X				
-	X				
-	X				
-	X				
0	X				
-	X				
-	X				
-	X				
+	X				
+			X		
+					X
+			X		
+		X			
+				X	
+	X				
+	X				
+	X				
-	X				
+			X		
+		X			
+					X
+				X	
+					X
+					X
+					X
+	X				
+					X
+		X			
+			X		
+	X				
+			X		
+					X
+					X
-	X				
-	X				
-	X				
-	X				
-	X				
+	X				
+			X		
-	X				
-	X				
-	X				

TABLE 15.

Alloy	Alloy Content (Balance Niobium), a/o	Thermal-Neutron Absorption Cross Section, barns per atom	Type of Niobium Base[a]	Exposure Time, days	Weight Change, mg per dm^2
N45	<0.08 Fe	1.15	H.P.	196	-182
N46	0.3 Fe	1.16	H.P.	112	-1180
169	4.9 Fe	1.22	C.P.	196	10
N47	10 Fe[c]	1.28	H.P.	28	-2000
N61	1 Ni[c]	1.18	H.P.	28	4[d]
N62	2.5 Ni[c]	1.23	H.P.	7	Cracked
N63	5 Ni[c]	1.32	H.P.	7	Disintegrated
N64	1 Pd[c]	1.21	H.P.	28	-834
N59	1 Y[c]	1.15	H.P.	56	-1020
N60	5 Y[c]	1.16	H.P.	56	-6420
N57	1 Ce[c]	1.13	H.P.	56	-1180
NL-10	9.6 Ti-3.3 Cr	1.75	H.P.	196	51
175	12 Ti-0.5 Cr	1.72	C.P.	196	66
176	20.2 Ti-2.1 Cr	2.12	C.P.	196	39
177	28.2 Ti-6.1 Cr	2.56	C.P.	196	20
NL-7	11.2 Ti-3.2 Mo	1.72	H.P.	196	55
172	12 Ti-4.2 Mo	1.78	C.P.	196	64
173	17.4 Ti-6.2 Mo	2.06	C.P.	196	54
NL-6	18.8 Ti-8.7 Mo	2.15	H.P.	196	53
174	23.1 Ti-7.8 Mo	2.35	C.P.	196	45
N49	2 V-2.5 Ti	1.34	H.P.	196	88
178	5 V-10.4 Ti	1.57	C.P.	196	56
179	8.4 V-16.1 Ti	1.80	C.P.	196	40
180	11 V-22.6 Ti	2.05	C.P.	196	48
N17	2.3 Zr-4 V	1.26	H.P.	196	60
NL-9	5.7 Zr-11.4 V	1.50	H.P.	196	23[d]
NL-8	9.9 Zr-9.4 V	1.39	H.P.	196	44[d]
N18	25 Zr-5 V[c]	1.10	H.P.	196	-284
N19	35 Zr-5 V[c]	1.00	H.P.	196	-352
N20	45 Zr-5 V[c]	0.90	H.P.	196	60
N21	10.9 Zr-5.1 Ti	1.24	H.P.	196	61
N22	25 Zr-5 Ti[c]	1.10	H.P.	196	-44
N23	25 Zr-15 Ti[c]	1.56	H.P.	196	48
N24	25 Zr-25 Ti[c]	2.04	H.P.	196	48
N25	35 Zr-5 Ti[c]	1.00	H.P.	196	71
N26	35 Zr-15 Ti[c]	1.50	H.P.	196	37
N28	45 Zr-5 Ti[c]	0.92	H.P.	196	71
NL-4	46.8 Zr-5.1 Ti	0.92	H.P.	196	92
N29	10 Zr-5 Mo[c]	1.13	H.P.	196	18[d]
N30	35 Zr-5 Mo[c]	0.88	H.P.	196	53
N31	45 Zr-5 Mo[c]	0.78	H.P.	196	70

(Continued)

Compared With "Best" 100 Nb[b]	Corrosion Resistance Compared With Zircaloy-2: Higher Weight Change >20 Per Cent	Higher Weight Change 10 to 20 Per Cent	Equivalent, ±10 per cent	Lower Weight Change 10 to 20 Per Cent	Lower Weight Change >20 Per Cent
-	X				
-	X				
+					X
-	X				
-	X				
-	X				
-	X				
-	X				
-	X				
+					X
+			X		
+					X
+					X
+				X	
+			X		
+				X	
+				X	
+					X
+	X				
+				X	
+					X
+					X
+			X		
+	X				
+	X				
-	X				
-	X				
+			X		
+			X		
-	X				
+					X
+					X
+			X		
+					X
+			X		
+	X				
+	X				
+				X	
+			X		

TABLE 15.

Alloy	Alloy Content (Balance Niobium), a/o	Thermal-Neutron Absorption Cross Section, barns per atom	Type of Niobium Base[a]	Exposure Time, days	Weight Change, mg per dm^2
N32	35 Zr-5 Al[c]	0.76	H.P.	196	62
N34	45 Zr-5 Al[c]	0.67	H.P.	196	60
N35	10 Zr-5 Cr[c]	1.14	H.P.	196	48
N37	45 Zr-5 Cr[c]	0.93	H.P.	196	48
N38	10 Zr-5 Fe[c]	1.12	H.P.	196	44
N50	2 V-2.3 Mo	1.29	H.P.	196	114
N51	2.2 V-0.54 Fe	1.24	H.P.	196	79
N53	1.8 V-<0.02 Cr	1.19	H.P.	196	58
N54	1.8 V-0.14 Al	1.19	H.P.	196	88
	Zircaloy-2	0.19	--	196	65

(a) C.P. designates commercial purity, H.P. designates high purity.
(b) Corrosion resistance, in terms of relative weight change to Sample N56; "-" designates greater weight change; "+" designates lower weight change.
(c) Nominal composition.
(d) Losing weight.

(Continued)

Compared With "Best" 100 Nb[b]	Corrosion Resistance Compared With Zircaloy-2				
	Higher Weight Change		Equivalent,	Lower Weight Change	
	>20 Per Cent	10 to 20 Per Cent	±10 per cent	10 to 20 Per Cent	>20 Per Cent
+			X		
+			X		
+					X
+					X
+					X
+	X				
+	X				
+			X		
+	X				
+			X		

TABLE 16. COMPARATIVE CORROSION RESISTANCE OF NIOBIUM ALLOYS IN 750 F STEAM

Alloy	Alloy Content (Balance Niobium), a/o	Thermal-Neutron-Absorption Cross Section, barns per atom	Type of Niobium Base[a]	Exposure Time, days	Weight Change, mg per dm^2	Corrosion Resistance		
						Compared With "Best"[b] 100 Nb	Compared With Zircaloy-2	
							Higher Weight Change (>20 Per Cent)	Lower Weight Change (>20 Per Cent)
--	100 Nb	1.15	C.P.	28	Disintegrated	-	x	
TP-37	100 Nb	1.15	H.P.	210	-4,570	0	x	
138	10.5 Zr	1.05	C.P.	210	-3,970	+	x	
142	9.4 Ti	1.58	C.P.	210	119	+		x
150	4.4 V	1.30	C.P.	210	-2,400	+	x	
147	6.6 V	1.38	C.P.	210	127	+		x
148	8.9 V	1.48	C.P.	210	118	+		x
NL-2	12.6 V	1.61	H.P.	210	89	+		x
152	2.45 Mo	1.18	C.P.	98	Disintegrated	-	x	
153	5.2 Mo	1.21	C.P.	210	-18,450	-	x	
NL-3	7.2 Mo	1.25	H.P.	70	Cracked	-	x	
169	4.9 Fe	1.22	C.P.	98	Disintegrated	-	x	
163	1.1 W	1.3	C.P.	210	-6,420	-	x	
NL-10	9.6 Ti-3.3 Cr	1.75	H.P.	182	-499	+	x	
NL-7	11.2 Ti-3.2 Mo	1.72	H.P.	266	36[c]	+	x	
NL-6	18.8 Ti-8.7 Mo	2.15	H.P.	266	53[c]	+	x	
NL-9	5.7 Zr-11.4 V	1.50	H.P.	182	-215	+	x	
NL-8	9.9 Zr-9.4 V	1.39	H.P.	182	-587	+	x	
NL-4	46.8 Zr-5.1 Ti	0.92	H.P.	266	251	+		x
--	Zircaloy-2	0.19	--	182	220	+		
			--	210	225	+		
			--	266	327	+		

(a) C.P. designates commercial purity, H.P. designates high purity.
(b) Corrosion resistance, in terms of weight change relative to sample TP-37; "-" designates greater weight change; "+" designates lower weight change.
(c) Losing weight.

in the vicinity of the reactor core. On the other hand, the corrosion rates of zirconium alloys, which possess adherent tarnish films, are unaffected by flow velocity. Only very small amounts of radioactive zirconium are detected in coolant waters. Similar behavior might be expected with niobium alloys. The corrosion behavior of those alloys with adherent films may be unaffected by flow velocity. On the other hand corrosion rates and product transport of those with less adherent films may increase with increasing flow velocity.

Based on the information obtained to date, it is not yet known whether hydrogen absorption in niobium during corrosion poses a problem as it does with zirconium alloys. Results indicate that hydrogen absorption is low in the more corrosion-resistant alloys and is high only in those alloys which exhibit high corrosion rates.

Oxygen contamination of niobium alloys also appears to be related to corrosion resistance. In general, high oxygen-diffusion coefficients were obtained with less resistant alloys. However, contamination of niobium alloys from oxygen in the oxide film does not appear to be a serious problem. Depth of contamination after 196 days' exposure to 680 F water was found to be less than 1 mil for the more corrosion-resistant alloys and less than 5 mils for less resistant alloys.

Theoretical Aspects

It is of interest to compare the observed effects of various binary alloy additions on the water corrosion resistance of niobium in the light of the principles which were developed[3] to explain alloying effects on the hot-air oxidation of niobium. In the case of water corrosion, the assumption is made that, as in hot air, the reaction rate depends primarily on the nature of the oxidation product formed at the niobium:water interface. Accordingly, the effects of alloying additions may be compared by the manner in which they influence the surface oxidation product formed on niobium in water. As shown earlier, the surface-oxidation product formed on niobium in 680 F water is the T-type Nb_2O_5, the same oxide which is predominantly formed on the surface of niobium heated in air at temperatures through 1470 F.

In the earlier Battelle work[3], three principles of alloying behavior were shown to be effective in governing the hot-air oxidation behavior of niobium. These are briefly summarized below:

Valence Effect: Niobium oxide is a semiconductor of the metal-excess or anion-deficit type. Accordingly, the addition of metal ions of higher valence than niobium decreases the number of interstitial metal ions or oxygen-ion vacancies in order to maintain electrical neutrality in the oxide. Since these defects are the means by which diffusion occurs through the scale, reducing their number decreases ionic-diffusion rates and thus the oxidation rate of the alloy. Adding metal ions of lower valence has the opposite effect, increasing the number of defects and increasing the alloy oxidation rate.

Size Effect: Metals of smaller ionic radii than niobium enter the oxide scale substitutionally where, because of their smaller size, they tend to lower the unfavorably high oxide:metal volume ratio of niobium. As a result, the mechanical stability of the scale is increased and it becomes more protective, i.e., the alloy oxidation rate is decreased. Conversely, metals of larger

ionic radii tend to decrease scale stability and increase oxidation by further increasing the oxide:metal volume ratio.

New-Scale Effect: In the range beyond the solubility limit for addition metal ions in the niobium oxide, new oxides must form. These may consist of mixed oxides or pure oxides of the alloying addition. Generally, if the new oxide(s) have improved thermodynamic, mechanical, or physical properties over that of the niobium oxide, improved oxidation resistance may result.

As implied above, valence and size effects are expected to predominate at low alloy levels (less than about 15 a/o) while new-scale effects can be expected at higher alloy levels.

The valences, ionic sizes, and oxide characteristics of each of the binary additions studied in water corrosion testing are listed in Table 17. Table 18 summarizes the anticipated and observed effects of these additions on the water corrosion behavior of niobium, assuming oxidation to be the primary corrosion mechanism.

Most of the binary additions were confined to low alloy ranges. Here, as indicated in Table 18, the size effect appears to overwhelmingly predominate the valence effect. Thus, five of six binary additions anticipated to improve the corrosion resistance of niobium through size effects actually do so. Of these, vanadium, which has the smallest ionic radius, appears most effective (on an equivalent atomic per cent addition basis). On the other hand, chromium and tungsten which should show increasingly beneficial effects actually did not. In these instances, it appears possible that larger additions of these metals may be required than were actually used in the present study.

Because of the wide range in 680 F corrosion rates observed for the various unalloyed niobium samples, it is not possible to accurately compare the behavior of the less-corrosion-resistant alloys. Nevertheless, the cerium, palladium, and yttrium alloys were among the least-corrosion-resistant materials tested, a behavior which might be explainable on the basis of their unfavorably large ionic radii.

The effectiveness of zirconium additions in improving the corrosion resistance of niobium can only be explained by the new scale effect. This thesis is supported by the X-ray evidence which showed that a double oxide, $6ZrO_2 \cdot Nb_2O_5$, was formed on the 45.7 a/o zirconium alloy exposed for 42 days in 680 F water.

Comparison of the hot-water corrosion and air oxidation behavior of niobium alloys shows several strong points of similarity.

First, in water corrosion as in air oxidation, size effects predominate over valence effects at low alloy concentrations.

Second, the most effective additions in improving air oxidation resistance were found to be those capable of forming new, stable, diffusion-resistant oxides. Again, in the water-corrosion work, the best combinations of low weight gain and adherent tarnish films were found with high-zirconium alloys and the 28.2 a/o titanium-6.1 a/o chromium alloy, both of which form new scales.

TABLE 17. VALENCE, IONIC SIZE, AND OXIDE CHARACTERISTICS OF ELEMENTS ADDED TO NIOBIUM[7,8,9]

Element	Valence	Goldschmidt Ionic Radius	Negative Free Energy of Formation of Oxide at 620 F, kcal per g-atom of oxygen	Oxide:Metal Volume Ratio
Cerium	4	0.94	107	1.16
Yttrium	3	0.92	125	1.39
Palladium	2	0.80	10.7	1.65
Zirconium	4	0.79	117	1.56
Nickel	2	0.69	43.9	1.65
Niobium	5	0.69	78.2	2.69
Titanium	4	0.68	99.6	1.73
Iron	3	0.64	52.8	2.14
Chromium	3	0.63	77.9	2.07
Molybdenum	6	0.62	47.9	3.24
Tungsten	6	0.62	54.7	3.25
Vanadium	5	0.59	62.1	3.19

TABLE 18. EFFECTS OF BINARY ALLOY ADDITIONS ON THE 680 F WATER-CORROSION BEHAVIOR OF NIOBIUM

	Effect of Additions on Corrosion Behavior			
Mechanism	Decreasing Corrosion Resistance (Increasing Weight Changes)	Negligible Effect	Negligible Effect or Slightly Increased Corrosion Resistance	Increasing Corrosion Resistance (Decreasing Weight Changes)
	Anticipated Behavior			
Valence effect	Nickel, iron, cerium, palladium, chromium, titanium, yttrium, zirconium	Vanadium		Molybdenum, tungsten
Size effect	Cerium, yttrium, palladium, zirconium, nickel			Titanium, iron, chromium, molybdenum, tungsten, vanadium
New scale effect				Titanium[a], zirconium[a]
	Generally Observed Behavior			
	Yttrium, chromium, cerium, tungsten, nickel, palladium		Iron, molybdenum	Zirconium, titanium, vanadium

(a) Placement based on high free energy of formation of oxide and more favorable oxide:metal volume ratio.

Finally, the additions (i. e., titanium, vanadium, and zirconium) found most effective in improving the corrosion resistance of niobium to water and steam were also among the most effective additions in improving the hot-air oxidation resistance of niobium.

These observations lend strong support to the beliefs that oxidation is the primary reaction involved in both hot water and air, and that the mechanism for forming more protective oxides, through alloying, against both media is basically the same.

Hot Hardness

The hardnesses of most of the fabricable alloys were determined, after vacuum annealing, at temperatures through 1650 F. These data are given in Table 19 and plotted as a function of temperature in Figures 9 to 16.

Hardness data were obtained for unalloyed niobium in two conditions: (1) as-received electron-beam-melted ingot, and (2) the same material after melting, cold rolling, and vacuum annealing. The curves for both materials were quite similar, as shown in Figure 9. Thus, the hardness of unalloyed niobium holds fairly constant at temperatures to 600 F after which it decreases fairly rapidly with increasing temperatures. Due to its higher interstitial content from contamination in processing, the sheet niobium maintained a higher hardness at all temperatures. Also, above 600 F, the hardness of sheet decreased less rapidly with increasing temperature than that for the higher purity ingot material.

Generally, the hardness curves for most of the alloys were similar. The general behavior was for hardness to decrease progressively at a uniform rate with increasing temperature to 1650 F. None of the alloy curves showed sharp breaks like those exhibited by the unalloyed niobium at 600 F.

The most notable exception to this general rule occurred for the binary and ternary alloys containing 1. 1 through 10 a/o zirconium. As shown in Figure 9, the hardnesses of binary alloys containing 10 a/o zirconium and less tended to increase at temperatures above 1200 F. Also, as illustrated in Figures 15 and 16, the same behavior occurs in ternary alloys containing 2. 3 through 10 a/o zirconium. It is concluded that zirconium increases the hardness during testing by gettering traces of oxygen from the test atmosphere to form a thin, hard subsurface oxide dispersion. The magnitude of this effect increases with temperatures above 1200 F. Also, the hardness-change data in Table 19 and the curves in Figure 17 indicate maximum susceptibility to hardness contamination occurs for zirconium contents of 5 to 10 a/o.

Binary titanium additions of 10 to 25 a/o appear to have a similar effect on niobium, though not nearly to the same degree as zirconium. Most of the other alloys show no evidence of this behavior.

The specific effects of binary molybdenum, titanium, vanadium, and zirconium additions on the hot hardness of niobium are more apparent from comparisons of Figures 17, 18, and 19 which show hardness plotted as a function of alloy composition. Initial additions of zirconium, vanadium, and molybdenum, in amounts through 30 a/o, 5 a/o, and 2. 5 a/o, respectively, result in approximately linear increases in the hot

TABLE 19. HOT HARDNESS OF SELECTED NIOBIUM-BASE ALLOYS

Alloy	Alloy Content (Balance Niobium)[a], a/o	Type of Niobium Base[b]	Hardness, VHN, at Temperature, F							Hardness Change[d], VHN
			75	600	900	1200	1400	1650	75[c]	
--	100 Nb	H.P.[e]	81	78	56	37	26	21	82	1
N40	100 Nb	H.P.[f]	97	95	74	65	54	46	93	-4
N2	1.1 Zr	H.P.	108	75	71	75	87	84	123	15
N3	2.2 Zr	H.P.	130	116	87	84	100	99	126	-4
N4	5 Zr[g]	H.P.	152	101	97	99	109	184	179	27
N5	10.2 Zr	H.P.	187	142	133	133	158	267	238	51
138	10.5 Zr	C.P.	197	143	145	150	152	175	211	14
139	26.1 Zr	C P	267	235	229	236	222	181	279	12
140	35.7 Zr	C.P	297	254	248	244	231	160	298	1
141	45.7 Zr	C.P.	294	245	233	233	182	148	296	2
N16	1.6 V	H.P.	103	67	65	66	63	58	114	11
150	4.4 V	C.P.	147	132	119	116	118	116	156	9
148	8.9 V	C.P.	191	150	144	134	146	147	200	9
149	10.7 V	C.P.	211	155	153	144	147	147	222	11
NL-2	12.6 V	H.P.	246	164	155	153	153	149	259	13
158	13 V	C.P.	287	213	205	205	209	195	290	3
151	24.2 V	C.P.	334	258	242	241	241	212	341	7
N11	3.2 Ti	H.P.	97	52	49	45	42	41	109	12
142	9.4 Ti	C.P.	133	77	74	75	67	74	143	10
N12	10.5 Ti	H.P.	121	69	63	58	57	66	141	20
143	18.8 Ti	C.P.	151	90	86	78	73	75	168	17
144	24.3 Ti	C.P.	157	102	99	87	87	87	179	22
N13	25 Ti[g]	H.P.	152	84	75	68	67	77	194	42
145	30.5 Ti	C.P.	165	109	97	88	82	77	200	35
146	33.8 Ti	C.P.	177	114	103	89	81	76	221	53
152	2.45 Mo	C.P.	134	102	108	95	95	87	142	8
153	5.2 Mo	C.P.	154	100	103	92	94	89	165	11
NL-3	7.2 Mo	H.P.	199	133	133	116	104	89	187	-12
154	7.4 Mo	C.P.	180	120	117	108	108	114	186	6
N45	<0.08 Fe	H.P.	98	72	76	60	60	52	97	-1
N46	0.3 Fe	H.P.	106	123	95	92	89	71	110	4
169	4.9 Fe	C.P.	143	109	109	97	96	84	141	-2
N47	10 Fe[g]	H.P.	251	182	187	182	172	119	235	-16
163	1.1 W	C.P.	128	96	97	81	78	77	130	2
164	4.7 W	C.P.	178	137	145	117	108	103	174	-4
N48	0.5 Cr	H.P.	120	82	78	77	77	64	123	3
N57	1 Ce[g]	H.P.	64	50	53	40	32	27	62	-2
N60	5 Y[g]	H.P.	102	91	79	82	75	63	96	-6
N64	1 Pd[g]	H.P.	107	77	77	63	62	51	102	-5

TABLE 19. (Continued)

Alloy	Alloy Content (Balance Niobium)[a], a/o	Type of Niobium Base[b]	Hardness, VHN, at Temperature, F							Hardness Change[d], VHN
			75	600	900	1200	1400	1650	75[c]	
N49	2 V-2.5 Ti	H.P.	119	75	66	68	71	69	129	10
N50	2 V-2.3 Mo	H.P.	134	83	77	71	69	66	134	0
N51	2.2 V-0.54 Fe	H.P.	143	104	101	103	104	85	149	6
N52	2.2 V-0.87 Ni	H.P.	168	139	135	128	124	94	171	3
N53	1.8 V-<0.02 Cr	H.P.	112	80	65	66	65	61	111	-1
N54	1.8 V-0.14 Al	H.P.	104	73	65	63	69	58	112	8
N65	5 V-2.5 Ti[d]	H.P.	146	104	98	97	97	82	155	9
N68	5 V-2.5 Cr[d]	H.P.	152	120	115	113	108	94	162	10
N70	5 V-2.5 Al[d]	H.P.	146	101	93	96	95	85	150	4
N55	2.5 V-2.5 Zr[g]	H.P.	141	114	103	100	113	115	144	3
N17	4.0 V-2.3 Zr	H.P.	159	117	115	106	119	145	179	20
NL-8	9.4 V-9.9 Zr	H.P.	277	212	194	186	185	212	291	14
NL-9	11.4 V-5.7 Zr	H.P.	275	188	181	186	194	245	293	18
N21	10.9 Zr-5.1 Ti	H.P.	207	135	130	135	151	223	239	32
N29	10 Zr-5 Mo[g]	H.P.	238	146	148	152	178	246	268	30
N35	10 Zr-5 Cr[g]	H.P.	208	173	169	166	169	221	236	28
N38	10 Zr-5 Fe[g]	H.P.	322	237	247	237	249	168	338	16
NL-4	46.8 Zr-5.1 Ti	H.P.	282	199	200	201	186	153	305	23
NL-7	11.2 Ti-3.2 Mo	H.P.	178	107	87	80	79	87	189	11
NL-10	9.6 Ti-3.3 Cr	H.P.	239	158	148	153	150	146	246	7

(a) By chemical analysis unless otherwise indicated.
(b) H.P. designates high-purity electron-beam-melted, C.P. designates commercial sintered.
(c) Hardness measured after heating samples to 1650 F in vacuum.
(d) Change in room-temperature hardness after heating to 1650 F.
(e) Sample taken directly from electron-beam-melted ingot 405-599-P37.
(f) Same material as (e) after inert-electrode arc melting, cold rolling, and vacuum annealing.
(g) Nominal compositions.

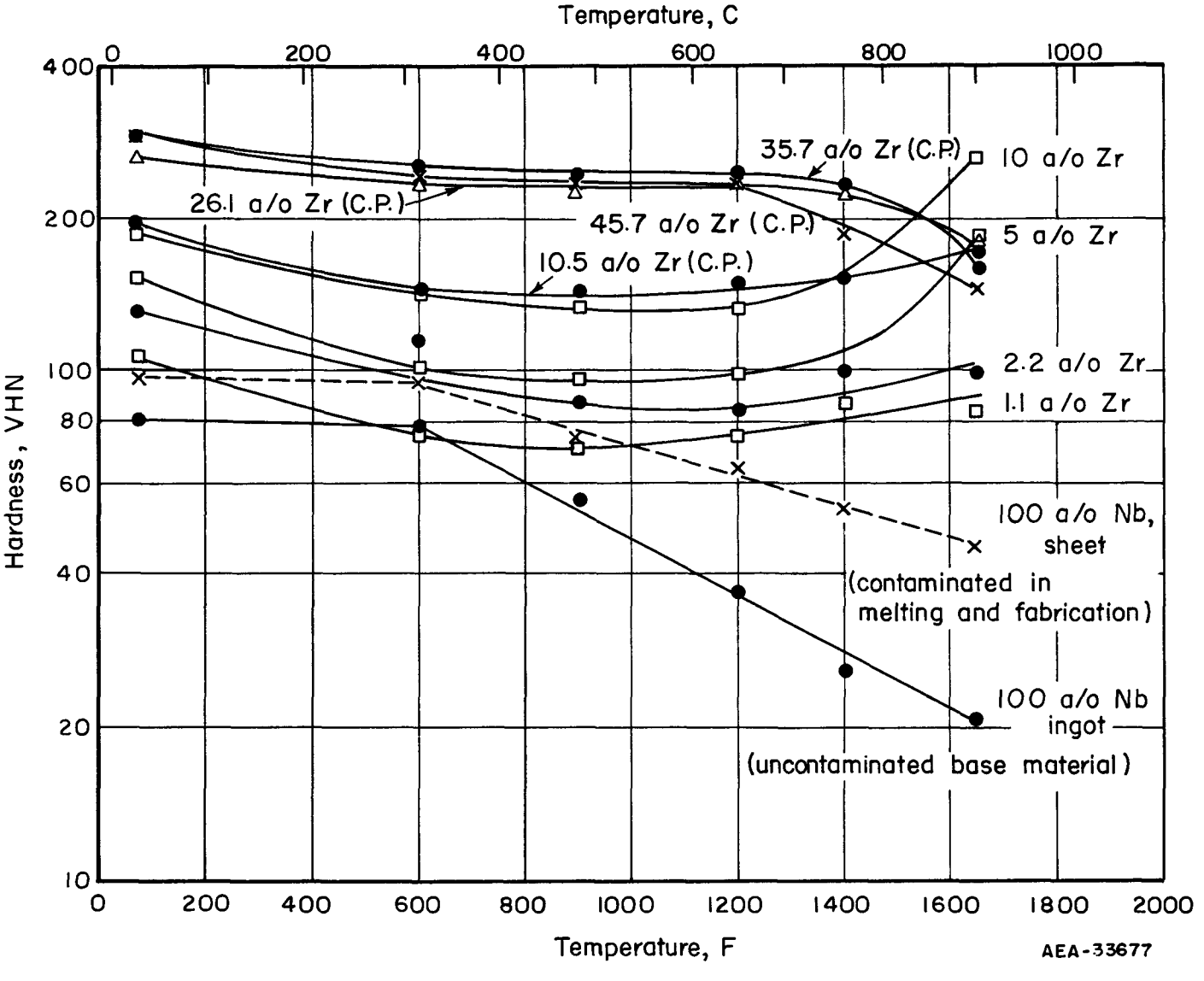

FIGURE 9. HOT HARDNESS OF NIOBIUM-ZIRCONIUM ALLOYS

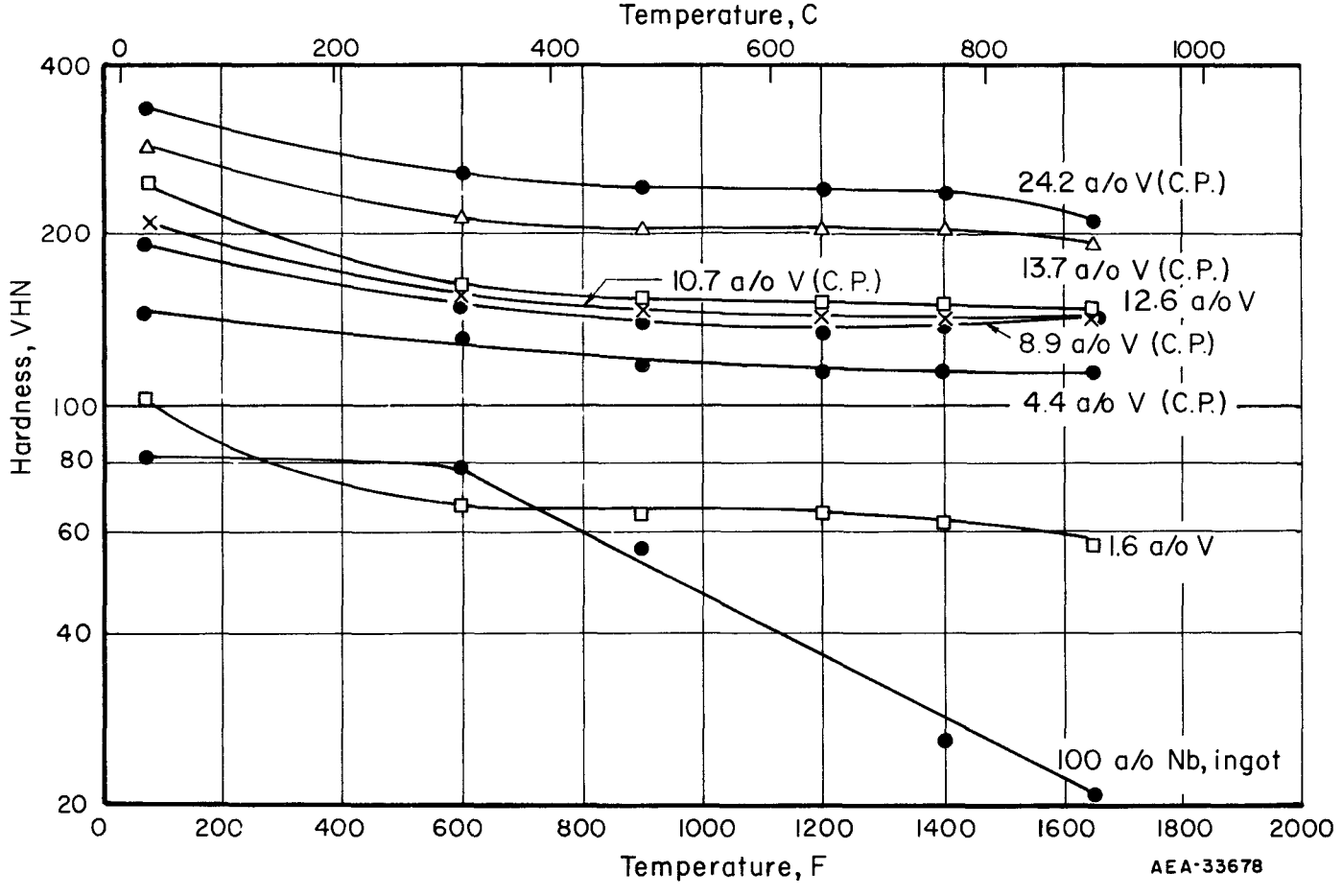

FIGURE 10. HOT HARDNESS OF NIOBIUM-VANADIUM ALLOYS

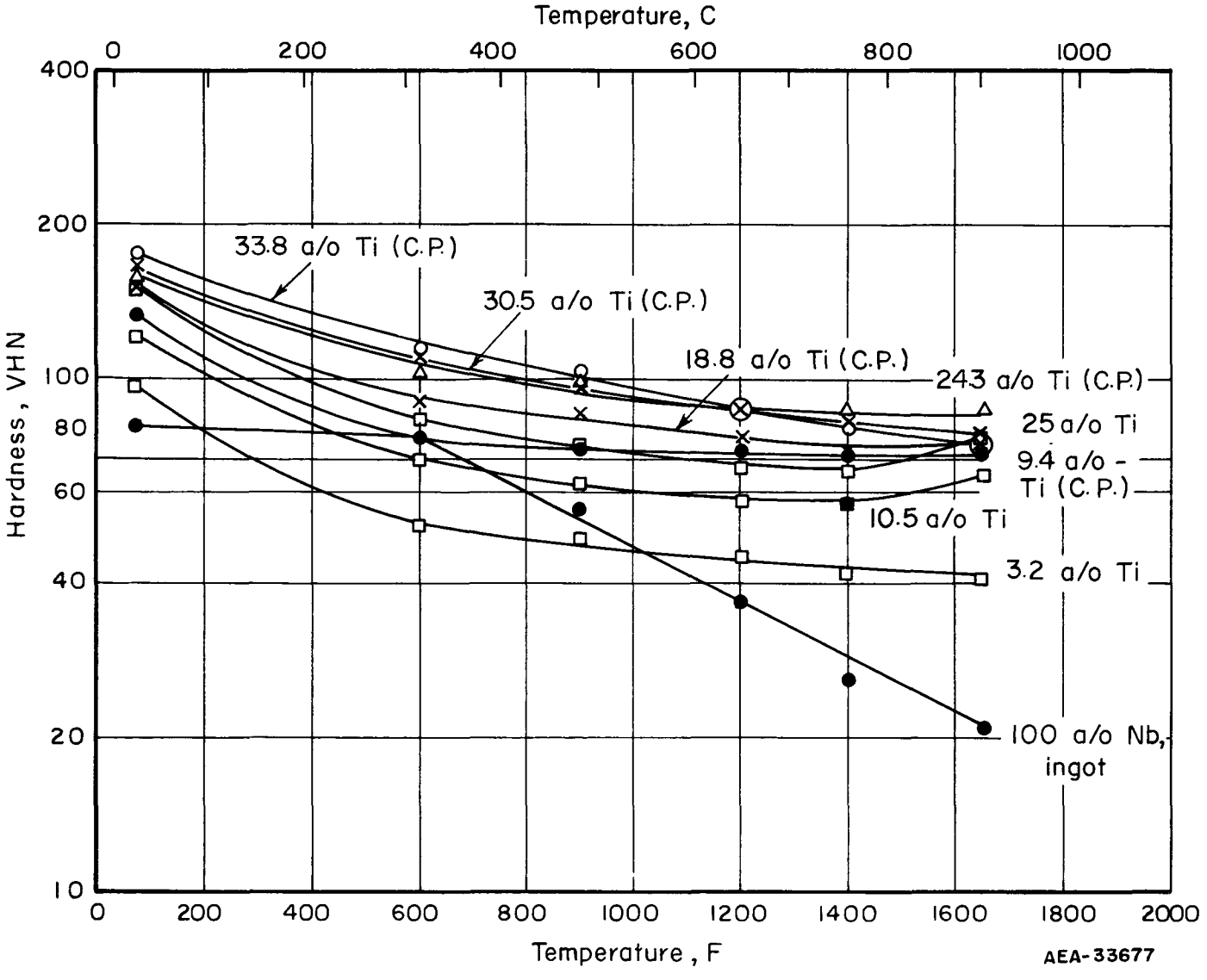

FIGURE 11. HOT HARDNESS OF NIOBIUM-TITANIUM ALLOYS

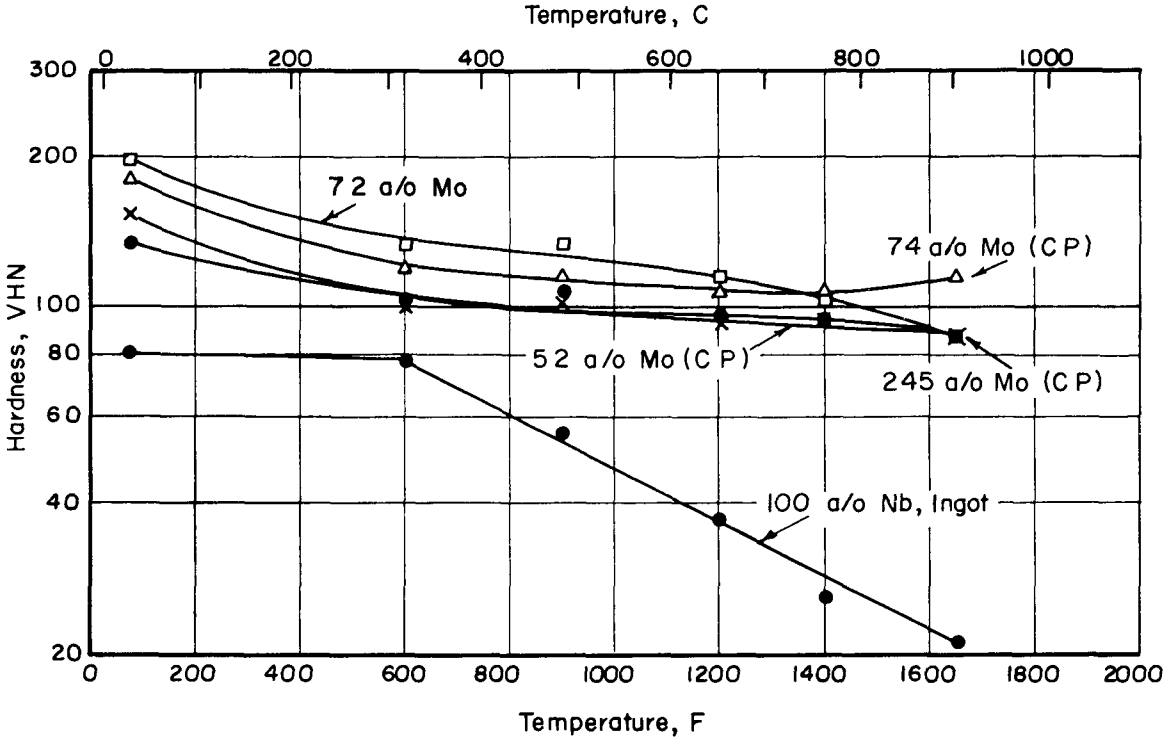

FIGURE 12. HOT HARDNESS OF NIOBIUM-MOLYBDENUM ALLOYS

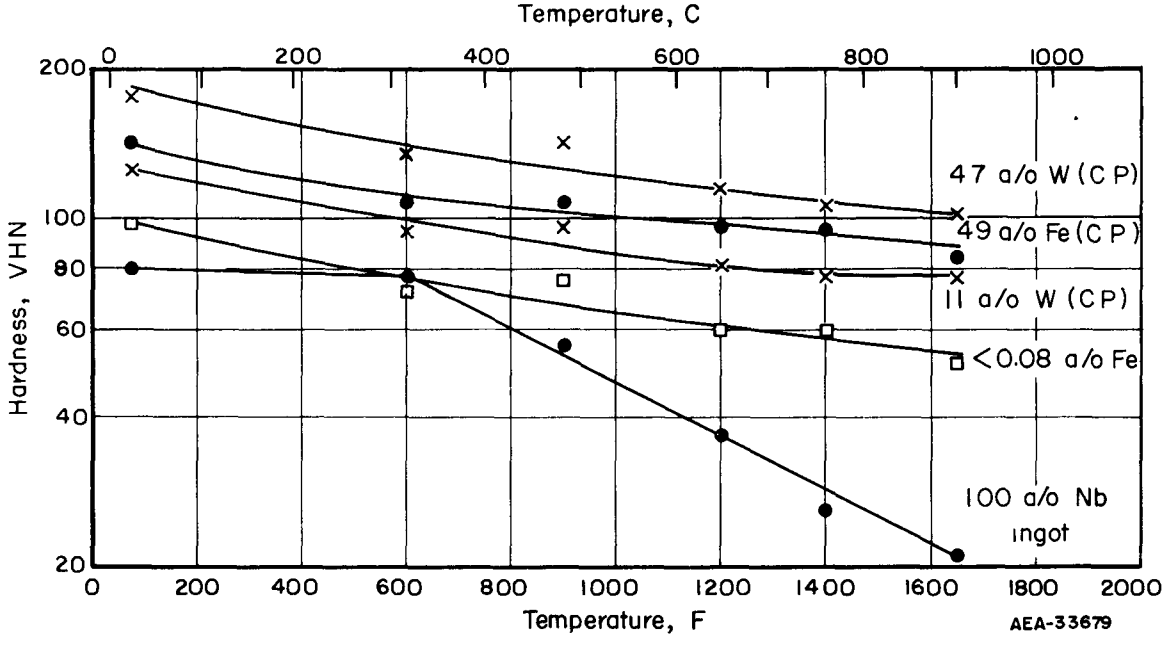

FIGURE 13. HOT HARDNESS OF NIOBIUM-TUNGSTEN AND NIOBIUM-IRON ALLOYS

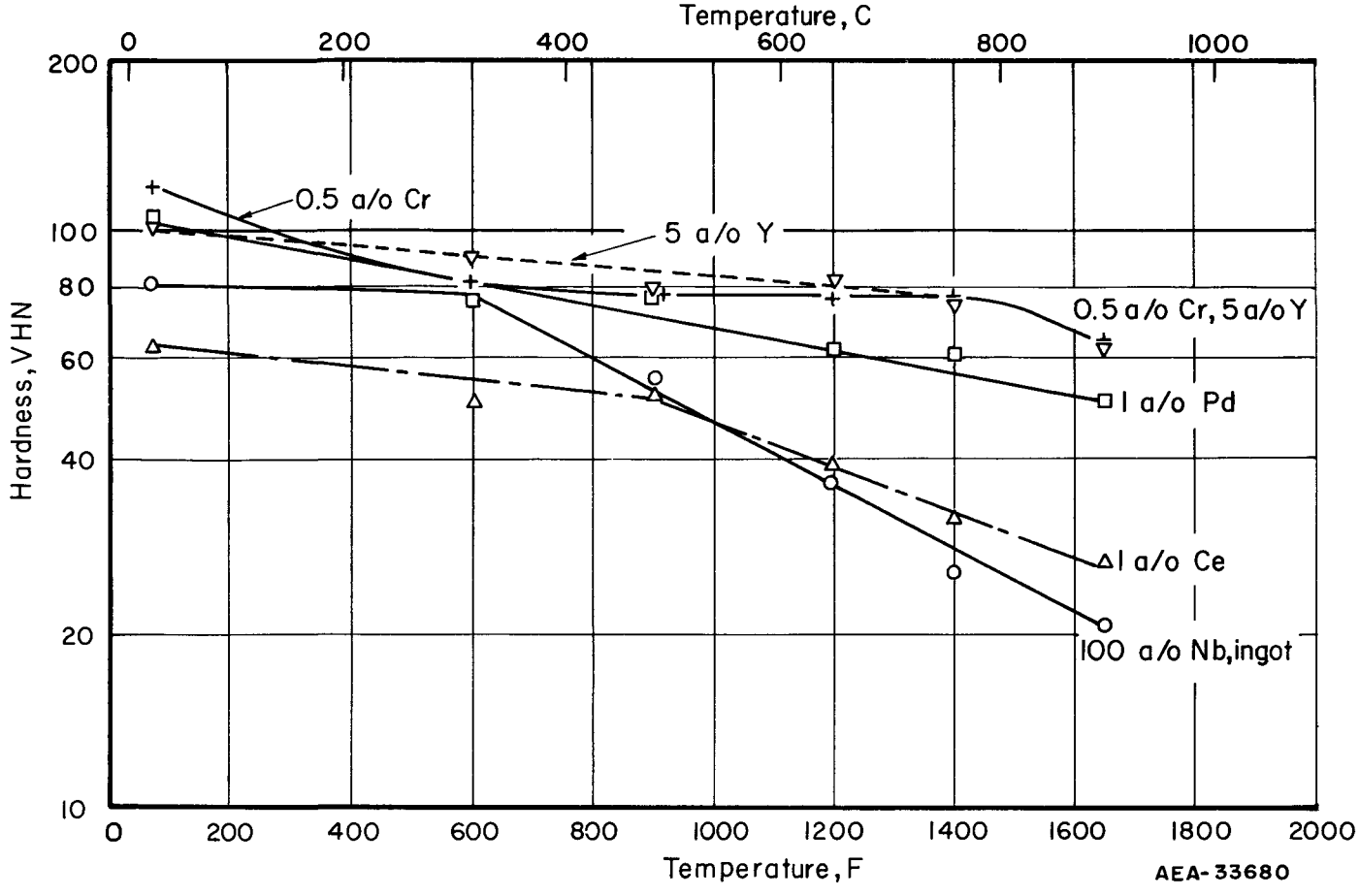

FIGURE 14. HOT HARDNESS OF MISCELLANEOUS BINARY NIOBIUM-BASE ALLOYS

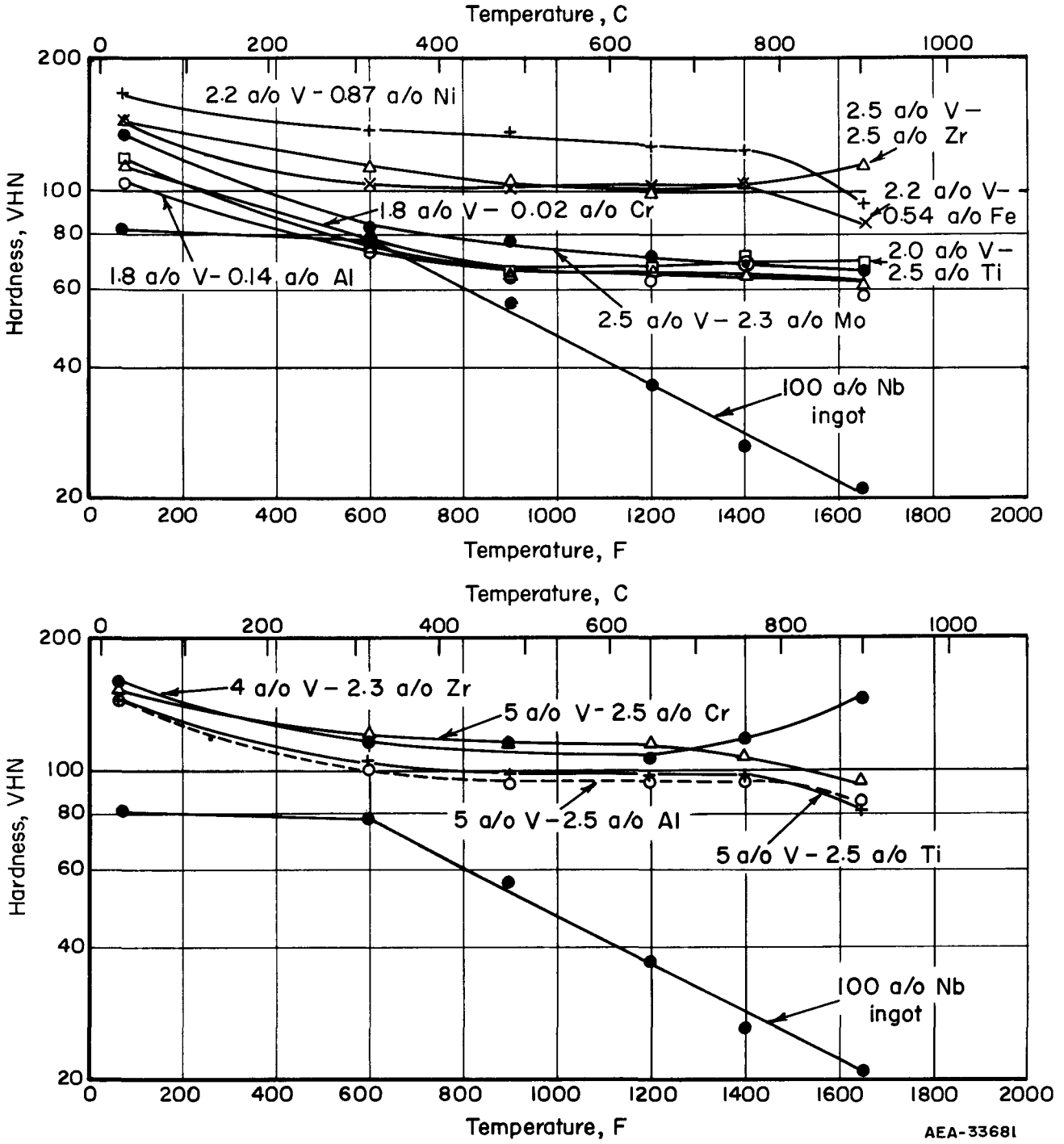

FIGURE 15. HOT HARDNESS OF TERNARY NIOBIUM-VANADIUM-BASE ALLOYS

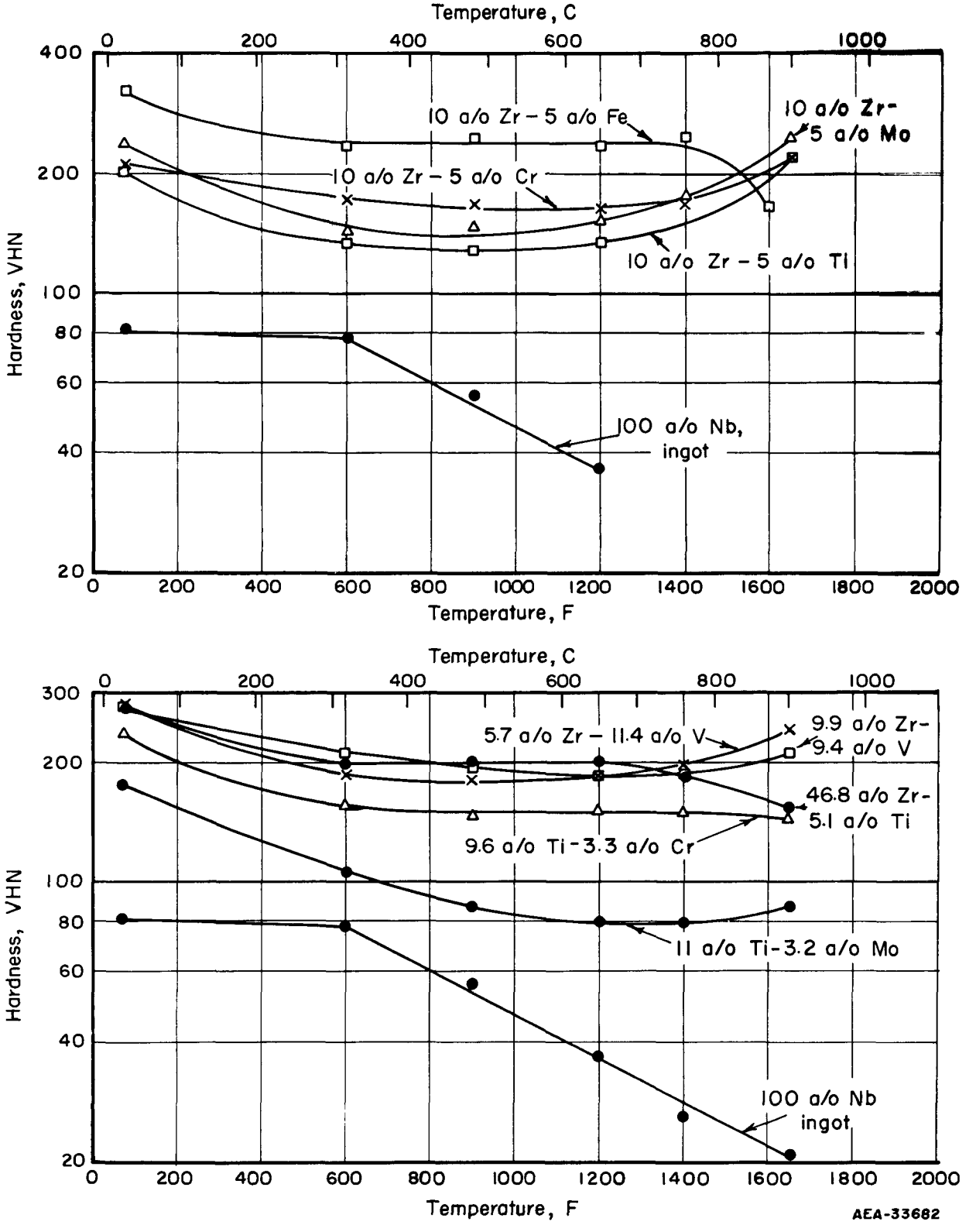

FIGURE 16. HOT HARDNESS OF TERNARY NIOBIUM-ZIRCONIUM- AND NIOBIUM-TITANIUM-BASE ALLOYS

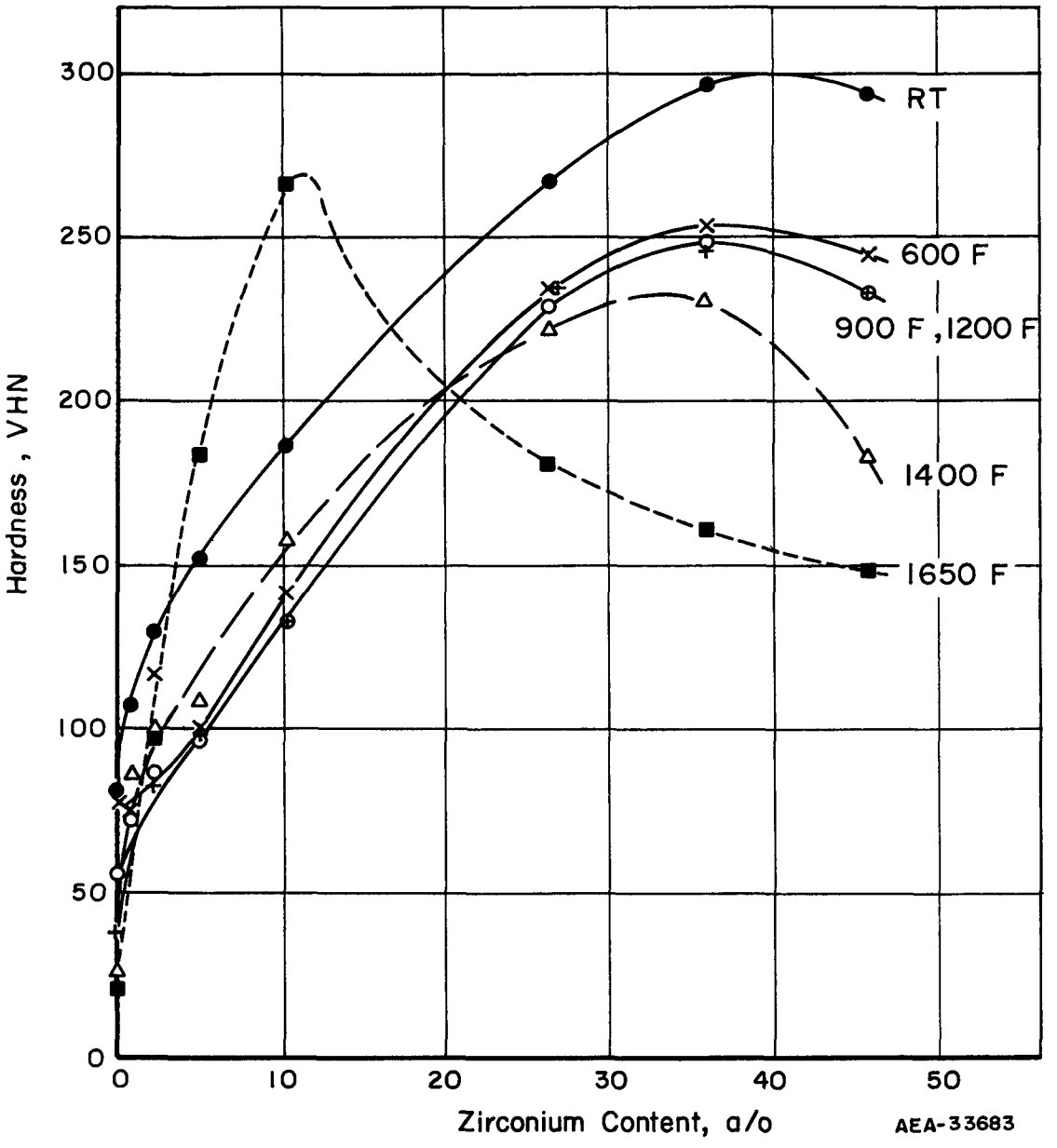

FIGURE 17. EFFECT OF ZIRCONIUM ON THE HOT HARDNESS OF NIOBIUM

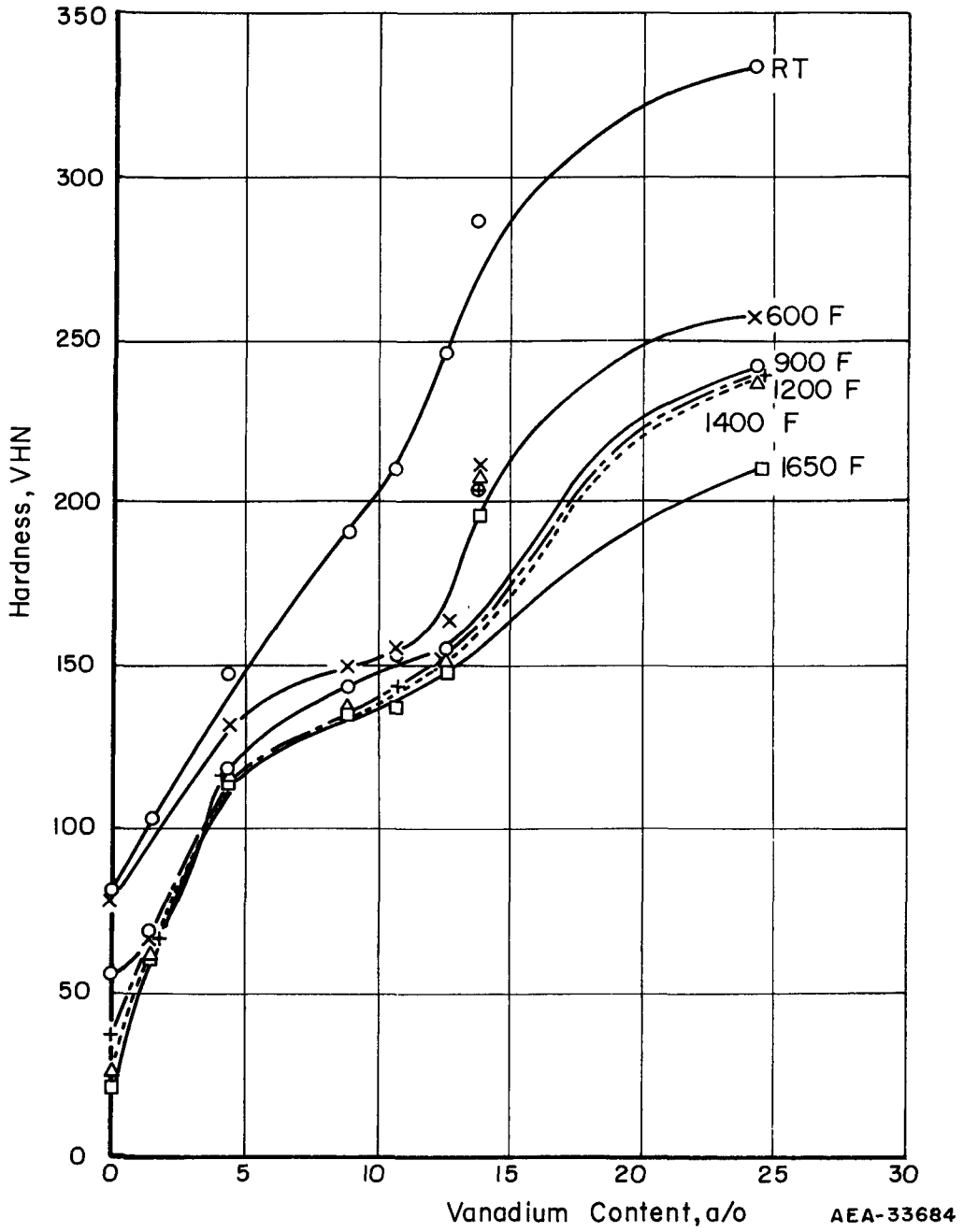

FIGURE 18. EFFECT OF VANADIUM ON THE HOT HARDNESS OF NIOBIUM

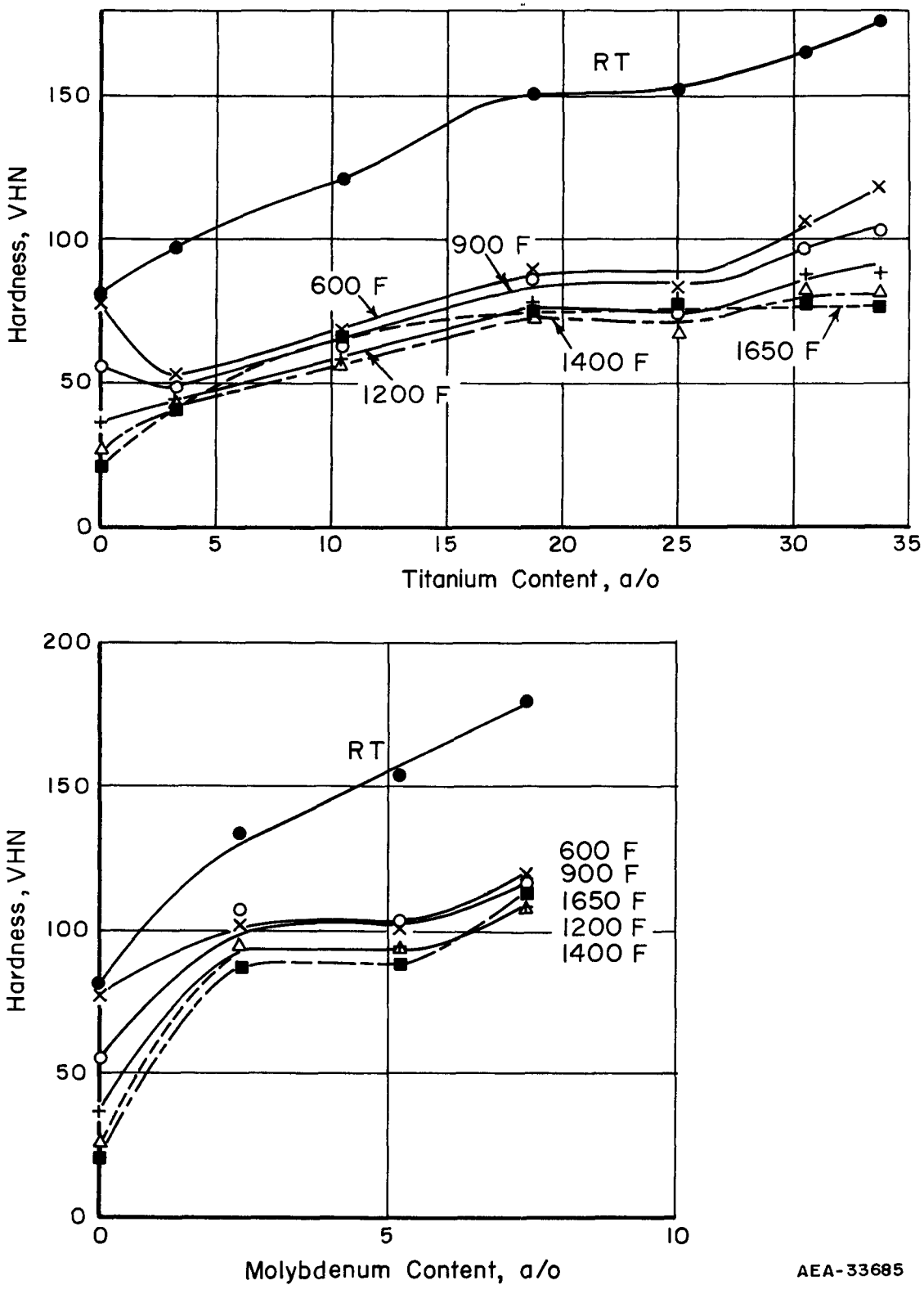

FIGURE 19. EFFECTS OF TITANIUM AND MOLYBDENUM ON THE HOT HARDNESS OF NIOBIUM

hardness of niobium. Binary additions of these metals in larger amounts have a lesser effect in further increasing the alloys' hardnesses. As shown in Figure 19, titanium is much less effective than any of these other elements in improving the hot hardness of niobium. Neglecting contamination effects, the order of these elements on an equivalent percentage (5 to 7 a/o) basis in increasing the hot hardness of niobium is titanium, zirconium, molybdenum, and vanadium.

Comparison of the ternary-alloy data shows that, in combination with vanadium or zirconium, iron and nickel additions appear more effective in increasing the hardness of niobium at elevated temperatures than similar amounts of molybdenum or titanium.

The effect of time on the hardness of the 12.6 a/o vanadium and 7.2 a/o molybdenum alloys at 1200 F was determined as shown in Figure 20. For both alloys, the resistance to deformation decreases slightly, at about the same rate, with increasing times up to 2000 sec.

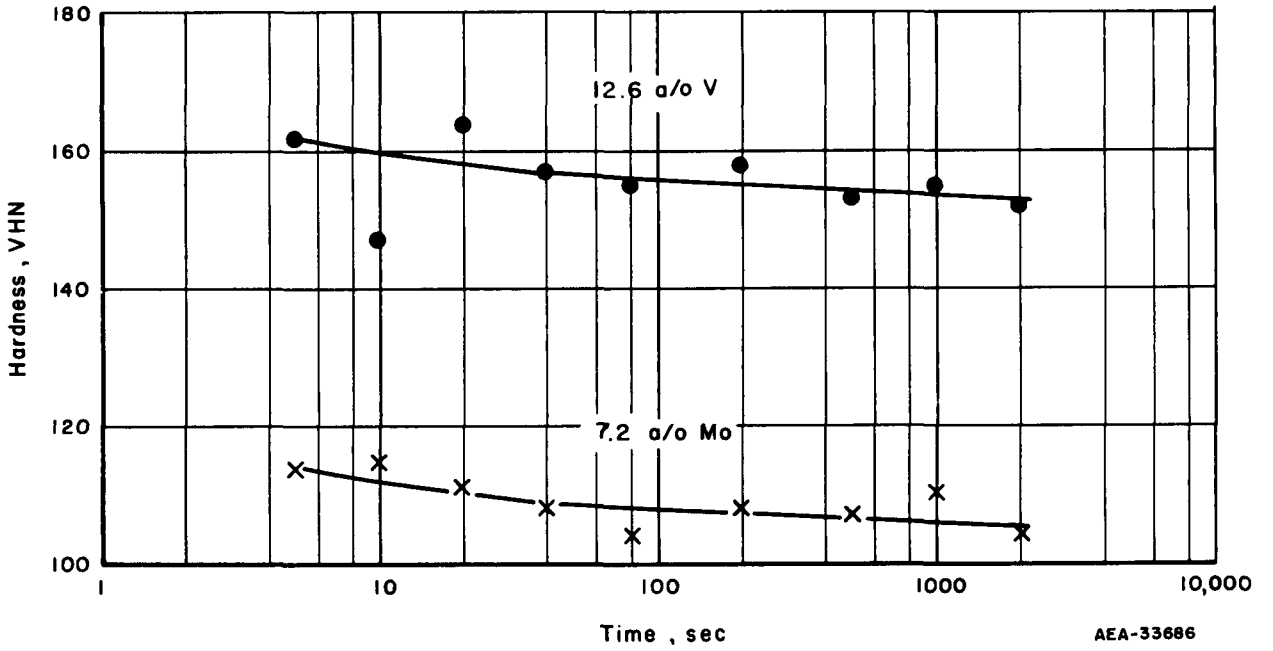

FIGURE 20. EFFECT OF TIME ON THE HARDNESS OF TWO NIOBIUM-BASE ALLOYS AT 1200 F

Tensile Properties

The tensile properties of the first scaleup alloys prepared were determined at temperatures through 1200 F, the highest temperature deemed of practical interest for pressurized water applications. Later, tests on some of the alloys were extended to 1500 F. The latter temperature was primarily selected for testing the screening alloys, for which only sufficient material for a single tensile sample was available. Here, the 1500 F ultimate tensile strength was calculated*, as being approximately equivalent to

*Calculated using the Larson-Miller parameter, $P = T(C + \log t)10^{-3}$ where T = absolute temperature, t = time, hr, and C = a constant having an estimated value of 20.

TABLE 20. TENSILE PROPERTIES AND BEND

Alloy	Alloy Content (Balance Niobium), a/o	Annealing Temperature, F	Minimum Bend Radius, T[(a)]	Tensile Room Temperature: 0.2 Per Cent Offset Yield Strength, 1000 psi	Tensile Room Temperature: Ultimate Strength, 1000 psi	Tensile Room Temperature: Elongation in 1 In., per cent
TP-37	100 Nb	2730	0	20.5	26	28
		2190	0	22	32	43
NL-11	7.6 V	2190	--	51.5	75	29
NL-12	8.7 V-0.26 N	2190	--	65.5	87	18
NL-13	7.3 V-2.4 Ti	2190	--	44	78	27
NL-14	7.6 V-2.3 Mo	2190	--	59	84	28
NL-2	12.6 V	2730	0	79	97	24
NL-3	7.2 Mo	2730	0-1.0	63	77	20
NL-4	46.8 Zr-5.1 Ti	2730	3->12.7	124	128	8
NL-6	18.8 Ti-8.7 Mo	2730	Brittle	--	~25	0
NL-7	11.2 Ti-3.2 Mo	2730	1.5-3.1	57	67	35
NL-8	9.4 V-9.9 Zr	2730	Brittle	--	91	0
NL-9	11.4 V-5.7 Zr	2730	Brittle	--	46	0
NL-10	9.6 Ti-3.3 Cr	2730	Brittle	--	73	0

(a) T-value expresses the ratio of smallest successful bend radius to thickness of the sheet used; generally T-values greater than 10 indicate brittle behavior.

(b) 1200 F and 1500 F tensile tests conducted in helium; all others carried out in air.

(c) Fracture of loading pin in shoulder occurred.

DUCTILITIES OF NIOBIUM-BASE SCALEUP ALLOYS

Properties at Temperatures Indicated								
600 F			1200 F[b]			1500 F[b]		
0.2 Per Cent Offset Yield Strength, 1000 psi	Ultimate Strength, 1000 psi	Elongation in 1 In., per cent	0.2 Per Cent Offset Yield Strength, 1000 psi	Ultimate Strength, 1000 psi	Elongation in 1 In., per cent	0.2 Per Cent Offset Yield Strength, 1000 psi	Ultimate Strength, 1000 psi	Elongation in 1 In., per cent
12	25	32	8.7	13	23	--	--	--
--	--	--	32	58	17	34	53	34
--	--	--	38	64.5	15	42	60	26
--	--	--	38	62	14	34	53.5	23
--	--	--	36	64	18	34	55	28
57	81	23	49	77	18	47	>69[c]	>8[c]
46	67	14	36	44	3	--	--	--
87	101	~6	--	78	3	--	--	--
17	17	~1	32	33	2	--	--	--
31	42	32	22	39	21	--	--	--
--	--	--	--	65	2	--	--	--
--	--	--	--	38	1	--	--	--
--	--	--	62	74	3	--	--	--

the 100-hr rupture strength of the alloys at 1200 F. Unfortunately, due to time limitations, it was not possible to test all of the screening alloys at 1500 F. Accordingly, the remainder were tested at room temperature.

The results of both room- and elevated-temperature tests on each on the scaleup alloys are given in Table 20. Table 21 summarizes the results of all of the room-temperature tensile data obtained on both the scaleup and screening alloys.

Room Temperature

The unalloyed niobium base, annealed for 1 hr at 2730 F, showed low yield and ultimate strengths (20,500 and 26,000 psi, respectively) characteristic of this high-purity material. The comparatively low tensile elongation, 28 per cent, of this sample was due to the extremely large grain size (see Figure 5a) which resulted from the 2730 F anneal. Recrystallizing this material at 2190 F gave a much finer grain size (similar to that shown in Figure 5b) and increased the tensile elongation value to 43 per cent. Yield and ultimate strengths were increased, accordingly, to 22,000 and 32,000 psi, respectively.

Generally, as expected, all of the alloying additions increased the strength of niobium at the expense of decreasing its ductility.

Of the few binary alloys tested, the results at the 1-5 a/o alloy level show that yttrium, palladium, and nickel, in that order, are increasingly more effective in strengthening niobium. The 2.5 a/o nickel addition approximately doubled the strength of the niobium and halved its tensile elongation. The strengths obtained with this alloy are quite high and compare favorably with the strengthening effect obtained by much larger (about 7.5 a/o) additions of molybdenum or vanadium. The best combination of high strength and ductility was obtained in the binary 12.6 a/o vanadium alloy which has yield and ultimate strengths of 79,000 and 97,000 psi, respectively, and an elongation of 24 per cent.

Of the various ternary alloys tested, good combinations of strength and ductility were generally obtained in all of those with a niobium-vanadium base excepting those containing 5 to 10 a/o zirconium. At the 2.5 to 5 a/o vanadium level, the addition of 0.5 a/o (0.09 w/o) oxygen – in combination with small amounts (0.25 to 0.5 a/o) titanium or zirconium – results in higher strengths and lower ductilities than the addition of 0.5 a/o (0.07 w/o) carbon. At 5 a/o vanadium, the nominal 2.5 a/o ternary additions of aluminum, chromium, and iron are not as effective in strengthening as are additions of nitrogen or oxygen. Similarly, at vanadium levels of 7.3 to 8.7 a/o, 0.26 a/o (0.04 w/o) nitrogen has a more potent strengthening effect than 2.5 a/o additions of either titanium or molybdenum. It is thus apparent that interstitial additions to niobium-vanadium alloys have a powerful strengthening effect yet do not seriously impair their room-temperature tensile ductility.

Despite its comparatively high total alloy content, the 11.2 a/o titanium-3.2 a/o molybdenum alloy is not as strong as either the binary 7.2 a/o molybdenum or 7.6 a/o vanadium alloys.

TABLE 21. SUMMARIZED ROOM-TEMPERATURE TENSILE PROPERTIES OF NIOBIUM-BASE ALLOYS

Alloy	Alloy Content (Balance Niobium), a/o	Annealing Temperature, F	Hardness, VHN	Tensile Properties		
				0.2 Per cent Offset Yield Strength, 1000 psi	Ultimate Strength, 1000 psi	Elongation, in 1 In., per cent
TP37	100 Nb	2190	--	22	32	43
		2730	81	20.5	26	28
N59	1 Y[a]	2190	94	24	36	19
N60	5 Y[a]	2190	109	31	42	20
N61	1 Ni[a]	2190	144	43	58	22
N62	2.5 Ni[a]	2190	171	50	69	20
N64	1 Pd[a]	2190	134	31	44	40
NL3	7.2 Mo	2730	199	63	77	20
N71	2.5 V-0.5 C[a]	2190	130	33	55	20
N77	2.5 V-0.5 Ti-0.5 C[a]	2190	127	30	53	29
N79	2.5 V-0.5 Zr-0.5 C[a]	2190	163	40.5	67	24
N80	5 V-0.5 Zr-0.5 C[a]	2190	198	49.5	82	25
N73	2.5 V-0.25 Ti-0.5 O[a]	2190	161	54	71	22
N75	2.5 V-0.25 Zr-0.5 O[a]	2190	158	57	71	10
N76	5 V-0.5 Zr-0.5 O[a]	2190	163	54	75	24
N67	5 V-2.5 Fe[a]	2190	169	48	70	20
N68	5 V-2.5 Cr[a]	2190	149	41	65	30
N70	5 V-2.5 Al[a]	2190	144	42	64	30
NL-11	7.6 V	2190	176	51.5	75	29
NL-12	8.7 V-0.26 N	2190	207	65.5	87	18
NL-13	7.3 V-2.4 Ti	2190	193	44	78	27
NL-14	7.6 V-2.3 Mo	2190	205	59	84	28
NL-2	12.6 V	2730	246	79	97	24
NL-8	9.4 V-9.9 Zr	2730	277	--	91	0
NL-9	11.4 V-5.7 Zr	2730	275	--	46	0
NL-10	9.6 Ti-3.3 Cr	2730	239	--	73	0
NL-7	11.2 Ti-3.2 Mo	2730	178	57	67	35
NL-6	18.8 Ti-8.7 Mo	2730	--	--	~25	0
NL-4	46.8 Zr-5.1 Ti	2730	282	124	128	8

(a) Nominal composition.

The highest room-temperature strength (128,000 psi ultimate) was obtained on the 46.8 a/o zirconium-5.1 a/o titanium alloy. However, the fairly small spread (4,000 psi) between the yield and ultimate strength of this alloy and its low tensile elongation (8 per cent) indicate its capacity for cold plastic deformation is quite limited.

As shown by the data of Tables 20 and 21, four of the ternary alloys proved to be quite brittle, as evidenced by their complete lack of tensile and bend ductility at room temperature. These include the 9.4 a/o vanadium-9.9 a/o zirconium, 11.4 a/o vanadium-5.7 a/o zirconium, 9.6 a/o titanium-3.3 a/o chromium, and 18.8 a/o titanium-8.7 a/o molybdenum alloys.

The brittle behavior of these vanadium-zirconium alloys is believed primarily due to their high interstitial content as a result of contamination in their preparation (see data of Table 5). As noted earlier, both of these alloys contained appreciable amounts of an inter- and intergranular zirconium-rich second phase (see Figure 1d). It appears possible, therefore, that the presence of this phase was also a contributing factor to the brittle behavior of these alloys.

The lack of ductility in the 9.6 a/o titanium-3.3 a/o chromium alloy probably resulted from chromium segregation and localized precipitation of a brittle phase based on $NbCr_2$ (see Figure 1f).

On the other hand, no explanation can be offered for the lack of ductility in the 18.8 a/o titanium-8.7 a/o molybdenum alloy.

Elevated Temperatures

The effects of temperature on the tensile properties of the scaleup alloys are given in Table 20. The same data are plotted, as a function of temperature, in Figures 21, 22, and 23.

The general behavior of the alloys with increasing temperatures through 1200 F is much the same. Thus, both strengths and ductilities decrease with increasing temperature over this interval. Because the strength drop-off with temperature is similar for most of the alloys, their relative order of 1200 F strengths, listed below, is about the same as at room temperature.

Alloy Content, a/o	1200 F Ultimate Strength, psi
100 Nb	13,000
11.2 Ti-3.2 Mo	39,000
7.2 Mo	44,000
7.6 V	58,000
7.3 V-2.4 Ti	62,000
7.6 V-2.3 Mo	64,000
8.7 V-0.26 N	64,500
12.6 V	77,000
46.8 Zr-5.1 Ti	78,000

At 1500 F, the tensile ductility in the alloys containing 7.3 to 8.7 a/o vanadium show a marked increase (Figure 23) over the 1200 F values. This indicates recovery for these alloys occurs at or slightly above 1200 F.

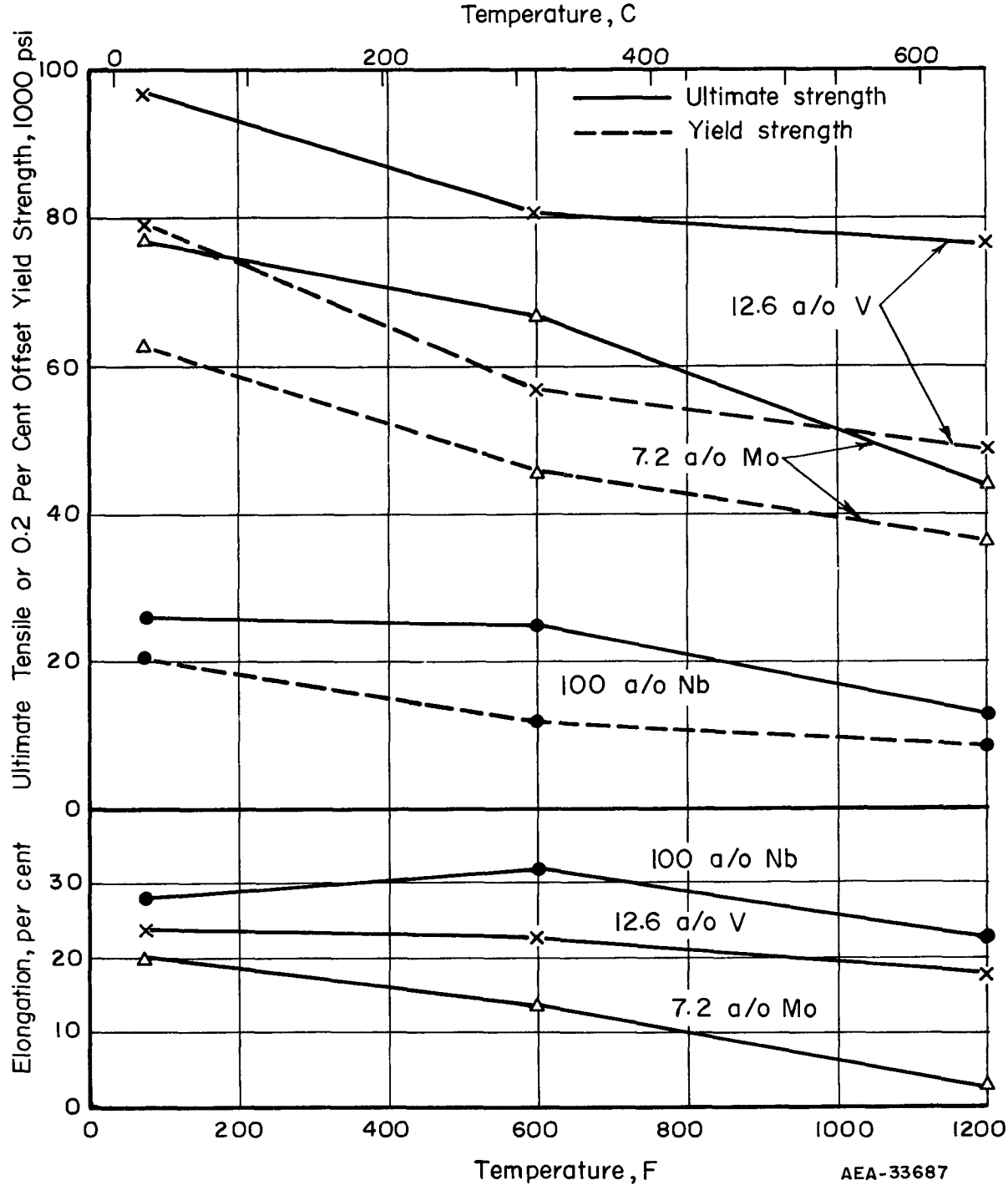

FIGURE 21. EFFECT OF TEMPERATURE ON THE TENSILE PROPERTIES OF NIOBIUM AND THE NIOBIUM-7.2 a/o MOLYBDENUM AND NIOBIUM-12.6 a/o VANADIUM ALLOYS, AS VACUUM ANNEALED 1 HR AT 2730 F

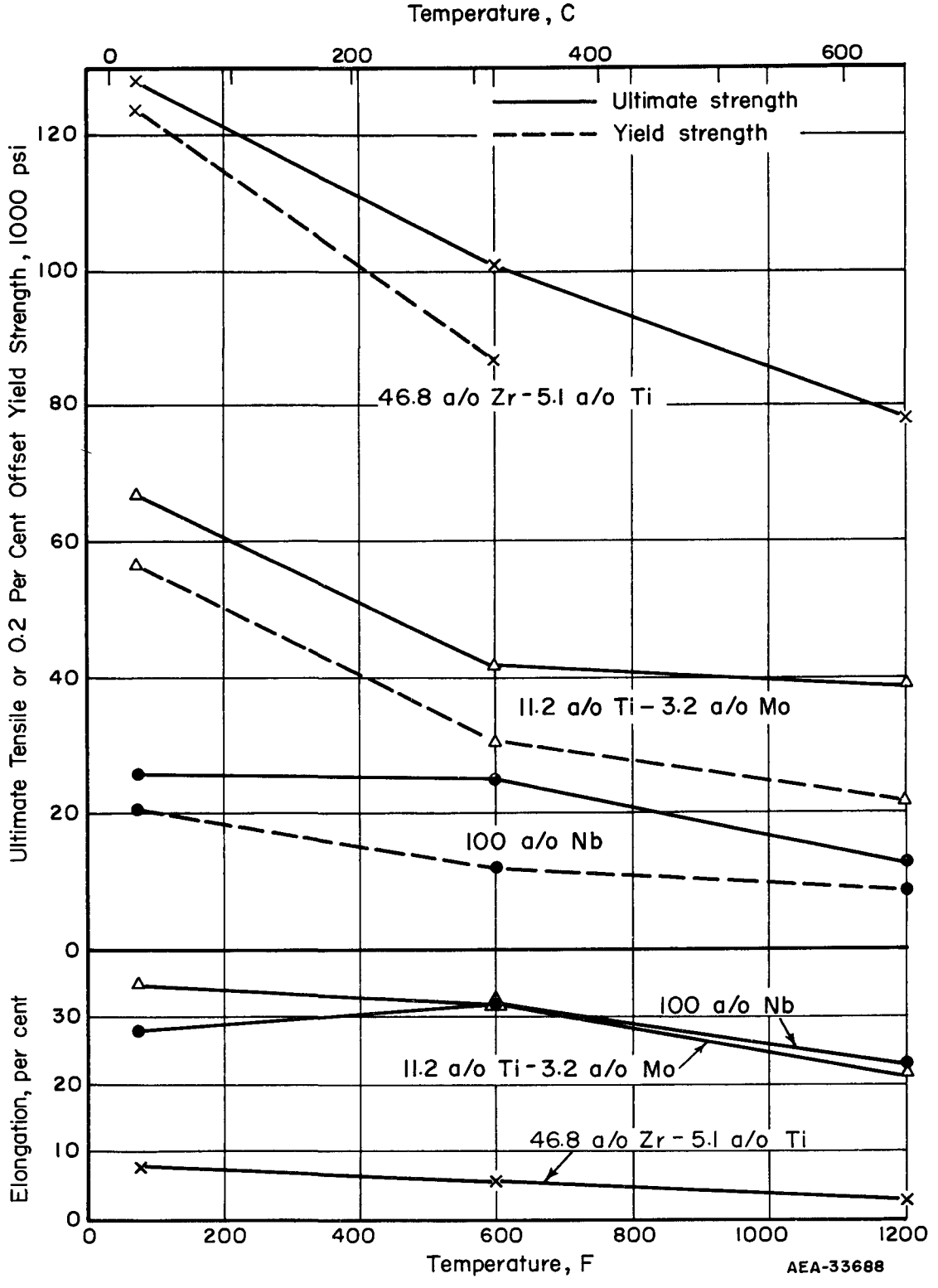

FIGURE 22. EFFECT OF TEMPERATURE ON THE TENSILE PROPERTIES OF NIOBIUM AND THE NIOBIUM-11.2 a/o TITANIUM-3.2 a/o MOLYBDENUM AND NIOBIUM-46.8 a/o ZIRCONIUM-5.1 a/o TITANIUM ALLOYS, AS VACUUM ANNEALED 1 HR AT 2730 F

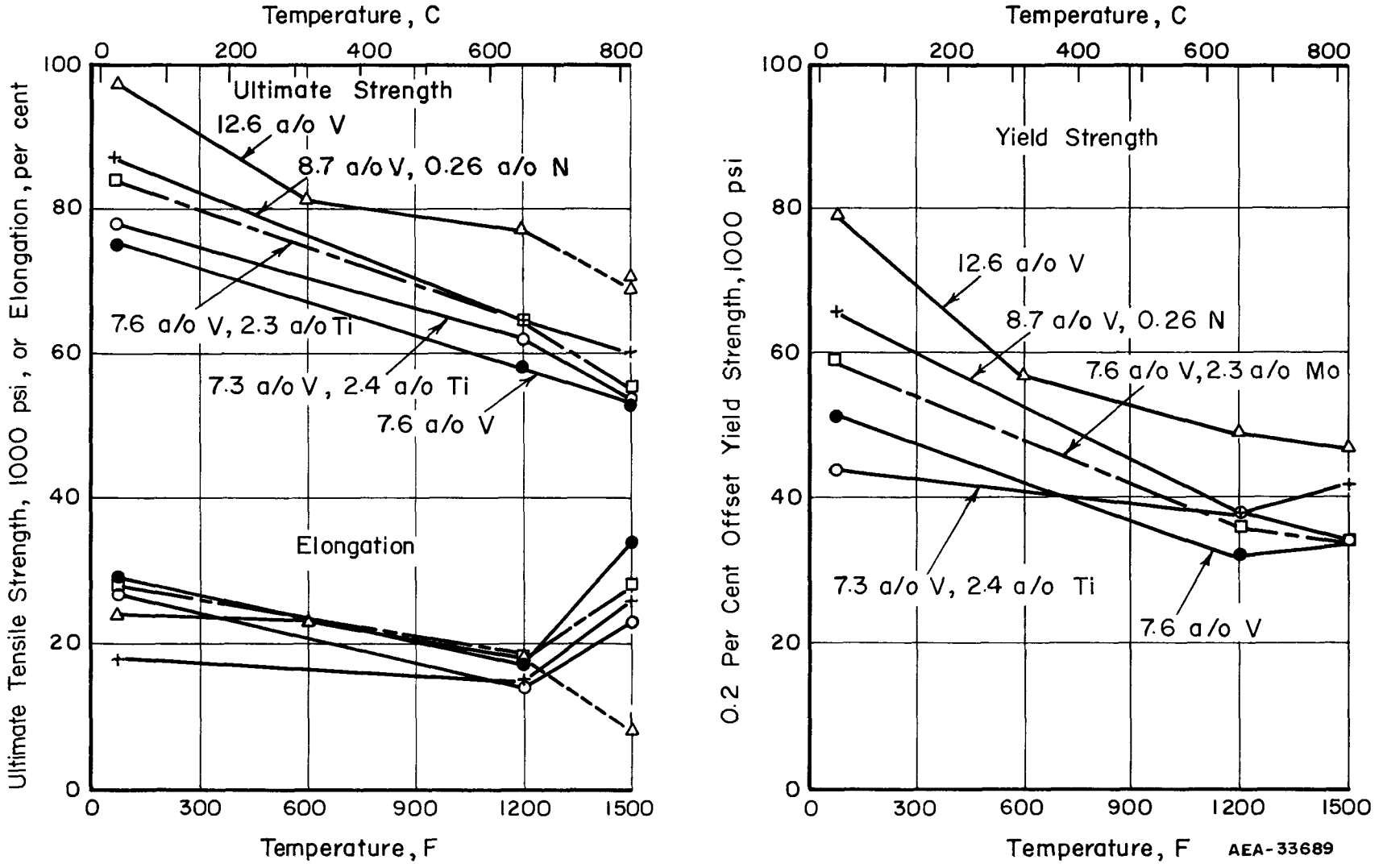

FIGURE 23. EFFECT OF TEMPERATURE ON THE TENSILE PROPERTIES OF NIOBIUM-VANADIUM-BASE ALLOYS

The 1500 F tensile properties of all of the alloys tested are summarized in Table 22.

Comparison of the binary-alloy data shows that additions of titanium through 10.5 a/o have no strengthening effect on niobium at 1500 F. While the addition of 2.2 a/o zirconium results in moderate strengthening, this alloy and each of the three ternary alloys containing zirconium are characterized by extremely low tensile ductilities at 1500 F. This undesirable effect is thus apparently carried over into vanadium-base ternary alloys where the effect of zirconium, at 5 a/o vanadium, is far more severe than the effect of interstitial contaminants (e.g., carbon and oxygen).

As illustrated in Figure 24, vanadium additions through 12.6 a/o result in almost linearly increasing the 1500 F strength of niobium. As pointed out previously, the higher tensile elongations at 1500 F for alloys containing vanadium additions up through about 8 a/o apparently results from partial recovery of these alloys at this temperature.

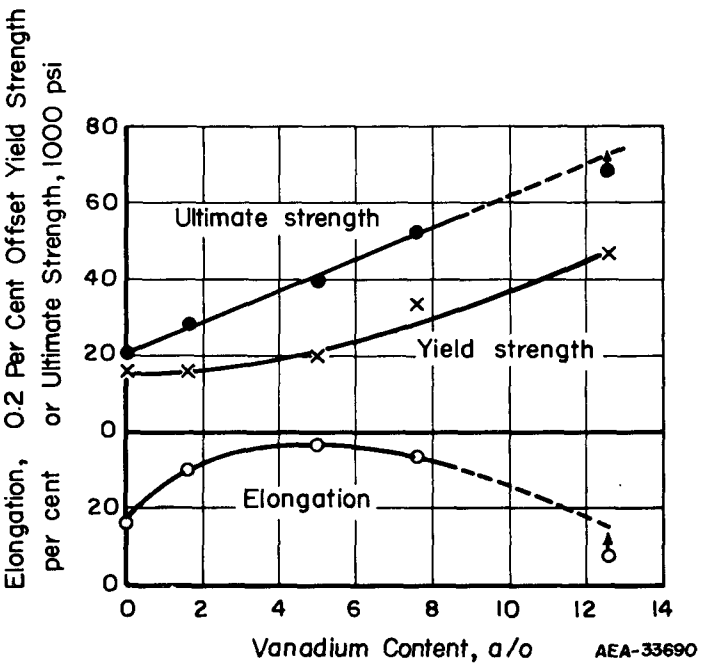

FIGURE 24. EFFECT OF VANADIUM ON THE TENSILE PROPERTIES OF NIOBIUM AT 1500 F

At vanadium levels from 2 to 7.5 a/o, additions of 2.5 a/o titanium or molybdenum are about equivalent in strengthening effect. However, neither titanium nor molybdenum is as effective in improving the hot tensile strength of the niobium-vanadium base as are smaller additions of iron, nickel, nitrogen, or carbon.

In an attempt to correlate the elevated-temperature tensile properties and hardnesses of all the alloys tested, these data were cross plotted with the results shown in Figure 25. As indicated, while the scatter is quite large, the ultimate and yield strengths of niobium alloys at temperatures through 1500 F may be roughly approximated from hot-hardness data through use of the following relationships:

$$UTS_{(psi)} = 400\ VHN$$

$$YS_{(psi)} = 333\ (VHN-10)\ .$$

TABLE 22. SUMMARIZED 1500 F TENSILE PROPERTIES OF NIOBIUM-BASE ALLOYS

Alloy	Alloy Content (Balance Niobium), a/o	Annealing Temperature, F	Tensile Properties		
			0.2 Per Cent Offset Yield Strength, 1000 psi	Ultimate Strength, 1000 psi	Elongation in 1 In., per cent
N40	100 Nb	2190	16	21	18
N57	1 Ce[a]	2190	8	15	30
N3	2.2 Zr	2190	30	32	5
N11	3.2 Ti	2190	14	17	11
N12	10.5 Ti	2190	12	20	12
N16	1.6 V	2190	16.5	28.5	30
N53	1.8 V-<0.02 Cr	2190	17	31	51
N54	1.8 V-0.14 Al	2190	16	30	38
N49	2 V-2.5 Ti	2190	19	35	18
N50	2 V-2.3 Mo	2190	21	34	29
N51	2.2 V-0.54 Fe	2190	25	43	31
N52	2.2 V-0.87 Ni	2190	38	47	52
N55	2.5 V-2.5 Zr[a]	2190	--	38	1
N17	4 V-2.3 Zr	2190	30	46	9
N81	5 V[a]	2190	20	40	37
N65	5 V-2.5 Ti[a]	2190	23	44	29
N66	5 V-2.5 Mo[a]	2190	24	43	9[b]
N72	5 V-0.5 C[a]	2190	30	48	32
N78	5 V-0.5 Ti-0.5 C[a]	2190	26	47	42
N74	5 V-0.25 Ti-0.5 O[a]	2190	35	51.5	28
NL-11	7.6 V	2190	34	53	34
NL-12	8.7 V-0.26 N	2190	42	60	26
NL-13	7.3 V-2.4 Ti	2190	34	53.5	23
NL-14	7.6 V-2.3 Mo	2190	34	55	28
NL-2	12.6 V	2730	47	>69[c]	>8[c]
NL-21	10.9 Zr-5.1 Ti	2730	34	37	2

(a) Nominal composition.
(b) Ruptured at pin in shoulder.
(c) Pin in shoulder of tensile sample ruptured.

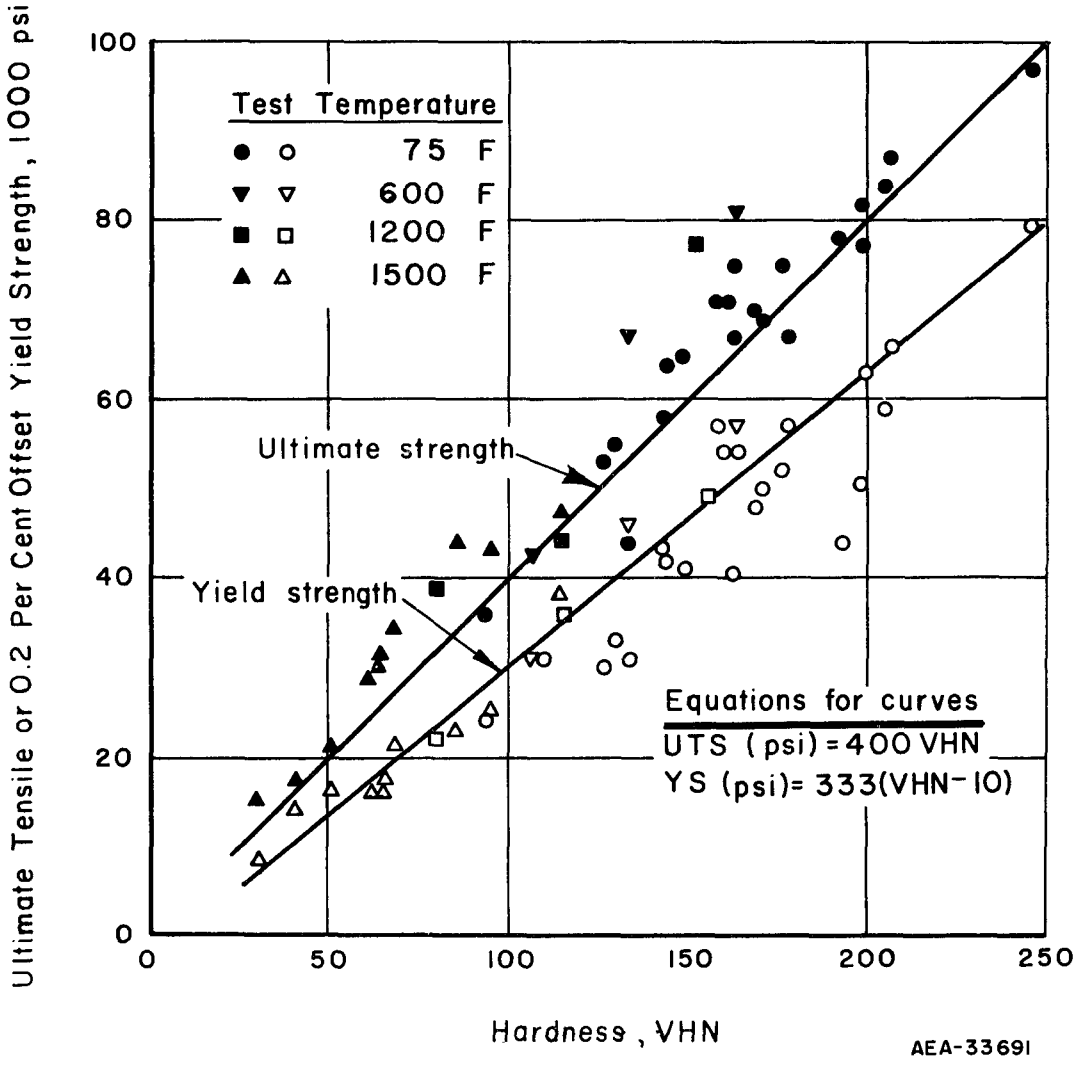

FIGURE 25. CORRELATION OF HOT HARDNESSES TO TENSILE AND YIELD STRENGTHS FOR NIOBIUM-BASE ALLOYS

Creep Properties

Creep tests were conducted on each of the fabricable scaleup alloys at 1200 and/or 1380 F. The creep-deformation and -rupture data from all tests are detailed in Table 23 and summarized in Table 24. Typical creep-deformation curves are illustrated in Figure 26.

Stressing the unalloyed niobium base to 6000 psi at 1200 F resulted in a continuously decreasing rate of creep, even though the total deformation approached 6 per cent in 265 hr. At the time this test was discontinued (265 hr), the creep rate had reached a minimum value of 0.0018 per cent per hr even though this sample was apparently still in first-stage creep. Increasing the stress level to 8000 psi resulted in an appreciable increase in the rate of deformation and rupture occurred in about 18 hr. As shown by the log-log plot of these data in Figure 27, the stress-rupture curve for unalloyed niobium is very flat.

Generally, the resistance to creep of all of the alloys tested at 1200 F and stresses to 20,000 psi was excellent. None of these alloys had a minimum creep rate greater than 0.0002 per cent per hr. Indeed, four of the alloys (12.6 a/o vanadium, 7.2 a/o molybdenum, 7.6 a/o vanadium-2.3 a/o molybdenum, and 7.3 a/o vanadium-2.4 a/o titanium) showed no measurable creep after exposure periods up to 500 hr. Further, six of these seven alloys showed 0.2 per cent or less total plastic strain as a result of the creep exposures.

Similarly, of the six alloys tested at 30,000 psi and 1200 F, excellent resistance to creep was shown by all excepting the 46.8 a/o zirconium-5.1 a/o titanium alloy. This alloy, which showed a superior ultimate tensile strength to the 12.6 a/o vanadium alloy at 1200 F (Table 20), ruptured with 3 per cent elongation after a 68-hr exposure to 30,000 psi while the vanadium alloy had a total deformation of only 0.2 per cent after a 500-hr exposure. The poor creep strength of this alloy appears attributable to its high zirconium content; i.e., at 1200 F, the alloy behaves much like a zirconium-base alloy.

The creep resistance of the two ternary alloys containing titanium was excellent although both of these alloys showed tendencies to undergo more pronounced deformation on loading than any of the other alloys tested (note the creep-deformation curve for the 7.3 a/o vanadium-2.4 a/o titanium alloy in Figure 26). In one instance, a sample of the 11.2 a/o titanium-3.2 a/o molybdenum alloy was inadvertently loaded to 8000 psi over its 22,000-psi yield strength at 1200 F. Although this sample elongated 2.4 per cent on loading, no measurable creep subsequently occurred in a period of 210 hr. This suggested that the creep resistance of this alloy would be quite amenable to strengthening by cold working. As proof of this hypothesis, another sample of this alloy was exposed to the same stress (30,000 psi) at 1200 F after an 18 per cent cold reduction. As indicated in Table 23, the cold-worked sample underwent a total plastic strain of less than 0.1 per cent and had an estimated minimum creep rate of 0.00003 per cent per hr after a 138-hr exposure.

Of all of the alloys tested, the most outstanding resistance to creep deformation was shown by the 12.6 a/o vanadium alloy. This is evident from comparison of the data in Table 24, which shows good creep strength is retained in this alloy at temperatures to 1380 F and stresses to 40,000 psi.

TABLE 23. CREEP-DEFORMATION AND -RUPTURE

Alloy	Alloy Content (Balance Niobium), a/o	Temperature, F	Stress, psi	Deformation Properties: Elongation on Loading, per cent	Total Deformation: Per Cent	Total Deformation: Time, hr	Creep Deformation(b): Per Cent	Creep Deformation(b): Time, hr
TP-37	100 Nb	1200	6,000	0.15	1	0.38	0.1	0.02
					2	3.9	0.2	0.05
					5	90	0.5	0.12
					5.8	265	0.75	0.30
							1.0	0.56
		1200	8,000	0.5	1	0.12	0.1	0.02
					2	0.44	0.2	0.04
					5	1.3	0.5	0.12
							0.75	0.20
							1.0	0.28
							2.0	0.60
							5.0	1.40
NL-2	12.6 V	1200	20,000	0.12	0.15	0.35	0.03	0.35
					0.16	0.4	0.04	0.4
					0.16	500	0.04	500
			30,000	0.24	0.24	0.1	0.0	1
					0.25	100	0.005	100
		1200	30,000	0.20	0.21	1	0.01	1
					0.21	500	0.01	500
		1380	40,000	0.35	0.35	1	0.05	21
					0.38	10	0.1	41
					0.59	100	0.2	84
					0.78	200	0.5	248
					0.94	307	0.59	307
NL-11	7.6 V	1200	20,000	0.28	0.30	1	0.05	92
					0.32	10	0.07	254
					0.33	100	0.08	303.9
					0.34	200		
					0.36	300		
					0.36	303.9		
NL-12	8.7 V-0.26 N	1200	20,000	0.27	0.30	1	0.05	120
					0.30	10	0.07	168
					0.31	100	0.08	256.4
					0.34	200		
					0.35	256.4		
		1200	30,000	0.48	0.50	1	0.05	6
					0.54	10	0.10	130
					0.57	100	0.12	142.2
					0.58	142.2		
NL-13	7.3 V-2.4 Ti	1200	20,000	0.60	0.80	1	0.10	0.1
					0.86	10	0.20	0.5
					0.86	220.4	0.26	3
							0.26	220.4

PROPERTIES OF SELECTED NIOBIUM-BASE ALLOYS[a]

Total Plastic Strain, per cent	Minimum Creep Rate, per cent per hr	Rupture Properties		Remarks
		Time, hr	Elongation, per cent	
5.8	0.0018	>265	>5.8	Test discontinued after 265 hr
17.9	3.0	10.1	17.9	
0.04	Nil	>500	--	Stress increased to 30,000 psi after 500 hr
0.1	0.00005	>100	--	Stress increased to 40,000 psi after 100 hr and held for an additional 145 hr, giving a total deformation of 0.3 per cent in 745 hr
0.03	Nil	>500	--	Test discontinued after 500 hr
0.7	0.0016	>307	--	Test discontinued after 307 hr
0.24	0.00021	>303.9	--	Test discontinued after 303.9 hr
0.23	0.00010	>256.4	--	Test discontinued after 256.4 hr
0.40	0.00022	>142.2	--	Test discontinued 142.2 hr
0.74	Nil	>220.4	--	Test discontinued after 220.4 hr

TABLE 23.

Alloy	Alloy Content (Balance Niobium), a/o	Temperature, F	Stress, psi	Elongation on Loading, per cent	Deformation Properties: Total Deformation, Per Cent	Total Deformation, Time, hr	Creep Deformation(b), Per Cent	Creep Deformation(b), Time, hr
NL-14	7.6 V-2.3 Mo	1200	20,000	0.13	0.14	1	0.05	200
					0.15	10	0.05	261.6
					0.17	100		
					0.18	261.6		
		1200	30,000	0.26	0.27	1	0.05	40
					0.29	10	0.05	117.3
					0.31	45		
					0.31	117.3		
NL-3	7.2 Mo	1200	20,000	0.12	0.12	1	0	1
					0.12	500	0	500
			30,000	0.25	0.25	1	0.01	4
					0.30	56	0.02	11
					0.30	172	0.05	56
							0.05	172
		1200	30,000	0.19	0.19	1	0.01	5
					0.21	10	0.02	10
					0.30	100	0.05	33
					0.35	200	0.10	88
					0.39	300	0.20	300
					0.41	400	0.23	432
					0.42	432		
		1380	30,000	0.24	0.4	1	0.2	1.5
					0.5	2	0.5	5.8
					1	9.2	1	12.8
					2	23.2	2	26.7
					5	65.6	5	69
					7.6	100	10	134
					10	131		
NL-7	11.2 Ti-3.2 Mo	1200	20,000	0.25	0.25	1	0.01	10
					0.26	10	0.02	73
					0.28	100	0.05	267
					0.30	200	0.08	500
					0.31	300		
					0.32	400		
					0.33	500		
		1200	30,000	2.41	2.41	1	0	1
					2.41	210	0	210
			35,000	3.82	--	--	--	--
		1200	30,000	0.17	0.20	1	0.01	0.5
					0.22	40	0.02	1
					0.22	138	0.05	40
							0.05	138

(Continued)

Total Plastic Strain, per cent	Minimum Creep Rate, per cent per hr	Rupture Properties		Remarks
		Time, hr	Elongation, per cent	
0.06	Nil	>261.6	--	Test discontinued after 261.6 hr
0.13	Nil	>117.3	--	Test discontinued after 117.3 hr
0	Nil	>500	--	Stressed increased to 30,000 psi after 500 hr
0.12	Nil	>172	--	Test discontinued after total time of 672 hr with a total deformation of 0.3 per cent
0.24	0.00012	>432	--	Test discontinued after 432 hr
23	0.066	177.3	23	
0.21	0.00010	>500	--	Test discontinued after 500 hr
2.2	Nil	>210	--	Stress increased to 35,000 psi after 210 hr and held for an additional 120 hr giving a total deformation of 3.8 per cent
3.6	--	>210		
0.05	0.00003	>138	--	Sample initially cold rolled to an 18 per cent reduction; test discontinued after 138 hr

TABLE 23.

Alloy	Alloy Content (Balance Niobium), a/o	Temperature, F	Stress, psi	Deformation Properties: Elongation on Loading, per cent	Total Deformation: Per Cent	Total Deformation: Time, hr	Creep Deformation(b): Per Cent	Creep Deformation(b): Time, hr
NL-4	46.8 Zr-5.1 Ti	1200	30,000	0.26	0.3	1	0.05	7.5
					0.3	5	0.10	19.6
					0.5	42.9	0.20	37.6
					0.75	56.5	0.50	56.9
					1.0	62.9	0.75	63.1
							1.0	68.0
		1200	40,000	0.37	0.37	0.1	0.05	3.1
					0.38	1	0.10	5.9
					0.40	2		
					0.50	7.7		

(a) All alloys initially vacuum annealed 1 hr at 2730 F excepting alloys NL-11 through NL-14, which were annealed at 2190 F.
(b) Creep deformation defined as total deformation minus elongation on loading.

(Continued)

Total Plastic Strain, per cent	Minimum Creep Rate, per cent per hr	Rupture Properties		Remarks
		Time, hr	Elongation, per cent	
3	0.0035	68.3	3	
0.5	0.18	--	--	Failed in grips after 7.7 hr with total deformation of 0.5 per cent

TABLE 24. COMPARISON OF CREEP-DEFORMATION PROPERTIES OF NIOBIUM ALLOYS

Alloy	Alloy Content (Balance Niobium), a/o	Total Deformation in 100 Hr, per cent	Total Plastic Strain		Minimum Creep Rate, per cent per hr
			Time of Test, hr	Strain, per cent	
		1200 F, 20,000 PSI			
NL-3	7.2 Mo	0.1	500	<0.1	Nil
NL-2	12.6 V	0.2	500	<0.1	Nil
NL-14	7.6 V, 2.3 Mo	0.2	262	<0.1	Nil
NL-7	11.2 Ti, 3.2 Mo	0.3	500	0.2	0.0001
NL-12	8.7 V, 0.26 N	0.3	256	0.2	0.0001
NL-11	7.6 V	0.3	304	0.2	0.0002
NL-13	7.3 V, 2.4 Ti	0.9	220	0.7	Nil
		1200 F, 30,000 PSI			
NL-2	12.6 V	0.2	500	<0.1	Nil
NL-3	7.2 Mo	0.3	432	0.2	0.0001
NL-14	7.6 V, 2.3 Mo	0.3	117	0.1	Nil
NL-12	8.7 V, 0.26 N	0.6	142	0.4	0.0002
NL-7	11.2 Ti, 3.2 Mo	2.4	210	2.2	Nil
NL-4	46.8 Zr, 5.1 Ti	>3	68	3	0.18[a]
		1380 F, 30,000 PSI			
NL-3	7.2 Mo	7.6	177	23	0.066[b]
		1380 F, 40,000 PSI			
NL-2	12.6 V	0.6	307	0.7	0.0016

(a) Ruptured in 68 hr.
(b) Ruptured in 177 hr.

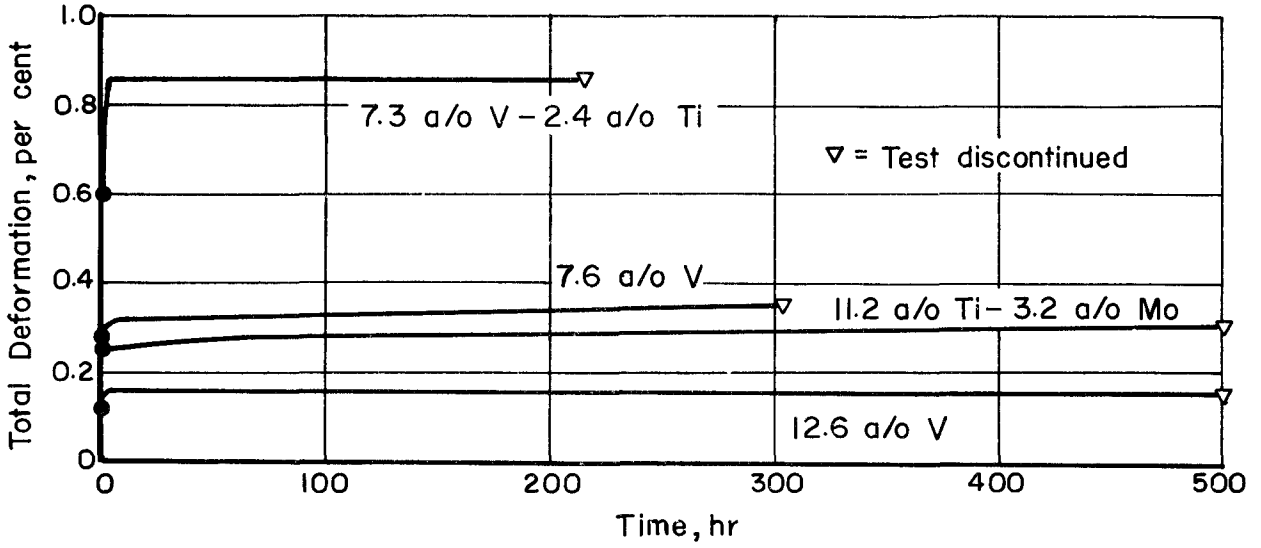

a. Tested at 20,000 PSI

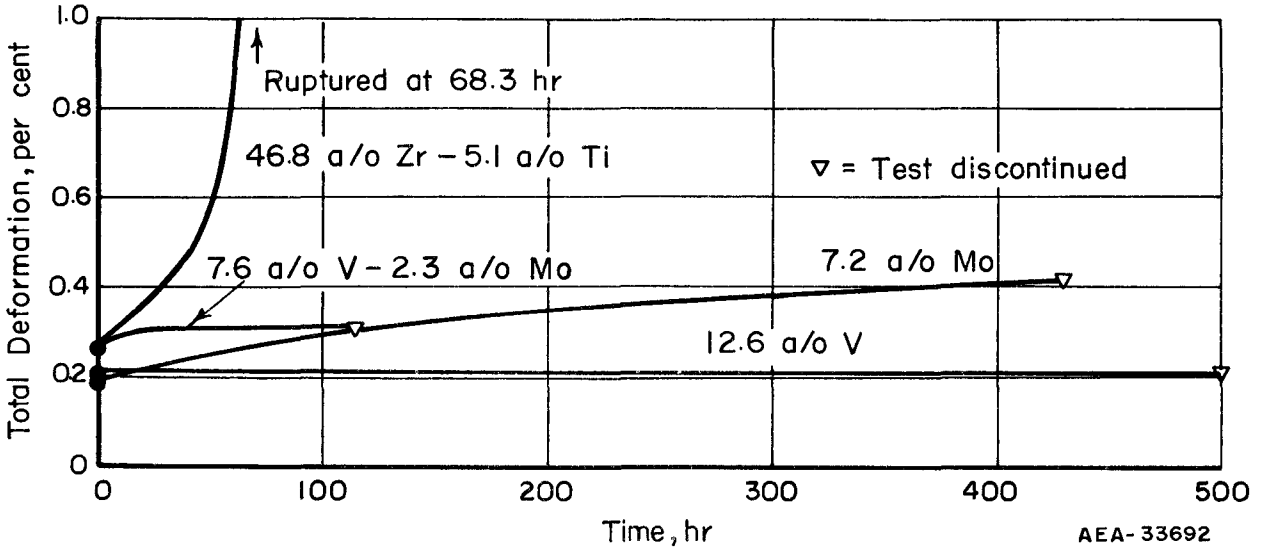

b. Tested at 30,000 PSI

FIGURE 26. CREEP-DEFORMATION CURVES OF VARIOUS NIOBIUM-BASE ALLOYS AT 1200 F

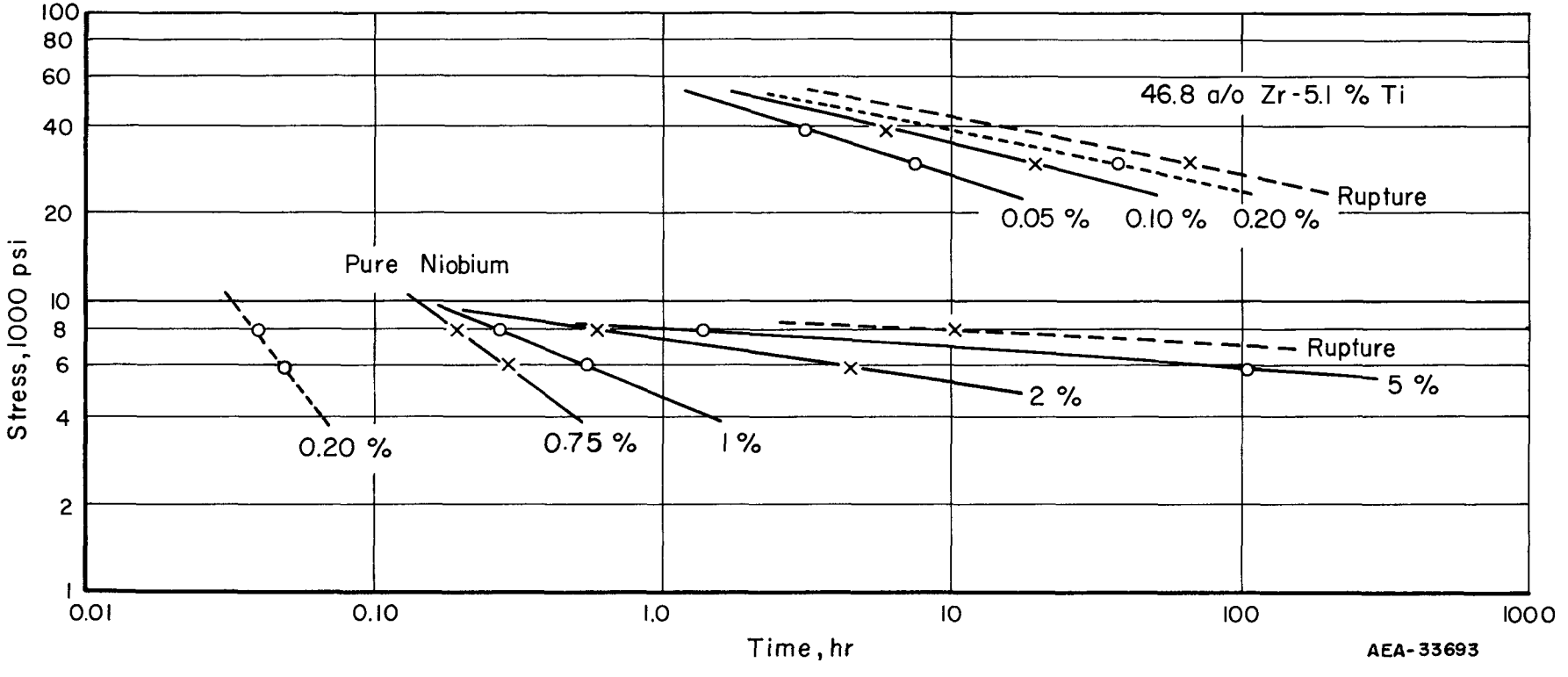

FIGURE 27. CREEP DEFORMATION OF RECRYSTALLIZED NIOBIUM AND NIOBIUM-46.8 a/o ZIRCONIUM-5.1 a/o TITANIUM ALLOY AT 1200 F

TABLE 25. EFFECT OF CREEP EXPOSURE ON THE ROOM-TEMPERATURE TENSILE PROPERTIES OF SELECTED NIOBIUM-BASE ALLOYS

Alloy	Alloy Content (Balance Niobium), a/o	History of Material[a]	Room-Temperature Tensile Properties: 0.2 Per Cent Offset Yield Strength, 1000 psi	Ultimate Strength, 1000 psi	Elongation in 1 In., per cent
TP-37	100 Nb	Annealed 1 hr at 2730 F	20.5	26	28
		Strained 5.8 per cent in 265 hr at 1200 F under 6,000 psi; annealed 1 hr at 2190 F	24	29	23
NL-2	12.6 V	Annealed 1 hr at 2730 F	79	97	24
		Strained 0.3 per cent in 745 hr at 1200 F under 40,000 psi; annealed 1 hr at 2190 F	81	100	31
		Strained 0.2 per cent in 500 hr at 1200 F under 30,000 psi	75	81	1
		Strained 0.9 per cent in 307 hr at 1380 F under 40,000 psi	80	82	1
NL-3	7.2 Mo	Annealed 1 hr at 2730 F	63	77	20
		Strained 0.3 per cent in 672 hr at 1200 F under 30,000 psi; annealed 1 hr at 2190 F	64	78	20
		Strained 0.4 per cent in 432 hr at 1200 F under 30,000 psi; surface ground to remove 2 mils of metal	57	69	18
NL-7	11.2 Ti-3.2 Mo	Annealed 1 hr at 2730 F	57	67	35
		Strained 0.3 per cent in 500 hr at 1200 F under 20,000 psi	58	60	1
		Strained 3.8 per cent in 330 hr at 1200 F under 35,000 psi	--	68	1

(a) Annealing treatments and creep exposure conducted in vacuum.

Several of the discontinued creep test samples were tensile tested at room temperature to check the effect of creep exposure on the subsequent room-temperature behavior. When brittle behavior was observed in two each of the 12.6 a/o vanadium and 11.2 a/o titanium-3.2 a/o molybdenum alloys tested "as-removed" from the creep apparatus, several experiments were performed to investigate this behavior. Hardness measurements on shoulder sections of the brittle room-temperature test samples were made and showed no increases indicative of gross contamination. Subsequently, additional room-temperature tensile tests were carried out on these and other alloy samples after (1) vacuum annealing at 2190 F to remove possible strain-hardening effects, or (2) simply surface grinding the creep test sample to remove 2 mils of metal. The results of all of these tests are summarized in Table 25.

As shown, in all cases, either surface grinding or subsequent vacuum annealing restored the original room-temperature properties to the alloys. These data indicate that the embrittlement observed in the original samples resulted from contamination of a thin surface layer of the alloys during creep exposure. Removal of the layer (either by grinding or diffusing it into the base metal) resulted in no detriment to the tensile properties.

CONCLUSIONS

On the basis of this research, the following conclusions are offered regarding the potential usefulness of niobium and niobium alloys in pressurized-water thermal reactors:

(1) High-purity niobium offers more resistance to corrosion by 600 and 680 F water and 750 F steam than commercial-purity niobium. However, neither grade is as resistant to attack as zirconium. Hence, niobium must be alloyed in order to obtain adequate corrosion resistance and improved strength for pressurized-water applications.

(2) Binary and ternary additions of chromium, iron, molybdenum, titanium, vanadium, and zirconium significantly improve the corrosion resistance of niobium. In binary combinations, the effects of titanium, vanadium, and zirconium are most outstanding.

(3) The fabricability of the vanadium and titanium alloys, in the ranges required for good corrosion resistance, is good to excellent while that for the zirconium alloys is marginal.

(4) Many binary and ternary alloys show as low or lower weight changes, after comparable exposure times, in 680 F water and 750 F steam than Zircaloy-2. However, of these alloys, only a ternary 28.2 a/o titanium-6.1 a/o chromium alloy and alloys containing 45 a/o or more zirconium develop a dense, adherent tarnish film.

(5) Base-metal purity does not appear to have a significant effect on the corrosion behavior of niobium alloys.

(6) The effects of alloying additions on the behavior of niobium in hot water are similar to their effects on the behavior of niobium in hot air. Hence, oxidation appears to be the primary reaction involved in both media and the alloying mechanism for improving the resistance of niobium to both media appears similar.

(7) Most of the niobium-base alloys tested show strength far superior to that of zirconium and Zircaloy-2 at temperatures from 900 through 1200 F.

(8) At temperatures through 1200 F, the tensile strength and creep resistance of binary vanadium and molybdenum alloys, at levels down to about 7.5 a/o, and ternary alloys of molybdenum, titanium, and vanadium are excellent. Comparably, at 1200 F, the creep resistance of high-zirconium-content alloys is quite low.

(9) On the basis of thermal-neutron-absorption cross section, fabricability, corrosion resistance, and hot strength, vanadium offers the greatest advantages in improving the properties of niobium for pressurized-water thermal-reactor applications.

REFERENCES

(1) Griess, J. C., et al., Solution Corrosion Group Quarterly Report, for the period ending April 30, 1957, CF 57-455 (Unclassified).

(2) Ivanov, O., and Grigorovich, V., "Structure and Properties of Zirconium Alloys", Paper No. 2046 presented at the 2nd International Conference on the Peaceful Uses of Atomic Energy, Geneva, Switzerland (September 1-13, 1958).

(3) Klopp, W. D., Maykuth, D. J., Sims, C. T., and Jaffee, R. I., "Oxidation and Contamination Reactions of Niobium and Niobium Alloys", Battelle Memorial Institute, Report No. BMI-1317 (February 3, 1959).

(4) Brauer, G., Z. anorg. u. allgem. Chem., 248, 1-31 (1941).

(5) Metallurgy of Zirconium, edited by B. Lustman and F. Kerze, McGraw-Hill Book Company, New York (1955), p 634.

(6) Ang, C. Y., "Activation Energies and Diffusion Coefficients of Oxygen and Nitrogen in Niobium and Tantalum", Acta Met., 1, 123 (March, 1953).

(7) Laves, F., "Crystal Structure and Atomic Size", Theory of Alloy Phases, American Society for Metals, Cleveland (1956), p 124.

(8) Coughlin, J. P., "Contributions to the Data on Theoretical Metallurgy", U. S. Bur. Mines Bull. 542 (1954).

(9) Kubaschewski, O., and Hopkins, B. E., Oxidation of Metals and Alloys, Butterworths, London (1953).

DJM:WDK:RIJ:WEB:FWF/all